ORNL/TM-2002/164

Life Sciences Division

Continuous Ethanol Production Using Immobilized-Cell/Enzyme Biocatalysts in Fluidized-Bed Reactor (FBR)

Nhuan P. Nghiem
Brian H. Davison

Prepared by
OAK RIDGE NATIONAL LABORATORY
Oak Ridge, Tennessee 37831-6226
Managed by
UT-BATTELLE, LLC
For the
U.S. DEPARTMENT OF ENERGY
Under contract DE-AC05-00OR22725

Acknowledgements

This report is a compilation of years of research science, and the authors gratefully acknowledge the collaboration and contributions of the following colleagues:

David Harshbarger

Mahesh M. Krishnan

Charles D. Scott

May Y. Sun

Frank Taylor

Orren F. Webb

Table of Contents

Executive Summary…….....1
1.0 Introduction…….....3
2.0 Ethanol production from corn starch…….....4
2.1 Ethanol production from soluble starch…….....4
2.1.1 Co-immobilized glucoamylase-*S. cerevisiae*.....4
2.2 Ethanol production from dry-milled corn starch…….....15
2.3 Mathematical model for ethanol production from starch in FBR…….....34
2.3.1 Fermentation kinetics of immobilized *Z. mobilis*……34
2.3.2 Hydrolysis kinetics of immobilized glucoamylase…….....35
2.3.3 Mathematical model of the biocatalyst bead…….....35
2.3.4 Modeling of the FBR…….....37
2.3.5 Results of the mathematical model…….....39
3.0 Ethanol production from lignocellulosic sugars……48
3.1 Materials and methods…….....49
3.1.1 Microorganisms…….....49
3.1.2 Fluidized-bed reactor (FBR)…….....49
3.2 Results and discussion……49
3.2.1 Plasmid-based strains…….....49
3.2.2 Chromosomally integrated strains…….....55
3.3 Economic analysis……..63
4.0 Scale-up of the FBR technology……64
5.0 Conclusions……66
References……..69

List of Figures

Figure 1. Schematic diagram of the fluidized-bed reactor (FBR) used for study of ethanol production from soluble starch solutions……..5

Figure 2. Example of concentration profiles along the length of the FBR using the glucose amylase-*S. cerevisiae* biocatalyst……7

Figure 3. The effect of starch mass loading on FBR performance with the glucose amylase-*S. cerevisiae* biocatalyst……...8

Figure 4. Determination of average ethanol yield by the glucose amylase-*S. cerevisiae* biocatalyst in the FBR……8

Figure 5. Example of concentration profiles along the length of the FBR using the glucose amylase-*Z. mobilis* biocatalyst……..11

Figure 6. Ethanol volumetric productivity at different sections of the FBR using the glucose amylase-*Z. mobilis* biocatalyst……..12

Figure 7. pH profiles along the length of the FBR using the glucose amylase-*Z. mobilis* biocatalyst……12

Figure 8. The effect of starch mass feed rate and time of operation on ethanol productivity in the FBR using the glucose amylase-*Z. mobilis* biocatalyst……...14

Figure 9. The contour plot of productivity versus starch mass feed rate and time to determine the optimum mass feed rate of the FBR using the glucose amylase-*Z. mobilis* biocatalyst……...14

Figure 10. Determination of average ethanol yield by the glucose amylase-*Z. mobilis* biocatalyst in the FBR……...15

Figure 11. Schematic diagrams of the simultaneous saccharification and fermentation (SSF) and separate hydrolysis and fermentation (SHF) processes……16

Figure 12. Comparison of soluble starch hydrolysis by fresh glycoamylase-*Z. mobilis* beads and spent (22 batch cycles) beads……...20

Figure 13. Volumetric ethanol productivity and dry-milled cornstarch-derived glucose feed conversion as a function of dilution rate for the SHF process……23

Figure 14. Volumetric ethanol productivity and synthetic glucose feed Conversion as a function of dilution rate for the SHF process……24

Figure 15. Overall volumetric ethanol productivity and ethanol concentrations obtained from hydrolyzed cornstarch feed by the SHF process using immobilized glucose amylase and *Z. mobilis*. The results are plotted as a function of the total residence time……25

Figure 16. Base case dry-mill corn starch to ethanol process……...27

Figure 17. FBR ethanol process……28

Figure 18. The mechanisms inside the reactor……..35

Figure 19. The reactions and mechanism inside the co-immobilized GA-*Z. mobilis* biocatalyst……..36

Figure 20. Mass flow and two effectiveness factors of the co-immobilized biocatalyst bead……..37

Figure 21. Stationary volume element ÄxÄyÄz through which fluid is moving……38

Figure 22. Starch concentration profile inside the bead along the radial distance from the center of the bead at the different bulk starch concentrations……40

Figure 23. The comparison of the mathematical model results solved using the plug flow boundary condition (simple) and the Danckwerts boundary condition (flow rate 0.6 L/hr, enzyme loading = 150 ml, and catalyst bead diameter = 0.2 mm)……..41

Figure 24. The comparison of the mathematical model results solved using the plug flow boundary condition (simple) and the Danckwerts boundary condition (flow rate 2 L/hr, enzyme loading = 375 ml, and catalyst bead diameter = 0.4 mm)……..42

Figure 25. The starch concentration profile comparison between the model results and the experimental data (experimental condition: flow rate = 0.6 L/hr, feed concentration = 110 g/L)……42

Figure 26. The starch concentration profile comparison between the model results and the experimental data (experimental condition: flow rate = 2 L/hr, feed concentration = 95 g/L)……43

Figure 27. The starch concentration profile in the catalyst bead at different bulk starch concentrations……...44

Figure 28. Glucose concentration profiles corresponding to the different starch bulk concentrations. Glucose concentration G1 corresponds to bulk starch……44

Figure 29. Starch and glucose concentration profiles at the different starch diffusivities. Bead radius = 2mm, starch bulk concentration Sb = 1.0, glucose bulk concentration = 0.0, starch S11, glucose G11 (Ds = 0.002 cm^2/hr), S12, G12 (Ds = 0.004 cm^2/hr); S13, G13 (Ds = 0.008 cm^2/hr)……...45

Figure 30. Starch and glucose concentration profiles for different sizes of catalyst bead. S0.1 is starch concentration, G0.1 is glucose concentration at r = 0.1 cm; S0.15; G0.15 (r = 0.15 cm); S0.2; G0.2 (r = 0.2 cm)……46

Figure 31. The comparison of concentration profiles in the reactor with different catalyst enzyme loading……..46

Figure 32. The comparison of concentration profiles in the reactor with different catalyst enzyme loading……..47

Figure 33. The influence of the feed flow rate on the concentration profiles in the reactor……48

Figure 34. Determination of stability of strain *Z. mobilis* 31821 (pZB5) in continuous FBR operation……52

Figure 35. Determination of stability of strain *Saccharomyces* 424A (LNH-ST) in continuous FBR operation……...56

Figure 36. Performance of *Z. mobilis* C25 in FBR using 40/20 glucose/ xylose feed at 4.2-h retention time with Red Star yeast extract as nutrient source……59

Figure 37. Performance of *Z. mobilis* C25 in FBR using 40/20 glucose/ xylose feed at 4.2-h retention time with Difco yeast extract as nutrient source……60

Figure 37. Performance of *Saccharomyces* 424A (LNH-ST) in FBR using 40/20 glucose/xylose feed at 4.6-h retention time with Difco yeast extract as nutrient source……..62

Figure 39. Continuous ethanol fermentation in the FBR by *E. coli* K011……63

List of Tables

Table 1. Simultaneous saccharification and fermentation (SSF) of maltodextrin and dextrins from dry-milled corn starch to ethanol using co-immobilized glucoamylase-*Z. mobilis* in the FBR……..21

Table 2. Fermentation of glucose obtained by enzymatic hydrolysis of dextrins from dry-milled corn starch to ethanol using co-immobilized glucoamylase-*Z. mobilis* in the FBR……22

Table 3. Fermentation of synthetic glucose feed to ethanol using immobilized *Z. mobilis* in the FBR……24

Table 4. FBR process cases used in the economic analysis……..31

Table 5. Capital costs comparison for base case and FBR processes (Cases 1 and 5)……...31

Table 6. Operating cost comparison of processing steps for base case process and FBR process (Cases 1 and 5)…….32

Table 7. Summary of operating costs for base case process and FBR process cases……..33

Table 8. Results of repeated batch experiments performed with immobilized *Z. mobilis* CP4(pZB5) biocatalyst……50

Table 9. Steady state results of FBR experiments performed with immobilized *Z. mobilis* CP4(pZB5) biocatalyst……50

Table 10. Results of fermentation of glucose-xylose mixture to ethanol during repeated batch experiments……51

Table 11. Steady state results of FBR experiments performed with immobilized *Z. mobilis* 31821(pZB5)……...53

Table 12. Steady state results of FBR experiments performed with immobilized *Z. mobilis* 31821(pZB5) and Arkenol's hydrolysate……53

Table 13. Steady state results of FBR experiments performed with immobilized *Saccharomyces* 424A(LNH-ST)…….57

Table 14. Steady state results of FBR experiments using a larger quantity of immobilized *Saccharomyces* 424A(LNH-ST) biocatalyst……..57

Executive Summary

The immobilized-cell fluidized-bed bioreactor (FBR) was developed at Oak Ridge National Laboratory (ORNL). Previous studies at ORNL using immobilized *Zymomonas mobilis* in FBR at both laboratory and demonstration scale (4-in-ID by 20-ft-tall) have shown that the system was more than 50 times as productive as industrial benchmarks (batch and fed-batch free cell fermentations for ethanol production from glucose). Economic analysis showed that a continuous process employing the FBR technology to produce ethanol from corn-derived glucose would offer savings of three to six cents per gallon of ethanol compared to a typical batch process. The application of the FBR technology for ethanol production was extended to investigate more complex feedstocks, which included starch and lignocellulosic-derived mixed sugars. Economic analysis and mathematical modeling of the reactor were included in the investigation. This report summarizes the results of these extensive studies. Based on these results, the following conclusions are made.

1. The FBR was a highly effective system for ethanol production from corn-derived and lignocellulosic sugars. Both feed stocks could be used to produce ethanol at yields very close to the theoretical values and at volumetric productivities at least one order of magnitude higher than those typically obtained in batch process using conventional stirred tank fermenters. The reactor could be operated continuously for over a month with very good stability. There was no loss of the biocatalyst beads from the reactor over the entire normal course of the operation and minimal deactivation. The κ-carrageenan-based immobilized biocatalyst was stable. There were no obvious signs of structural failure of these beads. Minimal sterility requirement were needed and the system was resistant to contamination due to the low liquid residence time.

2. Co-immobilized enzyme-microbe systems allow the potential to perform simultaneous saccharification and fermentation (SSF). Both co-immobilized biocatalyst systems, namely the glucoamylase-*S. cereviasiae* and glucoamylase-*Z. mobilis*, are suitable for production of ethanol from soluble starch. The average ethanol yield of the glucoamylase-*S. cereviasiae* system was 0.45 g ethanol/g starch consumed or 80% of the theoretical yield. In the case of the glucoamylase-*Z. mobilis* system the average ethanol yield was 0.49 g ethanol/g starch consumed or 89% of the theoretical yield.

3. When dry-milled corn starch was used for ethanol production, the solids in the feed streams had to be removed first because the FBR was unable to handle feed streams with high solid contents.

4. An SHF (separate hydrolysis and fermentation) system was much more effective for ethanol production from dry-milled corn starch than an SSF system because in the SHF it was possible to carry out the two consecutive steps, namely the hydrolysis of soluble starch by immobilized glucoamylase and the fermentation of the sugars to ethanol by immobilized *Z. mobilis*, at their different optimum conditions, rather than at a compromise non-optimal condition. In the SSF system to ensure viability of the organism the FBR had to be operated at temperatures below 35°C, at which the hydrolysis rate of glucoamylase was only about 15 to 20% of its optimum rate at 55°C.

The results clearly indicated the need for a highly effective thermophilic ethanol-producing organism, which will allow hydrolysis and fermentation to be carried out simultaneously in one single reactor at the temperature optimum for both the enzyme and the organism.

5. An SHF process using the FBR technology was developed for production of ethanol from dry-milled corn starch using immobilized glucoamylase and immobilized *Z. mobilis* in two consecutive reactors. An economic analysis was performed for this process with USDA. The results showed savings of one to three cents per gallon of ethanol produced compared to a traditional batch process using conventional stirred tank fermenters in a state-of-the-art dry-mill ethanol plant.

6. A mathematical model was developed for ethanol production from glucose or from soluble starch in the FBR. The model can be used to predict concentration profiles of starch and glucose within biocatalyst beads as well as the concentration profiles of starch, glucose, and ethanol along the length of the FBR under a set of process conditions such as feed concentration and feed flow rate. The predicted results allow determination of optimum bead size and optimum operating conditions of the FBR.

7. Five recombinant organisms were tested in the FBR for ethanol production from lignocellulosic sugars. These included two plasmid-based strains, *Z. mobilis* CP4(pZB5) and *Z. mobilis* 31821(pZB5), and three chromosomally integrated strains, *Z. mobilis* C25, *Saccharomyces* 424(LNH-ST), and *E. coli* KO11.

8. Strain *Z. mobilis* CP4(pZB5) was not suitable for continuous operation in the FBR. Even with tetracycline in the feed solutions the strain lost its xylose metabolism capability in about ten days. *Z. mobilis* 31821(pZB5) was a much more stable strain and was suitable for continuous use in the FBR. With tetracycline in the feed solutions it maintained its xylose metabolism capability for a period of 17 days. However, without tetracycline it lost this capability after five days of continuous operation.

9. *Z. mobilis* 31821(pZB5) had very high xylose conversion efficiency. With feed solutions containing 40 g/L glucose and 20 g/L xylose, and 50 g/L glucose and 10 g/L xylose, greater than 84% conversion of xylose was observed at a dilution rate of 0.24 h^{-1}. In both cases complete conversion of glucose was achieved. The xylose conversion rate was well above the goal of 75% xylose conversion set for a process using lignocellulosic sugars to produce ethanol.

10. *Z. mobilis* 31821(pZB5) was also tested with Arkenol's rice straw hydrolysate, which was obtained by the concentrated hydrolysis process. The hydrolysate displayed no toxicity toward the organism. It also was proven to be a good feed stock for ethanol production. At the highest sugar concentrations tested, which were 144 g/L glucose and 27 g/L xylose, and a dilution rate of 0.25 h^{-1}, the conversion rates of glucose and xylose were 98% and 83%, respectively. The ethanol concentration was 70 g/L, which gave a productivity of 17 g/L-h. This was almost ten times the typical productivity of 2 to 3 g/L-h obtained in batch fermentations using lignocellulosic sugars.

11. An economic model was developed for a process using the FBR technology with immobilized *Z. mobilis* biocatalyst for ethanol production from lignocellulosic sugars obtained by concentrated acid hydrolysis. The results indicated savings of about three cents per gallon of ethanol produced compared to a typical batch process using stirred tank fermenters.

12. Both *Saccharomyces* 424A(LNH-ST) and *Z. mobilis* C25 displayed loss of xylose metabolism capability with time. The yeast strain was able to maintain xylose metabolism at the level equal to the initial level for 13 days whereas the bacterial strain seemed to lose that capability sooner. Both of these strains showed an ethanol yield lower than the yield obtained with the plasmid-baased strain *Z. mobilis* 31821(pZB5) due to formation of by-products.

13. *E. coli* KO11 did not perform as well as the other two chromosomally integrated strains tested. Maximum glucose conversion of only 60% was achieved. This strain also displayed instability of xylose metabolism with time.

Overall the multiple configurations, immobilized-cell FBR systems have generally shown order of magnitude increases in ethanol volumetric productivity at high conversion with yields equal to or greater than that of free-cell systems. Economic analyses of several configurations have shown potential savings of 1 to 6 cents/gal due to both capital and yield improvements. The savings are valuable but below that for retrofit of existing plants. The technology is viable but appears to be a second-generation technology, worthy of consideration after improvements in other areas further drop the production cost.

1. Introduction

Fuel ethanol is produced in a batch or fed-batch process using the traditional stirred tank reactor. Significant efforts are ongoing to reduce ethanol production costs by investigating new inexpensive feedstock, e.g., woody biomass, and by process improvements in the fermentation and separation steps. Increasing reactor productivity is a potential method for reducing capital costs associated with new construction and expansion of existing facilities. Selection of fermentative organisms and the reactor configuration also affect operating cost factors such as yield, energy demand, and control of bacterial contamination.

A key element in the development of advanced bioreactor systems capable of very high conversion rates is the retention of high biocatalyst concentrations within the bioreactor and a reaction environment that ensures intimate contact between substrate and biocatalyst. Such strategies include cell recycle by filtration, sedimentation, entrapment by membranes, and immobilization in gel beads (Crueger and Crueger, 1982; Inloes et al., 1985). These retention schemes can then be used with various reactor configurations, including continuous stirred-tank (CSTR), packed-bed (PBR), and fluidized-bed (FBR). Typical batch reactors, which are commonly used in industry, have volumetric ethanol productivity between 2 and 5 g/L-h (Silman, 1984; Bajpai and Margaritis, 1985). On a total reactor volume basis, volumetric productivity for continuous systems with high conversion is reported as 6-8 g/L-h for a free-cell

CSTR, 10-16 g/L-h for an immobilized-cell CSTR, 10-30 g/L-h for a hollow fiber reactor, 16-40 g/L-h for vertical PBR, and 50-120 g/L-h for an immobilized-cell FBR (Godia et al., 1987; Davison and Scott, 1988). One very effective method is to use an immobilized biocatalyst that can be placed into a reaction environment that provides effective mass transport, such as fluidized bed. Previous studies at ORNL using immobilized *Zymomonas mobilis* in FBR have shown that this system may be more than 10-50 times as productive as industrial benchmarks (Davison and Scott, 1988; Webb et al., 1995). Economic analysis with Fluor-Daniels showed that a continuous process employing the FBR technology to produce ethanol from corn-derived glucose would offer savings of three to six cents per gallon of ethanol compared to a typical batch process (Harshbarger et al., 1995). A predictive model was also developed (Petersen and Davison1991; 1995). The FBR technology developed at ORNL received significant technical and financial support from a number of industrial concerns such as Tate and Lyle (formerly A. E. Staley Co.) of Decatur, Illinois and the National Corn Growers Association.

Impressive results obtained with simple glucose solution prompted investigation into use of the FBR technology for more complex feedstocks such as cornstarch and lignocellulosic hydrolysate. This report will summarize the results of these investigations.

2. Ethanol production from corn starch

Starch is the most abundant renewable carbon source and has been used extensively in ethanol production. Unfortunately, the two best ethanol-producing organisms, *Saccharomyces cerevisiae* and *Z. mobilis*, cannot metabolize starch. Therefore, the conversion of starch to ethanol normally requires two stages: hydrolysis of starch to glucose by acid or enzyme, and its subsequent conversion to ethanol. Since previous research at ORNL already examined ethanol production from glucose, which was produced from corn in wet-mill ethanol plants, our next level of efforts focused on ethanol production from dry-mill cornstarch. The first part of this study used synthetic solutions of soluble starch. The second part of the study used dextrins slurries, which were prepared from corn powder using the actual industrial process employed by dry-mill ethanol plants. Finally a mathematical model was derived to predict the performance of the FBR using soluble starch for ethanol production.

2.1 Ethanol production from soluble starch

Two biocatalyst systems were used in this study. These included co-immobilized glucoamylase-*S. cerevisiae* and co-immobilized glucoamylase-*Z. mobilis*.

2.1.1 Co-immobilized glucoamylase-*S. cerevisiae*

Materials and methods

The *S. cerevisiae* cells were immobilized in covalently crosslinked gelatin (6 wt%) and chytosan (0.25 wt%) with glucoamylase (GA). Crosslinking was accomplished by glutaraldehyde. Biocatalyst diameter ranged between 1.2 and 2.8 mm. This developmental

biocatalyst was supplied by Gist-Brocades (Delft, The Netherlands); this technology is now owned by Genencor, Inc. and the immobilization equipment is at FermPro International.

Feed solutions consisted of various concentrations of StarDri 100 starch (Tate and Lyle, Decatur, IL), 5 g/L Tastetone 900 AG yeast extract (Red Star, Junneau, WI), and 0.1% w/v antifoam B (Dow Corning, Midland, MI) in tap water.

The reactor shown in Fig. 1 was constructed of a 30-cm inlet section, which expanded from 1.27 to 2.5 cm in ID, three 30-cm sections of 2.5 cm ID jacketed glass pipe, and a 10-cm disengagement section of 9 cm ID with a screened sidearm for disengagement of the biocatalyst beads from the reactor effluent. Temperature was controlled at 34°C by recirculating water from a constant temperature water bath through the jacket. Feed solutions were introduced at the reactor bottom using a 7550-60 Masterflex peristaltic pump (Cole Parmer, Niles, IL). The pump was calibrated daily. The pump flow rates were adjusted to provide feed rates from 18 to 114 g starch per hour. The reactor was opened to the atmosphere for gas-liquid disengagement at the outlet.

Figure 1. Schematic diagram of the fluidized-bed reactor (FBR) used for study of ethanol production from soluble starch solutions.

Starch, glucose, and ethanol concentration in feeds and in the effluents were measured using a Shimadzu HPLC consisting of an RID6A refractive index detector, an SIL 10A autoinjector, an LC10AD pump, an SCL10A system controller, a CTD10A column oven, and a CR501 integrator. An Aminex HPX-87H (Bio-Rad Laboratories, Hercules, CA) column with a 5 mM H_2SO_4 mobile phase was used for separation of the constituents of the samples.

Minimal procedures were used for mitigation of contaminant growth. These included:

1. Changing feed lines with each new charge of feed carboy;
2. Replacement of feed carboys with each charge of fresh feed; and

3. Media were autoclaved prior to use, because significant amounts of contaminants existed in the yeast extract.

Previous studies demonstrated that sterile operation was not necessary. However, sterile operation was needed to keep the feed free of high levels of contamination, e.g., contamination at less than 10^8 cells/mL. The reactor was not sterilized or cleaned after the experiment began. The experiment lasted for ten weeks but no significant contamination was observed.

Results and discussion - Co-immobilized glucoamylase-*S. cerevisiae*

Operability of the reactor was good throughout the course of the experiment. The reactor system generally was operated without operator intervention. The pH within the reactor was not controlled and ranged from 6.5 at the inlet to 3.5 at the outlet of the reactor. The biocatalyst was used for ten weeks in the FBR without recharging. There was no noticeable loss of biocatalyst from the reactor. There also were no obvious signs of physical degradation of the biocatalyst except for a very small number of beads that demonstrated significant increases in size.

In the FBR, the fluid dynamics and reaction kinetics were coupled and were a complex function of reaction rate, starch and glucose concentration, biocatalyst loading, and gas-liquid-solid properties (Petersen and Davison, 1995; Webb et al., 1996); a predictive model was developed to simulate the conditions. Fluidization of the biocatalyst in the reactor changed rapidly with axial position due to significant changes in fluid flow rates and physical properties. Along the reactor axis, there were three zones that could be distinguished visually. The first zone, located at the bed entrance, was fluidized by the upward flow of the liquid. The second zone, which was fluidized by the gas product, started within the expansion section and encompassed most of the bed. The third zone, where disengagement of gas and liquid occurred, was characterized by high gas hold-up and significant mixing. The axial reaction rate in the FBR was a strong function of reactor biocatalyst concentration. Gas and liquid hold-up, and dispersion, which became larger in the upper parts of the reactor, reduced the biocatalyst concentration. Inside the biocatalyst matrix, starch was hydrolyzed by glucoamylase (GA) to form glucose, which then was converted to ethanol and carbon dioxide by the yeast:

$$(C_6H_{10}O_5)n + (n-1)\,H_2O \longrightarrow n\,C_6H_{12}O_6$$

$$n\,C_6H_{12}O_6 \longrightarrow 2n\,CH_3CH_2OH + 2n\,CO_2$$

The biocatalyst was loaded with sufficient GA to convert low concentrations of starch at significant rates. The GA reaction rates were thus expected to be rapid at higher starch concentrations.

Fig. 2 shows an example of concentration profiles for low-starch loading. The flow rate and mass loading were 10 mL/min and 60 g starch/h, respectively. Mass loading was moderate, since the range of starch mass loading for the ten-week experiment was from 20 to 120 g/h. Starch concentration decreased with distance from the inlet as GA conversion proceeded. Glucose was an intermediate of the two reactions in series. Therefore, the axial glucose concentration would be a function of both the GA and yeast reaction rates. Glucose accumulated in the first section of the reactor because of high GA conversion rates (high starch concentrations). The ethanol concentrations increased as glucose was made available by GA and

then was converted by the yeast. Glucose accumulation in the first section indicated that the yeast reaction was slower than the GA reaction because of high bulk starch concentrations. The rate of conversion of starch to glucose dropped in higher sections as the available starch was reduced. Although the starch conversion rate in these sections was still higher than the yeast reaction rate, its reduction caused a decrease in glucose concentration. This tendency continued upward along the length of the reactor.

Figure 2. Example of concentration profiles along the length of the FBR using the glucose amylase-*S. cerevisiae* biocatalyst.

The surface in Fig. 3 allows visualization of the effect of mass loading on reactor performance. This surface was generated with the Statistica software (StarSoft, Tulsa, OK). The data clearly demonstrated that as mass loading increased, glucose accumulation also increased. Bed position was also important as a variable to indicate the effect of contact time between substrates and the catalysts, i.e., GA and the yeast. Thus, as the contact time increased, the total conversion of starch and glucose also increased. The GA reaction was influenced greatly by starch concentration and to a minor extent by glucose concentration. The yeast, on the other hand, was limited at the reactor inlet by a lack of glucose. As ethanol was formed, it became inhibited. Fig. 3 also indicated that the reaction was limited to the yeast and not the enzyme. The data clearly demonstrated that as mass loading was increased, the accumulation of glucose increased. In actual practice, the GA activity would ideally be balanced against the yeast activity to maintain a low glucose concentration throughout the reactor.

Figure 3. The effect of starch mass loading on FBR performance with the glucose amylase-*S. cerevisiae* biocatalyst.

The overall ethanol productivity was 25 to 44 g/L-h. The ethanol yield was calculated from the slope of the line plotted in Fig. 4 (ethanol production versus substrate conversion). The average yield was 0.45 g ethanol/g starch converted. This was about 80% of the theoretical yield. This rather low yield probably was due to the formation of other fermentation by-products or by nutritional limitation.

Figure 4. Determination of average ethanol yield by the glucose amylase-*S. cerevisiae* biocatalyst in the FBR.

2.1.2 Co-immobilized glucoamylase-*Z. mobilis*

Materials and methods

Z. mobilis NRRL-B-14023 was used. The stock culture was maintained in 25% glycerol and kept at –70°C. To obtain the cells for use in preparation of the biocatalyst beads, *Z. mobilis* was grown in a 75-liter fermentor (New Brunswick Scientific Co., Edison, NJ). The inoculum was grown in a three-liter fernbach containing two liters of medium. The medium contained 50 g/L glucose, 5 g/L Tastetone 900 AG yeast extract, and 6 g/L KH_2PO_4. The medium was adjusted to pH 5 with concentrated phosphoric acid. It was sterilized by autoclaving at 121°C for 20 minutes. One stock vial containing 1.7 mL liquid culture was used to inoculate the fernbach. The fernbach was incubated at 30°C with gentle mixing for 36 hours before its entire contents were used to inoculate the fermentor. The fermentor medium had the same composition as the fernbach medium. The temperature of the fermentor was maintained at 30°C and its pH at 5.0 using 2N NaOH. After about 20 hours, when 90% of the glucose had been consumed, the cells were recovered by centrifugation using a continuous Sharples Super-Centrifuge AS26NF. The recovered cell paste was stored at 4°C until it was ready for use in the biocatalyst preparation.

A developmental immobilized GA was used to prepare the biocatalyst. This immobilized GA product was a gift from Genencor International (Rochester, NY). The enzyme was immobilized on a proprietary solid matrix having average particle diameter of about 1.5 mm. Before the immobilized GA was used in preparation of the co-immobilized *Z. mobilis*-GA biocatalyst, it was ground in a ceramic mortar placed on ice until the particle diameter was less than 0.1 mm. A small sample was centrifuged and the supernatant tested for GA activity at 35°C using soluble starch at 80 g/L as substrate. In this test no glucose was observed, which indicated that the grinding process did not result in loss of GA from the solid matrix. The activity of the ground immobilized GA was measured at 35°C and pH 5.0. One hundred milliliters of buffer (6 g/L KH_2PO_4 adjusted to pH 5.0) was used to wash 2 mL of ground immobilized GA into a 250-mL flask. The flask was then placed in a 35°C water bath and its contents mixed with a stir bar. When the temperature of the flask contents was the same as that of the bath, 100 mL of a 80 g/L soluble starch in the same buffer was quickly added. Samples were taken at intervals, quickly centrifuged on a microcentrifuge to separate the immobilized GA, and glucose concentration in the supernatant was determined on a YSI glucose analyzer (Yellow Springs Instruments, WI). The specific activity of the ground immobilized GA at an initial starch concentration of 40 g/L was calculated as 1.16 g glucose/mL enzyme-h.

The co-immobilized GA-*Z. mobilis* biocatalyst beads were prepared as follows. Forty grams κ-carrageenan (Type NSAL 798 from FMC Corporation) was slowly dissolved in 700 mL de-ionized water in a beaker kept in a water bath at 70°C. Mixing was provided with a stir bar. After all the κ-carrageenan was dissolved, the beaker was transferred to a water bath maintained at 35°C. When the temperature of the solution reached 35°C, 40 g of *Z. mobilis* cell paste was added, followed by 150 mL ground immobilized GA. Finally, de-ionized water was added to bring the total volume to one liter. In the original procedure Fe_2O_3 was added to the mixture to increase the density of the biocatalyst beads. In this work, the addition of Fe_2O_3 was not necessary and therefore omitted since the solid matrix onto which GA was immobilized already made the density of the beads sufficiently high to prevent it from floating in the FBR.

The microbial cell-immobilized GA mixture was stirred in a beaker placed in a water bath maintained at 35°C. A Masterflex peristaltic pump delivered the gel solution to a nozzle, which actually was a 100-mL pipette tip. Vibration energy was provided by attachment of a vibrator transducer to the side of the flexible delivery tubing. The gel solution exited the nozzle as a stream of small droplets, which were collected in a cold fixing solution (0.3M KCl). The fixing solution was stirred gently to prevent the beads from coalescing with each other before they were hardened. A strobotac (General Radio Company, Concord, MA) was used to observe the size of the droplets coming out of the nozzle. The average diameter of the biocatalyst beads was 1.5 to 2 mm. These beads were stored at 4°C in a solution at pH 5 containing 0.3M KCl and 7.5 g/L KH_2PO_4.

The FBR was same as the one used for the co-immobilized GA-*S. cerevisiae* system.

Results and discussion, Co-immobilized glucoamylase-*Z. mobilis*

The operability of the reactor was good throughout the course of the experiment. The biocatalyst beads were used continuously for 22 days in the FBR without the need of recharging. There was no noticeable loss of biocatalyst from the reactor. There also were no obvious signs of structural failure of the beads.

Inside the biocatalyst matrix, starch was hydrolyzed by GA to glucose; the glucose then produced was converted to ethanol and CO_2 by *Z. mobilis*. Fig. 5 shows an example of concentration profiles of starch, glucose, and ethanol along the reactor axis. Starch concentration decreased with vertical position in the reactor as GA conversion proceeded. In this particular experiment, 65% conversion of starch was obtained. Glucose was an intermediate of the series of two consecutive reactions, and therefore, its concentration was a function of both GA and *Z. mobilis* conversion rates. Glucose concentrations were extremely low (near zero) at all positions in the reactor. This indicated that glucose production rate was much slower than its consumption rate. In other words, the hydrolysis of starch by GA was the rate-limiting step. Glucose was converted to ethanol and CO_2 immediately after it was produced, and therefore did not accumulate in the reactor. These results were different from those obtained with the GA-*S. cerevisiae* system. In the GA-*S. cerevisiae* system, starch conversion rate was much faster than glucose consumption rate, and glucose accumulated in the middle section of the reactor. Starch diffusion and GA accessibility may account for this difference. In the GA-*S. cerevisiae* system, GA was in its free form before it was co-immobilized with the yeast. In the GA-*Z. mobilis* system, the enzyme was immobilized on a solid matrix before it was co-immobilized with *Z. mobilis*. This double immobilization increased the restriction of starch diffusion into the active sites of the enzyme. Consequently, the concentrations of starch at these locations were low, and therefore, the conversion rate to glucose was slow.

Figure 5. Example of concentration profiles along the length of the FBR using the glucose amylase-*Z. mobilis* biocatalyst.

Ethanol volumetric productivity was calculated for the three sections of the reactor. The results are shown in Fig. 6. In the bottom section of the reactor, the ethanol volumetric productivity was 50 g/L-h. The productivity decreased to 17 and 3 g/L-h for the middle and the top sections, respectively. This decrease was related to fluid dynamics, phase hold-up, and reaction kinetics in the reactor. The fluidization of the biocatalyst bed changed rapidly with the axial position because of significant changes in fluid flow rates and physical properties (9,10). At the entrance to the reactor, the biocatalyst beads were fluidized by the liquid, and in the middle section by both liquid and the CO_2 gas. The uppermost section was characterized by high gas hold-up. The reaction rates in the reactor were a strong function of the biocatalyst concentration. This concentration was reduced in the upper part of the reactor by larger gas hold-up and liquid dispersion. The bottom section had the highest biocatalyst concentration, and consequently had the highest productivity.

An example of the pH profile along the reactor is shown in Fig. 7. The pH gradually decreased from 5.5 at the reactor entrance to 4.0 at the exit. The production of ethanol also generated CO_2, some of which dissolved in the liquid and decreased the pH. Since the feed solutions were not buffered, the decrease of the liquid pH along the reactor was directly proportional to the quantities of CO_2 dissolved in it. In the bottom section of the reactor, where the rates of ethanol and CO_2 production were highest, the decreasing rate of pH also was fastest. For the same reason, the decreasing rate of pH in the middle section was faster than that in the top section. Although the pH dropped more than one unit in the reactor, at the exit, the pH still was within the range suitable for ethanol production by *Z. mobilis* (Doelle et al., 1993).

Figure 6. Ethanol volumetric productivity at different sections of the FBR using the glucose amylase-*Z. mobilis* biocatalyst.

Figure 7. pH profiles along the length of the FBR using the glucose amylase-*Z. mobilis* biocatalyst.

Fig. 8 illustrates the effects of starch mass loading and operation time on the reactor performance. The results showed that the ethanol volumetric productivity decreased with time. For example, the ethanol volumetric productivity obtained on day four, at a mass flow rate of 71.4 g/h, was 38.5 g/L-h; it dropped to 17.3 g/L-h on day 16, at a similar mass flow rate of 66 g/h. During the course of the experiments, no significant loss of the biocatalyst beads was observed. Therefore, the decrease of productivity could only be caused by lower activities of the beads. In all the experiments, glucose concentrations stayed very close to zero in the reactor. Therefore, under the conditions of decreasing volumetric productivity, starch hydrolysis was still the rate-limiting step. The decrease in the rate of starch hydrolysis with time was probably the result of cell growth. At the beginning of the experiment, the cell concentrations inside the beads were low, and starch molecules could easily diffuse to the active sites of the immobilized GA. When the cells grew, they covered some of the active sites of the enzyme inside the beads. They could also form an outer layer, which would then severely restrict the diffusion of starch molecules into the beads. It has been shown by mathematical modeling (Sun et al., 1997, 1998a, 1998b) that even without a surface layer of microbial cells, starch concentration decreased rapidly along the radial direction, toward the center of the beads. Near the surface of the beads, more starch was available, which resulted in higher glucose formation and more cell growth. Conversely, near the center of the beads starch concentration dropped to zero and no glucose was produced. The highest volumetric productivity of ethanol obtained was 38.5 g/L-h. Since 150 mL ground immobilized GA having a specific activity of 1.16 g glucose/mL-h, was used to prepare 1 L of biocatalyst beads, and 350 mL of beads was placed in the reactor, having a working volume of 0.6 1iter, the ethanol volumetric productivity that could be expected in the reactor would be 51.8 g/(Lh). This was calculated assuming a yield of 0.51 g ethanol/g glucose consumed, and assuming that the co-immobilization of the ground immobilized GA with *Z. mobilis* did not increase restriction to starch diffusion into the biocatalyst beads. The highest ethanol volumetric productivity obtained, therefore, was 74% of the calculated value. This highest volumetric productivity obtained was slightly lower than the productivity obtained for co-immobilized GA-*Z. mobilis* in sodium alginate in a packed-bed reactor, but significantly higher than the productivity obtained with the same system co-immobilized in κ-carrageenan (Kim et al., 1988). Fig. 9 is a contour plot of the starch mass feed rate, operation time, and ethanol volumetric productivity. It can be seen that the optimum mass feed rate was between 120 and 180 g/h.

Fig. 10 shows a plot of ethanol production versus starch consumption. The slope of the best-fit line gives an average yield of 0.49 g ethanol/g starch consumed. HPLC analysis of the substrate indicated that the starch used in these experiments contained greater than 95% maltotetraose. The theoretical yield would be 0.55 g ethanol/g starch consumed. The average yield obtained, therefore, was 89% of the theoretical value. This was slightly lower than the yield obtained in other studies using immobilized *Z. mobilis* with glucose as substrate in an FBR (96% of the theoretical value) (Davison and Scott, 1988).

Figure 8. The effect of starch mass feed rate and time of operation on ethanol productivity in the FBR using the glucose amylase-*Z. mobilis* biocatalyst.

Figure 9. The contour plot of productivity versus starch mass feed rate and time to determine the optimum mass feed rate of the FBR using the glucose amylase-*Z. mobilis* biocatalyst.

Figure 10. Determination of average ethanol yield by the glucose amylase-*Z. mobilis* biocatalyst in the FBR.

2.2 Ethanol production from dry-milled corn starch

In the previous studies, ethanol production from synthetic soluble starch (maltodextrin) solutions was studied in a simultaneous saccharification and fermentation (SSF) process using co-immobilized GA-*S. cerevisiae* and GA-*Z. mobilis*. The SSF process facilitates the use of a single reactor for both hydrolysis and fermentation, and also minimizes the contamination risk because of the presence of ethanol in the fermentation broth. However, a drawback of this process is that the operating conditions cannot be optimized for both steps simultaneously. The maximum temperature at which *Z. mobilis* can ferment efficiently in a continuous process is 35°C (Davison and Scott, 1988), which is well below the optimum temperature of glucoamylase at 55°C (Genencor Product Data Sheet); hence a SSF process will suffer from low enzyme activity. In fact, it has been observed that in such a process, the enzymatic hydrolysis was indeed the rate-limiting step (Lee et al., 1983; Kim et al., 1992).

In this investigation, the production of ethanol from dry-milled corn starch was first studied in a SSF process using co-immobilized GA-*Z. mobilis* biocatalyst beads in a FBR. Ethanol production by separate hydrolysis and fermentation (SHF) was then studied using immobilized glucoamylase in a packed-bed reactor and immobilized *Z. mobilis* biocatalyst beads in a FBR. The two process schemes are shown in Fig. 11.

Figure 11. Schematic diagrams of the simultaneous saccharification and fermentation (SSF) and separate hydrolysis and fermentation (SHF) processes.

Materials and methods

Microorganism

The *Z. mobilis* strain, its maintenance, and the production of the cell mass for use in the preparation of the co-immobilized GA-*Z. mobilis* biocatalyst were the same as described previously for the study on ethanol production from soluble starch.

Enzymes

The α-amylase used for starch liquefaction and dextrinization was supplied by Morris Ag-Energy, (Morris, MN). Glucoamylase immobilized on porous diatomaceous earth as a support was supplied by Genencor International (Elkhart, IN). The immobilized enzyme particle diameter was between 1.0 and 1.5 mm. The specific activity of the immobilized enzyme at 55°C and pH 4.2 is 881 units/g on a dry weight basis (Lantero et al., 1995). One unit of activity represents the amount of enzyme that will produce one micromole of glucose in one minute under the assay conditions.

Corn Starch Hydrolysis

Dry-milled corn starch was supplied by Morris Ag-Energy (Morris, MN). The moisture content of the corn starch was determined to be 13%. Liquefaction and hydrolysis of the corn starch were carried out at 95°C and pH 6.3-6.5 using 0.2% (v/w) α-amylase for 1.5 hours. Enzyme activity in the starch slurry was maintained by adding 150 ppm calcium ions in the form of $Ca(OH)_2$. The hydrolysis was carried out in 10-L batches in a 20-L steel container. Mixing was achieved by using a high-speed laboratory mixer equipped with a 3-in (7.6-cm) propeller (Cole Parmer Instrument Company, Vernon Hills, IL) at 700-1000 rpm. The starch hydrolysis was carried out until the slurry gave a starch negative test (no violet coloration) with iodine solution. Experiments were conducted with 15% and 28% solids. For an industrial dry-milled corn starch-to-ethanol process, a solids loading of ~28% is commonly used (Corn Starch Hydrolysis Standard Operating Procedure, Morris Ag Energy, Morris, MN). In preliminary experiments, it was observed that the solids in the 28% slurry could not move through the FBR. This prompted us to test the flow of a dilute slurry with 15% solids in the FBR. However, the solids caused plugging of the FBR after a few hours of continuous operation. Therefore, these solids were removed by centrifugation using a Sorvall centrifuge (DuPont Instruments, Newtown, CT) at 4000 rpm for 10 min. The wet solids cake was washed thoroughly with 1:1 (w/w) water and recentrifuged. The liquid recovered from this step was mixed with the liquid obtained from the first centrifugation step. This combined dextrins mixture was used as the substrate for the ethanol production experiments. It should be pointed out that a 1:1 (w/w) ratio of water to wet solids was used in the laboratory experiments to minimize feed dilution. Extraction experiments indicated that the dextrin recovery in this case was ~57% of the dextrins still trapped in the solid cake. In large-scale operation, a greater ratio of water to wet solids can be used to improve dextrin recovery. The dilute dextrin stream then obtained can be recycled to the starch liquefaction tank. This process scheme will minimize the loss of fermentable substrate associated with the removed solids.

Biocatalyst

Preparation of the co-immobilized GA-*Z. mobilis* biocatalyst beads followed the same procedure as described previously for the study on ethanol production from soluble starch.

The protein contents of the fresh and spent beads were measured as follows. Ten mililiters of beads was mixed vigorously in deionized water. A spatula was used to crush the beads and release the cells. The suspension was centrifuged at 4000 rpm for 5 min and the supernatant was discarded. Ten milliliters of 1.0N HCl was added to the pellet and thoroughly mixed. The

suspension was centrifuged again and the supernatant was discarded. Ten milliliters of solution (1.0N NaOH+0.47 wt % NaCl) was added to the pellet and mixed thoroughly in a test tube, which was then placed in a boiling water bath for 15 min to dissolve the proteins. The solution was cooled in water. The suspension was centrifuged, and the supernatant was assayed for protein using the Bio-Rad (Hercules, California) procedure, which determines protein by the Bradford method. Bovine serum albumin was used as the standard.

Fluidized-Bed Bioreactor (FBR)

The FBR, as shown in Fig. 11, was a jacketed glass column with 5.1 cm inside diameter and 47 cm in length. The volume of the FBR was 0.9 L. The FBR was cleaned with 50% ethanol and hot water before the biocatalyst beads were loaded. The volume occupied by the beads was 600 mL. The pH in the upper part of the FBR was controlled at 5.0 using 0.5 M NaOH. The base injection was placed very close to the pH probe in order to avoid pH overshoot. The temperature of the FBR was maintained at 35°C when the co-immobilized biocatalyst was used and at 30°C when only immobilized *Z. mobilis* was used.

Z. mobilis was allowed to grow within the beads for 4-5 days. When co-immobilized glucoamylase-*Z. mobilis* beads were used, this was accomplished by pumping feed solutions containing 150 g/L StarDri 100 starch (A. E. Staley Co., Decatur, Illinois), 0.05 M KCl and 5 g/L yeast extract (Red Star, Juneau, Wisconsin) through the FBR at residence times of 2-3 h. The pH of the feed was adjusted to 5.8 using phosphate buffer. The feed was sterilized by autoclaving at 121°C for 1 h. When immobilized *Z. mobilis* beads were used, the soluble starch in the feed was replaced by 150 g/L dextrose (Tate and Lyle, Decatur, IL).

Following colonization of the biocatalyst beads by the microorganism, feed solutions of maltodextrin with 5 g/L yeast extract or hydrolyzed corn starch (supplemented at times with 15% v/v light steep water) were pumped through the FBR to give residence times in the range of 1-4 h. All the feed solutions contained 0.05 M KCl for stabilization of the biocatalyst beads. The feed lines were changed when the empty feed reservoir was replaced. For each set of experimental conditions, at least six residence times were allowed for the FBR to reach steady state before samples were analyzed for dextrins, glucose, and ethanol.

Immobilized Glucoamylase Packed-Bed Reactor

The reactor was a jacketed glass column with a 2.54 cm inside diameter and 60 cm in length. The volume of the reactor was 0.3 L. Immobilized glucoamylase occupied 80% of the column volume. The column was operated in the upflow mode, and the temperature was maintained between 50 and 55°C. The pH of the feed was adjusted to 5 with phosphoric acid.

Analytical Methods

Dextrins, glucose, and ethanol were analyzed using a high performance liquid chromatography (HPLC) system consisting of a Waters 410 RI detector, a Waters 717 Plus Autosampler and an Alltech 425 HPLC pump. The column was an Aminex HPX-87H (BioRad Laboratories, Hercules, CA) column. The mobile phase was 5 mM H_2SO_4 pumped at a flow rate of 0.6 mL/min. Data acquisition and analysis were performed using the Waters Millennium software. The chromatograms of maltodextrin and hydrolyzed starch samples showed three

distinct peaks. These peaks were quantified using pure maltotetraose, maltotriose and maltose standards (Sigma Chemical Company, St. Louis, MO). Maltodextrin consisted of 91.9% (w/w) maltotetraose, 5.7% (w/w) maltotriose, and 2.4% (w/w) maltose. Maltotetraose was the predominant component of the hydrolyzed starch samples as well. The dextrin concentration was determined by adding the concentrations of all three components.

Results and discussion - Ethanol production from dry-milled corn starch

Activity of Co-immobilized Biocatalyst Beads

In the previous study with the co-immobilized glucoamylase-*Z. mobilis* biocatalyst, maximum ethanol productivity of 37 g/L-h was achieved. However, the productivity declined with time even when the same experimental conditions were maintained. This prompted us to investigate the activity of the biocatalyst over an extended time period. A repeated batch experiment was conducted using maltodextrin as the substrate prior to experiments in the FBR. Each batch cycle lasted 24 h. A total of 22 cycles were carried out. Samples were taken at periodic intervals to analyze for maltodextrin, glucose, and ethanol. The batch media consisted of 100 g/L maltodextrin, 25% (v/v) light steep water (nutrient source), and 0.05M KCl. The experiment was conducted in a 250 mL Erlenmeyer flask at 35°C, 100 rpm, and pH 5. The diameter of the beads was between 1 and 2 mm. The flask contained 20 mL of biocatalyst beads in 100 mL of medium. At the end of each cycle, the beads were recovered and washed with deionized water before being placed in fresh medium for the next batch cycle. The pH of the fermentation medium dropped from 5 to 4.3 (on an average) during each batch run. Maltodextrin conversions and ethanol concentrations at the end of each cycle were in the range of 80-95% and 37-48 g/L, respectively. Average ethanol yield obtained was 0.46 g ethanol/g maltodextrin (81% of the theoretical yield). Typical of batch processes, productivity of 3 g/L-h was obtained.

The cell loadings of the used beads (after 22 batch cycles) and fresh beads were determined by measuring their protein contents. The protein contents of the fresh and used beads were 0.35 g/L and 0.44 g/L, respectively. This 26% increase in protein contents indicated significant growth of *Z. mobilis* within the biocatalyst beads. For comparison of maltodextrin conversion, the cells in used and fresh beads were inactivated by treatment with 40% (w/v) ethanol. Under these conditions, the beads retained only the glucoamylase activity. Following inactivation of the immobilized *Z. mobilis*, the beads were tested for maltodextrin hydrolysis in batch experiments at 35°C and pH 5. The results of these experiments are shown in Fig. 12. Almost identical concentration profiles of maltodextrin and glucose were obtained with the fresh and used beads, indicating that the growth of *Z. mobilis* within the beads did not restrict the diffusion of the substrate into these beads. In addition, the data showed that the immobilized glucoamylase was stable and retained its activity over a period of 22 days at 35°C.

Figure 12. Comparison of soluble starch hydrolysis by fresh glucoamylase-*Z. mobilis* beads and spent (22 batch cycles) beads.

The biocatalyst beads were also tested in a batch experiment (one cycle) using the same medium as described previously, but at pH 4. The objective of this experiment was to determine whether it would be feasible to operate the FBR without pH control. The initial maltodextrin concentration was 91.4 g/L, and at the end of 23 h, an 80% maltodextrin conversion was obtained. However, only 0.8 g/L ethanol was produced and up to 76.7 g/L glucose accumulated in the medium. Although the *Z. mobilis* cells showed very little activity, they were not irreversibly deactivated. This was verified qualitatively by the evolution of CO_2 when these beads were washed and resuspended in the medium at pH 5. These results indicate that a decline in ethanol production in the continuous FBR will occur when a pH of 5 is not maintained.

Simultaneous Saccharification and Fermentation (SSF)

In these experiments, both synthetic maltodextrin solutions and dextrin solutions obtained by hydrolysis of dry-milled corn starch were used as feeds for the FBR. In the latter case, a 15% dry-milled corn starch feed was hydrolyzed to dextrins using α-amylase. After solids separation and washing of the wet cake, the solids-free feed was used in the FBR experiments. The results for synthetic maltodextrin and corn starch hydrolysate feeds are summarized in Table 1.

For synthetic maltodextrin, two feed concentrations of 108 g/L and 188 g/L were used. These feeds were representative of the dextrins concentration obtained by the hydrolysis of 15% and 28% dry-milled corn starch, respectively. Yeast extract (5 g/L) was provided as a nutrient source. For the 108 g/L feed, a single-pass conversion of 66.6% was achieved at a residence time of 2.2 h. However, for the 188 g/L feed, the single-pass conversion was 31.3% at a similar residence time (1.9 h). By increasing the residence time to 3.7 h, the maltodextrin conversion

improved to 53.1%. Volumetric ethanol productivity in the range of 12 to 15 g/L-h was obtained. Average ethanol yields of 0.47 g ethanol/g starch were obtained, corresponding to 84% of the theoretical yield (0.56 g ethanol/g starch).

For the starch hydrolysate feed, no additional nutrients were supplied. The single-pass conversions ranged from 54 to 89% and volumetric ethanol productivity was in the range of 9.1 to 15.1 g/L-h. Average ethanol yields were identical to those obtained with the synthetic maltodextrin feed.

Table 1. Simultaneous saccharification and fermentation (SSF) of maltodextrin and dextrins from dry-milled corn starch to ethanol using co-immobilized glucoamylase-*Z. mobilis* in the FBR.

Feed (g/L)	Dilution rate (h^{-1})	Conversion (%)	Ethanol (g/L)	Productivity (g/L-h)
		Synthetic maltodextrin		
108.7	0.46	66.6	32.1	14.8
188.1	0.54	31.3	28.0	15.1
188.1	0.27	53.1	45.3	12.2
		Dextrins in 15% starch hydrolyzate		
95.9	0.66	53.6	22.9	15.1
99.3	0.54	63.2	27.7	15.0
104	0.42	66.9	32.6	13.7
100.3	0.25	89.3*	36.44	9.1

* Glucose in the effluent during this run was 11.7 g/L due to failure of the pH controller. The pH dropped to 4.60 before it was readjusted to 5.0.

The above experiments with synthetic maltodextrin and starch hydrolysate feeds were performed continuously over a period of 22 days. During this time period, no structural failure of the biocatalyst was observed. In all the experimental runs, steady-state glucose concentrations in the effluent remained at low levels (below 4 g/L). It was also observed that the glucose concentration in the effluent increased in the absence of pH control (i.e., when the pH dropped below 5). The steady-state data shown in Table 1 indicates that the hydrolysis of soluble starch to glucose was the rate-limiting step. The glucoamylase used has the highest activity at a temperature range of 55-65°C (Genencor Product Data Sheet). The experiments were performed at 35°C to avoid thermal inactivation of the immobilized *Z. mobilis*. At this temperature, the enzyme activity was only 16% of the maximum activity (Genencor Product Data Sheet). In order to achieve higher conversion of the hydrolyzed starch to ethanol, longer residence times are needed. This can be accomplished by either increasing the column length or decreasing the feed flow rates. However, at high residence times the probability of contamination during continuous operation of the FBR will increase and channeling of the feed occur due to poor fluidization. A cascade arrangement of FBRs can also be used. Besides providing greater

residence time, this configuration can also help in the disengagement of the CO_2. This can lower the gas hold-up in the FBR, thereby improving mass transfer between the substrate in the liquid phase and the biocatalyst beads.

*Separate Hydrolysis and Fermentation (SHF***)**

By carrying out the dextrins hydrolysis and fermentation steps sequentially, it would be possible to perform both steps under more optimal conditions. Therefore, this process configuration was also investigated.

Solids-free solution of 150-160 g/L dextrins (obtained by hydrolysis of 28% dry-milled corn starch) at pH 5 was fed to the immobilized glucoamylase column at a rate of 0.3 L/h, thereby giving a residence time of 1 h. The temperature of the column was maintained at 55°C. The conversion of soluble starch to glucose was greater than 95% and gave a product stream of 162-172 g/L glucose. This glucose product stream from the immobilized enzyme column was used as the feed for the FBR containing immobilized *Z. mobilis* at 30°C. The pH of the feed to the FBR was adjusted to 5.8 using 50% (w/v) NaOH, and 0.05 M KCl was added for stabilization of the beads.

Table 2 summarizes the glucose feed concentrations (from the immobilized enzyme column) and the ethanol concentrations obtained at different dilution rates. The results are also plotted in Fig. 13. At a residence time of 2 h, a 94.2% single-pass conversion of the glucose feed and an effluent ethanol concentration of 70.3 g/L were achieved at steady state without adding any additional nutrients in the feed. At shorter residence times of 1.56 h and 1 h, the glucose conversion declined to 59.3% and 47.7%, respectively. Nutrient limitation was shown to be a possible explanation for this observation. Upon use of 15% (v/v) light steep water as an additional nutrient source, improvements in glucose feed conversion to 75.0 and 75.6% were achieved at residence times of 1.5 h and 0.9 h, respectively. These results showed that nutrient limitation effects could limit feed conversions at short residence times in the continuous FBR. An average ethanol yield of 0.45 g ethanol/g glucose was obtained in the above experiments.

Table 2. Fermentation of glucose obtained by enzymatic hydrolysis of dextrins from dry-milled corn starch to ethanol using immobilized *Z. mobilis* in the FBR.

Glucose (g/L)	Dilution rate (1/h)	Conversion (%)	Ethanol (g/L)	Productivity (g/L-h)
162.4	0.50	94.2	70.3	35.2
162.4	0.64	59.3	45.3	29.0
153.6*	0.66	75.0	48.6	32.1
172.1	1	47.7	32.6	32.6
162.9*	1.1	75.6	47.2	51.9

* In these runs, 15% (v/v) light steep water was added to the feed to provide an additional nutrient source.

Figure 13. Volumetric ethanol productivity and dry-milled cornstarch-derived glucose feed conversion as a function of dilution rate for the SHF process.

The performance of the immobilized *Z. mobilis* beads in the FBR was also investigated after switching to synthetic glucose feeds consisting of 165-172 g/L glucose and 5 g/L yeast extract as a nutrient source. The process performance at different residence times in the FBR is summarized in Table 3. The results are also plotted in Fig. 14. Single-pass glucose conversions ranged from 98.2% at a residence time of 2 h to 70.8% at a residence time of 0.9 h. These results were comparable with those obtained with the hydrolyzed dextrins feed supplemented with 15% (v/v) light steep water. The highest volumetric ethanol productivity achieved was 68.8 g/L-h at a residence time of 1h with 82.2% conversion of the synthetic glucose feed. An average ethanol yield of 0.43 g ethanol/g glucose was achieved in these experiments.

Table 3. Fermentation of synthetic glucose feed to ethanol using immobilized *Z. mobilis* in the FBR.

Synthetic glucose (g/L)	Dilution rate (1/h)	Conversion (%)	Ethanol (g/L)	Productivity (g/L-h)
167.9	1.1	70.8	48.4	53.2
166.5	1	82.2	68.8	68.8
165.5	0.73	90.4	63.6	46.4
167.9	0.68	90.7	63.6	43.3
172.3	0.67	91.4	64.8	43.4
165.5	0.56	94.1	67.3	37.7
165.5	0.54	93.6	65.8	35.5
167.9	0.51	98.2	64.9	33.1

Figure 14. Volumetric ethanol productivity and synthetic glucose feed conversion as a function of dilution rate for the SHF process.

To control the pH in the FBR, a dilute NaOH solution (0.5 M) was used to avoid overshoot. The use of this dilute solution caused some dilution effect in the effluent due to periodic injection of the base. Based on daily base consumption, it is estimated that the effluent was diluted between 5-10%. This might be the cause for the apparently low ethanol yield since lactic acid (<5 g/L) was the only other product detected in the effluent samples. It should also be noted that in some of these experimental runs, ethanol yields in the range of 0.47 to 0.49 g ethanol/g glucose (corresponding to 92%-97% of the theoretical yield) have been obtained. This is in agreement with the yields reported by others (Davison and Scott, 1988). The FBR with immobilized *Z. mobilis* beads was run continuously with synthetic glucose and hydrolyzed dextrins feeds over a period of 27 days without structural failure of the beads.

The overall volumetric ethanol productivity for the process was calculated by taking into account the residence time of the feed in the immobilized glucoamylase packed column and in the FBR. The overall productivities and ethanol concentration as a function of total residence time for the hydrolyzed starch feed is plotted in Fig. 15. At a total residence time of 3 h, a steady-state effluent ethanol concentration of 70.3 g/L was achieved at a feed conversion of 94.2%, resulting in an overall productivity of 23.4 g ethanol/L-hr. This is a substantial improvement over the volumetric ethanol productivity obtained in typical industrial batch processes (2-3 g/L-h). These results also showed that higher productivities and ethanol concentrations were achieved in the continuous SHF process in comparison with the continuous SSF process in the FBR.

Figure 15. Overall volumetric ethanol productivity and ethanol concentrations obtained from hydrolyzed cornstarch feed by the SHF process using immobilized glucose amylase and *Z. mobilis*. The results are plotted as a function of the total residence time.

Process design and economic analysis - Ethanol production from dry-milled corn starch

The experimental results discussed in the previous section clearly demonstrated the superiority of an SHF process over an SSF process for production of ethanol from dry-milled corn starch. In the continuous SSF process carried out at 35°C, the single-pass conversion of 100-g/L dextrin feeds ranged from 54 to 89% and volumetric ethanol productivities of 9–15 g/L-h were obtained. Hydrolysis of dextrins to glucose was found to be the rate-limiting step, owing primarily to the low activity of glucoamylase at 35°C. This limitation was overcome in the SHF process, in which the hydrolysis and fermentation steps were performed at their optimum temperatures of 55 and 30°C, respectively. Single-pass conversions of 150-g/L dextrin feeds ranged from 75 to 94%, and overall volumetric ethanol productivities of 19–25 g/L-h were obtained.

In this section, an economic analysis of ethanol production from dry-milled corn starch employing the FBR technology in an SHF process is discussed. This will be referred to as the FBR process. The economic analysis was performed for a 15-million gal/yr ethanol facility, which is a typical size for a dry-mill corn-to-ethanol plant. Laboratory-scale experimental results were used to generate process information for the Aspen Plus simulations. For both the conventional (or base-case) and the FBR technology, process flowsheets with material and energy balances were developed and cost analysis was carried out to obtain operating and capital cost estimates. The objective of the economic analysis was to compare operating and capital costs of the base-case and the FBR processes.

FBR process description

The FBR process, incorporating an immobilized glucoamylase-packed column for saccharification and a fluidized-bed bioreactor for fermentation, was evaluated in comparison with a base-case, state-of-the-art process for ethanol production. In both processes, dry-milled corn is used as the feedstock. A leading designer of dry-mill ethanol plants (Delta-T Corp., Williamsburg, VA) generously provided some of the details of the base-case process shown in Fig. 16. In this process, the corn is cooked with hot evaporator condensate and distillation bottoms. With this arrangement, the requirement for fresh make-up water is minimal. The conversion of starch to glucose is 95%. Continuous-cascade fermentors are used to ferment the saccharified corn mash to ethanol using yeast. The conversion of glucose is 100%, and the fermentation yield of ethanol is 95.4% of the theoretical maximum. The saccharified mash entering the fermentors contains 23 wt % corn (dry solids), and the stream passing from the fermentors to the distillation columns contains 94 g/L ethanol. Stillage from distillation is sent through centrifugation, evaporation, and drying steps to obtain Distillers' Dried Grains with Solubles (DDGS), a coproduct in the ethanol plant.

In the FBR process shown in Fig. 17, the saccharification tank is replaced by a packed column containing immobilized glucoamylase. Since coarse solids cannot be accommodated in the packed column, the mash is centrifuged before being fed to the saccharification reactor. A Mercone® screening centrifuge (Dorr-Oliver, Oak Brook, IL) is used for centrifugation of the mash and washing of the wet solids. Separation is based on particle size, with the centrifugal force providing for flow through the screen. For the fermentation, the continuous-cascade fermentors are replaced with FBRs containing *Z. mobilis* immobilized in κ-carageenan gel beads.

Figure 16. Base case dry-mill corn starch to ethanol process.

Figure 17. FBR ethanol process.

By using *Z. mobilis* for glucose conversion to ethanol, a higher ethanol yield (98% of theoretical) is expected compared with that of yeast (95% of theoretical) because of reduced substrate flux to cell mass production. The maximum ethanol concentration in the effluent from the FBR is 72.2 g/L, which is lower than in the base case. However, much higher volumetric ethanol productivity could be achieved in the FBR. In the economic analysis, three residence times in the FBR were examined: 20, 60, and 120 min. Although the 20-min residence time was not tested experimentally, it was included in the analysis so that the impact of the FBR residence time on the process economics could be fully realized. The sensitivity effects of ethanol concentration and yield were also investigated. Ethanol yields of 95.4%, which is equal to that of the base case process, and 98% of the theoretical were used in the simulations, with product ethanol concentrations of 70.3 and 72.2 g/L, respectively.

Z. mobilis has received GRAS (generally regarded as safe) status (Zhang et al., 1995) and has been cleared by the FDA for use as animal feed. Also it has been reported that DDGS with *Z. mobilis* showed 34% protein, which is higher than with yeast (H. Doelle, Microbiological Resources Center, Brisbane, Australia, 1997, personal communication). Another advantage of DDGS with *Z. mobilis* is that it has no glycerol, which is a precursor for cholesterol. In the FBR process, the used immobilized *Z. mobilis* beads from the reactor have cell loading of the order of 40 g/L of beads (Davison and Scott, 1988). This is significantly higher than the cell densities obtained in the base-case process. These gel beads can be blended with the DDGS and used as animal feed, thereby making the DDGS valuable in the FBR case as well.

Detailed cost analysis of each process was carried out using the Aspen Plus simulation developed for the dry-mill corn-to-ethanol process at the Eastern Regional Research Center of the United States Department of Agriculture. Cost quotations and process parameters for the Mercone® screening centrifuge were obtained from Dorr-Oliver and used in the Aspen Plus simulation. Factors and assumptions used to size and cost the equipment and to calculate the operating costs were the same for both processes. Total capital investment (depreciated evenly over 9 years) was estimated to be three times the total equipment purchase cost. The operating labor and total costs of corn were assumed to be the same for both processes.

a. Process information for saccharification used in the FBR model

Glucoamylase immobilized on porous diatomaceous earth (Genencor International, Elkhart, IN) was used for hydrolysis of starch to glucose. In the model, it was assumed that conversion of 140–160 g/L starch to glucose was complete at 50°C with a residence time of 30 min in a packed column. This result has been achieved in laboratory-scale experiments as well. The bulk density of the immobilized enzyme was 575 kg/m^3, and its volume was 80% that of the packed column. The cost per kilogram of the immobilized enzyme was assumed to be 20% greater than that of the commercially available soluble glucoamylase in order to account for the immobilization costs. Based on discussions with Genencor International, it was also assumed that the packed column was emptied and reloaded with fresh immobilized glucoamylase every 3 months.

b. Process information for fermentation used in the FBR model

Z. mobilis immobilized in κ-carageenan beads was used for fermentation of glucose to ethanol in the FBR. A 100% conversion of 150-g/L glucose feed to ethanol was used in the simulations at residence times of 20, 60 and 120 min in the FBR. Complete conversion of 150

g/L-glucose feed to ethanol has been achieved for residence times of 50 min or greater in laboratory-scale experiments (6). Experimental results also indicated that complete conversion could be achieved at a residence time of 20 min by using a biocatalyst with improved activity. Therefore, simulation of the case of a 20-min residence time was also performed in order to give a more complete understanding of the impact of residence time on the overall operating cost.

A bulk biocatalyst volume of 60% of the FBR volume and a void fraction of 0.3 were used. It was also assumed that fresh biocatalyst beads were loaded into the FBR every 3 months. Two fractions of the theoretical yield (0.51 g ethanol/g glucose) were used in the process simulation: 0.954 (low) and 0.98 (high). Corresponding to these yields, two ethanol concentrations - 70.3 g/L (low) and 72.2 g/L (high) - were used. An ethanol yield fraction and concentration of 0.954 and 94 g/L, respectively, were used in the base case process simulation.

c. *Centrifugation and cake washing*

Two C-600 Mercone® screening centrifuges (Dorr-Oliver, Oak Brook, IL) with a total capacity of 300 gal/min were used in the process simulation. The Mercone® is essentially a conical screen that rotates about a vertical axis and can perform separations more effectively than an ordinary screen because of the influence of high-gravity forces on the separating action. The corn mash enters the high-speed rotor through a feed inlet spout and is brought up to speed and distributed within the rotor by a set of vanes. In the rotor, the mass of slurry is thrown against the screen surface by the centrifugal force and the liquid, plus "fines", flows through the perforations in the screen and is collected in an effluent housing. Oversized solids are retained on the screen. The centrifugal force is sufficient to overcome the capillary action, which causes liquid and small solids to adhere to the surface of the larger particles; thus, a low moisture cake, is discharged. Helical blades within the rotor rotate at a different speed than the screen, and these conveyer flights regulate the passage of oversized material down the screen surface to the point where it is discharged. Cake washing is also performed within the Mercone® using the spray nozzles located on the helix. A wash water flow of 3 times the liquid content of the cake was used in the process simulation. A starch recovery of 99.5% was assumed. A cost quote of $480,000 for both units was obtained from the vendor.

Economic analysis results and discussion

Simulations for the FBR process were performed for the six cases shown in Table 4, and the results were compared with those for the base case process. As previously described, three different FBR residence times were evaluated, along with two levels of ethanol yield and concentration. Tables 5 and 6 show the capital and operating costs of different processing sections only for the base case and for FBR Cases 1 and 5, while the net savings or losses for all six cases are shown in Table 7. Total capital costs (Table 5) were estimated at 3 times the equipment purchase cost. Operating costs (Table 6) include depreciation of capital and related expenses such as maintenance, taxes, insurance and administration, as well as utilities and raw materials (excluding corn) for each section. The net operating cost (Table 7) includes the costs for corn (at $2.50/bushel) and operating labor, which are the same for all cases.

Table 4. FBR process cases used in the economic analysis

	Residence time in FBR (min)		
[EtOH], yield	20	60	120
72.2 g/l, 0.98	Case 5	Case 1	Case 3
70.3 g/l, 0.954	Case 6	Case 2	Case 4

The FBR process resulted in lower capital and operating costs in the fermentation section compared with the base case. For the 120-min residence time, four 51,440-L FBRs (three in operation and one on standby) replaced the four 912,500-L stirred tanks used in the base case process. For the 60-min residence time, the volume of each FBR was reduced to 25,720 L. For the 20-min residence time, the volume was further reduced to 12,860 L, with two in operation and one on standby.

The centrifugation section also had a lower cost contribution in the FBR process because of the use of the Mercone®, which is less expensive than a conventional centrifuge. The Mercone® cannot be used in the base case because the yeast present in whole stillage interferes with the sieving or filtration separation of spent grains. The cost contributions for the distillation and thin stillage evaporation sections were higher than in the base case process due to the lower ethanol concentrations achieved in the FBR process. However, it should be noted that advances in distillation technologies have allowed an economical recovery of dilute ethanol solutions with only a marginal increase in capital investment (Madson and Locco, 1999). Hence, with the advanced distillation technologies, the recovery costs for a 72.2-g/L feed ethanol concentration would be similar to those for a 94-g/L concentration. This would increase the capital and operating cost savings for the FBR process even further.

Table 5. Capital costs comparison for base case and FBR processes (Cases 1 and 5)

	Base Case $	FBR Case 1 $	FBR Case 5 $
Corn receiving, storage and milling	2,130,600	2,130,600	2,130,600
Liquefaction and saccharification	1,866,900	2,124,000	2,124,000
Fermentation	3,645,900	3,147,900	1,793,100
Distillation	2,805,000	3,128,400	3,128,400
Centrifugation	3,055,500	1,420,200	1,420,200
Thin stillage evaporation	4,068,300	5,418,600	5,418,600
DDGS drying	1,098,000	1,037,400	1,037,400
Product storage, denaturation and shipping	1,084,500	1,084,500	1,084,500
Wastewater treatment	1,104,000	1,104,300	1,104,300
Total capital costs	20,858,700	20,595,900	19,241,100

Table 6. Operating cost comparison of processing steps for base case process and FBR process (Cases 1 and 5)

	Base case (cents/gal)	FBR Case 1 (cents/gal)	FBR Case 5 (cents/gal)
Corn @ $2.50/bushel	91.19	89.15	89.15
Corn receiving, storage and milling	2.95	2.88	2.88
Liquefaction and saccharification	9.31	8.65	8.65
Fermentation	7.27	5.51	3.46
Distillation	10.44	12.37	12.37
Centrifugation	4.30	1.94	1.94
Thin stillage evaporation	5.92	7.93	7.93
DDGS drying	5.96	5.35	5.35
Product storage, denaturation and shipping	1.52	1.49	1.49
Wastewater treatment	1.60	1.56	1.56
Operating labor	13.81	13.51	13.51
DDGS revenue	(43.10)	(40.23)	(40.23)
TOTAL	111.17	110.11	108.06

Table 7 summarizes the net operating cost and savings (or loss) for each case relative to the base case. For Case 1 (60-min residence time, 0.98 fraction of theoretical yield, 72.2-g/L ethanol), the cost savings are 1.06 cents/gal, or 1% over the base case. These savings drop to 0.19 cents/gal or 0.2% for Case 2, in which the FBR residence time is maintained at 60 min but the ethanol concentration and fractional ethanol yield drop to 70.3 g/L and 0.954, respectively. This finding indicates that the ethanol concentration and yield are sensitive parameters and contribute significantly to the overall cost savings. For Case 3 (120-min residence time, 0.98 fraction of theoretical yield, 72.2 g/L ethanol), the cost of producing ethanol by the FBR process would actually be higher than in the base case by 1.23 cents/gal, or 1.1%. At a fractional ethanol yield of 0.954 and ethanol concentration of 70.3 g/L (Case 4), the ethanol cost with the FBR process is 2.17 cents/gal or 2% higher than in the base case process. Previous experimental results indicated that complete conversion of glucose to ethanol at a residence time of 20 min in the FBR could be achieved by improvements in biocatalyst activity. This scenario was also evaluated in the simulations by taking Case 5 into consideration (20-min residence time, 0.98 fraction of theoretical yield, 72.2-g/L ethanol). As seen from Table 4, the potential cost savings in this case would be 3.12 cents/gal or 2.8% over the base case. For a fractional ethanol yield of 0.954 and ethanol concentration of 70.3 g/L (Case 6), the potential cost savings are 2.24 cents/gal or 2% over the base case. Because this analysis uses specific assumptions to compare technologies, the comparative benefit is emphasized, not the absolute value, which varies greatly with the assumptions. It is estimated that the overall error in the comparison of costs between cases is ± 1 cent/gal.

T7

This analysis shows that in the most realistic case (i.e., Case 1), an operating cost savings of 1.06 cents/gal can be realized over the base-case process. These operating cost savings are very sensitive to the residence time in the bioreactor or, in other words, to the size of the bioreactor. The other sensitive parameters are ethanol concentration and ethanol yield. This analysis also shows that lowering the residence time in the FBR to 20 min (by improvements in biocatalyst activity) would allow a higher cost savings of 3.12 cents/gal. These results indicate that operating and capital cost savings can be realized by using this technology in a new plant producing ethanol from starch.

2.3 Mathematical model for ethanol production from starch in FBR

To be able to design bioreactors, predictive mathematical models based on fundamental principles and accepted correlations that describe the important physical phenomena must be developed and verified. These models must be generic in nature such that they can be easily applied to a diverse set of applications and operating conditions. A mathematical model for ethanol production from glucose in the FBR has been derived (Petersen and Davison, 1995). The predictions of this model were verified by experimental results (Davison and Scott, 1988; Webb and Davison, 1996). The situation becomes much more complex when starch is used as a substrate in the FBR. In this part of the study we derived a mathematical model which included two consecutive reactions carried out by the immobilized biocatalyst, namely, the hydrolysis of starch and the fermentation of the released glucose to ethanol. In order to explicitly describe the model for a starch-to-ethanol process in an FBR, several main aspects must be addressed. Fig. 18 shows the mechanism inside the reactor. There are two key parts of the model: bicatalyst and reactor. The biocatalyst model includes fermentation kinetics of the immobilized *Z. mobilis*, saccharification kinetics of glucoamylase, and transport phenomena of the reactants and products by diffusion within the biocatalyst beads. In the FBR model, the dispersion coefficient and the fraction of the bed's cross section that is occupied by the gas, liquid, and solid phases is a function of the CO_2 produced and the liquid feed flow rates through that portion of the bed. All these factors affected the species concentration at each axial point in the bed and therefore must be addressed. (Sun et al., 1997, 1998ab)

2.3.1 Fermentation kinetics of immobilized Z. mobilis

The first assumption concerning *Z. mobilis* kinetics is that the immobilized cell employs the same mechanisms as the free cell. Therefore, the kinetic equations developed for free cells can also be used to describe the immobilized *Z. mobilis* reaction. Models have been developed and evaluated for ethanol production by *Z. mobilis* (Aiba et al., 1973; Rogers et al., 1978). The models were based on the assumption that the predominating factors influencing the kinetics of *Z. mobilis* are substrate limitation, product inhibition and substrate inhibition at high substrate levels. Lee and Rogers (1983) modified the basic equation to be consistent with the observed *Z. mobilis* kinetic behavior.

Figure 18. The mechanisms inside the reactor.

2.3.2 Hydrolysis kinetics of immobilized glucoamylase

Several kinetic studies of the enzyinatic hydrolysis of starch by glucoamylase have been carried out. The simplest equation to express the reaction kinetics of glucoamylase is the classical Michaelis-Menten kinetic model. Hamdane et al. (1988) used the differential gradientless reactor to determine the kinetic parameters for glucoamylase immobilized on crushed corn stover having average particle size of 200 μm. The substrate used was a soluble starch. Compared to other systems used to evaluate glucoamylase kinetic parameters (Miranda, 1991; Fujii, 1985), Hamdane's system was neares the conditions used in our investigation. Therefore, Hamdane's kinetic parameters were used in our model.

2.3.3 Mathematical model of the biocatalyst bead

Within a biocatalyst bead the substrate and products are transported by molecular difflision. In addition, it is here that the biocatalyst actually converts the substrates to products. Thus, the

reactions that produce the desired products are not dependent on the bulk fluid concentrations, but rather on the local conditions within the biocatalyst bead. The theory of combined reaction and diffusion has been well developed by academic and industrial researchers.

In this investigation, starch pore diffusion affects the ethanol production rate. Starch is converted to glucose by glucoamylase in the biocatalyst beads. Glucose then serves as substrate for the microorganism. It is assumed that the microorganism is distributed uniformly in the beads and the microorganism can obtain the glucose immediately after it is produced inside the bead. The effectiveness factor is usually employed to account for the effect of diffusion on the reaction rate. Most effectiveness factor calculations are about the single immobilization in which only one step reaction is involved. In order to calculate the actual reaction rate of glucoamylase and *Z. mobilis* in the co-immobilized biocatalyst, the two effectiveness factors relating these two reactions must be calculated. Fig. 19 shows the reactions inside the co-immobilized GA-*Z. mobilis* biocatalyst.

Figure 19. The reactions and mechanism inside the co-immobilized GA-*Z. mobilis* biocatalyst.

The following assumptions were made to predict the effective glucoamylase and *Z. mobilis* activity of the co-immobilized biocatalyst:

1. Negligible resistance of external diffusion
2. Steady state

3. Spherically shaped biocatalyst beads of uniform size
4. Homogeneous distribution of enzyme and microorganism inside the biocatalyst
5. Constant diffusion coefficient throughout the biocatalyst bead

The first effectiveness factor ς_1 of glucoamylase is defined as the ratio of the actual starch consumption rate of the enzyme within the biocatalyst bead to the consumption rate of starch if the enzyme were exposed to the exterior bulk concentration. The second effectiveness factor ς_2 is similarly defined for the immobilized microorganism. The calculation of the effectiveness factor ς_2 for the conversion of glucose to ethanol by the microorganism is more complicated than the calculation of ς_1. In order to calculate the effectiveness factor ς_2, a conservation of glucose for the whole bead is needed. Fig. 20 shows the two possible mass flow situations. The diffusion direction of glucose totally depends on the glucose concentration gradient in the particle near its outer surface. The glucose inside the bead could diffuse out or the bulk glucose could diffuse into the beads, depending on the glucose concentration inside the catalyst and the glucose concentration in the bulk solution. Both of these situations are considered in the model.

Figure 20. Mass flow and two effectiveness factors of the co-immobilized biocatalyst bead.

2.3.4 Modeling of the FBR

A rectangular coordinate system was first chosen to set up the equations for the cylindrical fluidized bed reactor because these coordinates are much easier to visualize. Then the rectangular coordinates are switched to cylindrical coordinates. The mathematical model developed for process simulation starts with the law of conservation of mass for starch (S) in a stationary volume element Ax Ay Az (Fig.21) through which the fluid is flowing. The system is assumed to be isothermal.

Figure 21. Stationary volume element ÄxÄyÄz through which fluid is moving.

Time rate of change of mass S in the volume element	=	Rate of mass of S in	-	Rate of mass of S out	-	Rate of production of S by chemical reaction

The mass balance equations can be written for the three faces of the element. The rectangular coordinates then are converted to cylindrical coordinates using the derivative operators (Bird et al., 1960). Based on the initial mathematical structure, different assumptions for different systems could be made. For the fluidized bed reactor system in this work, the following assumptions are valid:

1. Steady state
2. No radial dispersion
3. Uniform distribution of substrate, product, and biocatalyst at cross-sectional area
4. The volumetric flow rate is constant along the reactor.

There are two possible boundary conditions for this system: (1) the plug flow boundary condition (simplified boundary condition) assumes that the starch flows in a plug flow fashion at the inlet of the reactor (z = 0); (2) the Danckwerts boundary condition expresses the fact that the rate at which starch is fed to the reactor is equal to the rate at which it crosses plane z = 0 by

combined flow and dispersion (Danclcwerts, 1953). Solving of the Danckwerts boundary condition needs much more numerical effort than plug flow boundary condition. Therefore, if the difference of the results with respect to these two different boundary conditions is not significant, the plug flow boundary condition will be used in the model calculation. The comparison of these two boundary conditions will be addressed in the next section.

The axial dispersion coefficient of three-phase fluidized beds has been studied in detail by Kim and Han (1992). Their results are used to calculate the axial dispersion coefficient for our FBR. The same procedure is used to obtain the equations for glucose.

The vast majority of the $C0_2$ produced from fermentation will move into the gas phase and produce bubbles. These bubbles will then occupy some of the reactor volume, reducing the amount of volume that is available for the biocatalyst. Several researchers have shown that the solid holdup is a function of both the gas and liquid superficial velocities within a fluidized bed. Thus, as $C0_2$ is produced and the gas velocity increases, not only the gas but also the solid holdup will be affected. To predict the gas, liquid, and solid holdup, the widely accepted correlation of Begovich and Watson (1978) is used. Previously, Davison (1990) measured the various phase holdup within fluidized-bed bioreactors similar to the system used in this study. Based upon the 39 hydrodynamic experiments reported by Davison, the parameters of the Begovich and Watson correlation low density catalyst beads are calculated. A complete set of the equations used in the mathematical model can be found in a thesis (Sun et al, 1997, 1998; Sun, 1998).

2.3.5 Results of the mathematical model

The results of the mathematical model for the FBR with co-immobilized biocatalyst will be compared with the experimental data. The general applications of the model will also be addressed. Base case analysis represents the results of the model under the experimental conditions. The general case analysis discusses the generic and predictive applications of the model under different conditions.

Performance of the co-immobilized biocatalyst

Mathematical model equations for the biocatalyst bead are solved numerically and the starch concentration profile inside the bead is generated using the solution of the differential equations. Fig. 22 represents the starch concentration inside the bead along the radial distance from the center of the bead at the different bulk starch concentrations. It can be seen that the higher the bulk starch concentration, the more starch diffuses into the beads. When the bulk starch concentration is above 100 g/L, starch penetrates throughout the bead. At this condition, the catalyst is fully utilized. With the bulk starch concentration below 100 g/L, starch only diffuses into part of the bead volume. For example, at 45 g/L bulk starch concentration only 85% of the bead volume is used for reaction. While the bulk concentration is reduced, the used bead volume is reduced as well. At very low bulk starch concentrations such as below 0.5 g/L, starch only diffuses in the very thin ring of the bead and only a very small portion of each bead is used for reaction. In the fluidized bed reactor, the bulk starch concentration varies with the different axial positions. The catalyst can be used more efficiently at higher bulk substrate concentrations. In the FBR the starch concentration decreases along the axial position (this will be discussed in more detail in a later section). Therefore, the biocatalyst beads located at the lower position of

the reactor are used more efficiently than the beads at the higher position of the reactor. This explains the phenomenon observed during the experiments: the beads at the bottom always appeared different from those at the top. At the bottom of the reactor, the starch concentration was higher and more starch diffuses into the beads. As a result, for the consecutive reactions, more glucose could be produced and there was more glucose available for growth of the microorganism and the production of products. These two processes make the beads at the bottom of the reactor look different from those at the top. Generally they had a lighter color and produced more ethanol. Consequently, ethanol productivity of the bottom section of the reactor was higher than other sections. This further explains the experimental data discussed earlier. The experimental data showed that the volumetric productivity decreased from the bottom to the top of the reactor.

Figure 22. Starch concentration profile inside the bead along the radial distance from the center of the bead at the different bulk starch concentrations.

Performance of the FBR

The boundary conditions of the differential equations for the FBR will be considered first. Relative to the plug flow boundary condition, the Danckwerts boundary condition equation needs much more numerical effort to be solved. The necessity of the Danckwerts boundary condition for this system was tested under different conditions. Results using the plug flow

boundary condition and Danckwerts boundary condition are compared in Figs. 23 and 24 under various conditions. In Fig. 23, the flow rate is 0.6 L/h, the enzyme loading is 150 ml, and the catalyst bead diameter is 0.2 mm. In Fig. 24, the flow rate is 2 L/hr, the enzyme loading is 375 ml, and the catalyst bead diameter is 0.4 mm. Numerical results from the model show no difference between two different boundary conditions; however, using the plug flow boundary condition reduces the numerical effort and calculation time. Therefore, in order to reduce the complexity of the calculation, the plug flow boundary condition can be used without introducing error.

Figure 23. The comparison of the mathematical model results solved using the plug flow boundary condition (simple) and the Danckwerts boundary condition (flow rate 0.6 L/hr, enzyme loading = 150 ml, and catalyst bead diameter = 0.2 mm).

The concentration profiles along the reactor axis will be considered next. The concentration profiles generated under different operation conditions are compared with the experimental data. The predicted concentrations of starch, glucose, and ethanol are presented in Figs. 25 and 26. These two experiments were conducted under different flow rate and feed concentration. In general, the model predictions compared favorably with the experimental data. The model results show the correct concentration profile trends and behaviors such as decreasing starch concentration, increasing ethanol concentration, and very low glucose concentration along the axial position of the reactor. The model results predict more conversion than actually occurred. The difference observed between the model predictions and the experimentally determined profiles may be due to a variety of factors. For example, some errors may be due to experimental uncertainty, such as uncertainty in the density of the beads, and in the amount of enzyme immobilized within each bead. The beads at the top of the reactor were generally less dense than the beads at the bottom of the reactor. This probably was caused by reduction in enzyme particle

loading. Reduction of enzyme caused less starch conversion and less ethanol production. Therefore, there are greater differences between the model results and experimental data at the top of the reactor. Additional errors may be due to the mathematical model assumptions such as the one that assumes all the beads are uniform geometrically and characteristically, or that each bead has the same enzyme loading and the same composition.

Figure 24. The comparison of the mathematical model results solved using the plug flow boundary condition (simple) and the Danckwerts boundary condition (flow rate 2 L/hr, enzyme loading = 375 ml, and catalyst bead diameter = 0.4 mm).

Figure 25. The starch concentration profile comparison between the model results and the experimental data (experimental condition: flow rate = 0.6 L/hr, feed concentration = 110 g/L).

Figure 26. The starch concentration profile comparison between the model results and the experimental data (experimental condition: flow rate = 2 L/hr, feed concentration = 95 g/L).

Once the model has been verified by experimental data it can be used to predict the performance of the system. These predicted results give a better understanding of the system and are great tools to optimize it. Some examples are discussed in this report.

The first example is the prediction of the biocatalyst performance. Fig. 27 represents the starch concentration profile in the catalyst at different bulk starch concentrations. A 2 mm bead with an enzyme loading of 375 mL is used. The maximum dimensionless bulk concentration, S_b = 1, corresponds to 225 g/L of starch. Higher bulk starch concentrations result in higher diffusion rates into the beads. As a result, a greater concentration of the intermediate (glucose) occurs, which is then available as a substrate for the microorganism. Fig. 28 shows glucose concentration profiles corresponding to the starch concentrations in Fig. 27. It can be seen that higher bulk starch concentrations causes higher glucose concentration in the bead. Fig. 27 shows that starch only partially diffuses into the bead. Even at the highest starch concentration, starch can only be observed at a radial distance of 0.65. This indicates that only 72% of the catalyst volume is used. Besides the bulk concentration influence, starch diffusivity has a significant impact on the concentration profile. Fig. 29 shows starch and glucose concentrations inside the beads at different starch diffusion coefficients. High starch diffusivity increases the starch concentration inside the bead and increases the usable volume of the biocatalyst. At the high starch diffusion coefficient (Ds = 0.008 cm^2/hr), starch diffuses into the bead as far as r = 0.4. This means that about 93.6% of the catalyst volume is used. In this case, glucose can penetrate all the way to the center of the bead and this will increase the catalyst efficiency.

Figure 27. The starch concentration profile in the catalyst bead at different bulk starch concentrations.

Figure 28. Glucose concentration profiles corresponding to the different starch bulk concentrations. Glucose concentration G1 corresponds to bulk starch.

Figure 29. Starch and glucose concentration profiles at the different starch diffusivities. Bead radius = 2mm, starch bulk concentration Sb = 1.0, glucose bulk concentration = 0.0, starch S11, glucose G11 (Ds = 0.002 cm^2/hr); S12, G12 (Ds = 0.004 cm^2/hr); S13, G13 (Ds = 0.008 cm^2/hr).

Another issue concerning the biocatalyst efficiency is the bead size. In cases where a low starch diffusion coefficient occurs, reducing the size of the bead could save immobilization carrier material and enzyme. Fig. 30 shows different concentration profiles at different bead radii. It can be seen that for a small bead (r = 1 mm), starch can penetrate to the center of the bead. In this situation, the catalyst bead is used completely. However, for a large bead (r = 2 mm), starch can only reach 72% of the bead volume and glucose concentration becomes zero at a dimensionless radial distance of 0.65, therefore, large beads are not used efficiently.

The second example is the prediction of the FBR performance. Enzyme loading influences the activity of the catalyst, which affects the overall performance of the reactor. Figure 31 shows that the starch concentration in the effluent of the reactor with higher enzyme loading is lower than the one with lower enzyme loading. Obviously, starch consumption will be higher in the reactor with higher enzyme loading. Consequently, more ethanol is produced. In the actual experimental process, the enzyme loading is limited by the bead making process. There is a difficulty for making beads when there is too much enzyme in the gel solution. High concentrations of the immobilized enzyme in the gel solution can block the outlet nozzle due to high solid contents and high viscosity.

Figure 30. Starch and glucose concentration profiles for different sizes of catalyst bead. S0.1 is starch concentration, G0.1 is glucose concentration at r = 0.1 cm; S0.15; G0.15 (r = 0.15 cm); S0.2; G0.2 (r = 0.2 cm).

Figure 31. The comparison of concentration profiles in the reactor with different catalyst enzyme loading.

As discussed previously, the size of the catalyst affects its efficiency. Fig. 32 shows the concentration profiles inside the reactor with different sizes of bead. For the same total volume of the catalyst, which is loaded in the reactor, the smaller catalyst performs better. For the smaller catalyst bead, a larger portion of each bead is used. This in turn allows a larger portion of the total volume of the catalyst bed to be used. Therefore, more starch is consumed with a smaller size catalyst and a higher concentration of ethanol is obtained at the outlet of the reactor. However, this does not mean that the beads should be made as small as possible. The size of the catalyst bead should be decided with the consideration of the other experimental conditions. For example, industrial feed solutions may contain solids. In this situation, beads that are too small may be washed out and it will be difficult to separate the catalyst from the effluent by using simple sieving method.

Figure 32. The comparison of concentration profiles in the reactor with different catalyst enzyme loading.

The performance of the reactor is also affected by the operating conditions. Fig. 33 shows the concentration profiles in the reactor under different feed flow rates. For the same feed concentration, a higher flow rate causes less starch consumption, mainly because the high flow rate corresponds to the short residence time. The starch in the feed does not have enough time to be converted before it flows through the reactor. However, a higher flow rate introduces better fluidization, better external mass transfer, and also high productivity. One way to overcome this problem is to build a closed loop system. In such system the effluent from the reactor is pumped back into the reactor forming a closed loop. This operation can be continued until the starch conversion rate reaches the desired level. A longer column can be another way to reduce the starch concentration of the effluent. However, these two reactor configurations have the same disadvantage, which is $C0_2$ build up in the reactor. To overcome this problem, staged columns can be an alternative. A gas disengaging system can be built between each columns. The inlet $C0_2$ of the next column will be reduced.

Figure 33. The influence of the feed flow rate on the concentration profiles in the reactor.

3. Ethanol production from lignocellulosic sugars

Lignocellulosic biomass is a low-cost renewable resource that can be used to meet the projected increase in fuel ethanol demand. These feedstocks are comprised of cellulose, hemicellulose and lignin. Lignocellulosic hydrolysates produced either chemically or enzymatically contain both pentoses and hexoses. Glucose derived from cellulose is the major hexose sugar while the pentoses derived from hemicellulose are comprised of xylose and arabinose. While glucose can be fermented to ethanol by a number of microorganisms, the conversion of xylose and arabinose to ethanol is more difficult. Since pentoses, which are predominantly comprised of xylose, can account for 8-28% of the raw material (Ladish et al., 1983), their efficient conversion to ethanol is necessary for an economical process. Advances in metabolic engineering have led to the construction of several xylose-fermenting microorganisms. These include recombinant bacterial strains of *Escherichia coli* (Burchardt and Ingram, 1992), *Zymomonas mobilis* (Zhang et al., 1995) and a recombinant *Saccharomyces* yeast (Ho et al., 1998). The genes required for xylose metabolism in the recombinant strains of *Z. mobilis* and *Saccharomyces* were placed either on a plasmid or integrated into the chromosome of the hosts. The genes required for enhanced ethanol production in *E. coli* were incorporated into the chromosome of the host. We investigated ethanol production by both plasmid-based and chromosomally integrated strains in the continuous FBR.

3.1 Materials and methods

3.1.1 Microorganisms

The plasmid-based strains included *Z. mobilis* CP4(pZB5) and *Z. mobilis* 31821(pZB5). The chromosomally integrated strains included *Z. mobilis* C25, *Saccharomyces* 424A(LNH-ST), and *E. coli* KO11. The three *Z. mobilis* strains were obtained from NREL. The *Saccharomyces* strain was obtained from Dr. Nancy Ho at Purdue University and the *E. coli* strain was obtained from Dr. Lonnie Ingram at the University of Florida. The stock cultures were maintained in 25% glycerol at -70°C. The procedures used for production of the cell mass and preparation of the immobilized biocatalyst were the same as described previously.

3.1.2 Fluidized-bed bioreactor (FBR)

The FBR was the same as the one used in the investigation of ethanol production from dry-milled corn starch (described previously).

Feed solutions included synthetic solutions of glucose and xylose mixtures at various concentrations and the actual rice straw hydrolysate obtained from Arkenol. This hydrolysate was produced by the Arkenol's patented concentrated acid hydrolysis process. The synthetic sugar solutions were prepared when needed. The hydrolysate was kept refrigerated until use. All the feed solutions contained 10 g/L yeast extract, 2 g/L KH_2PO_4, and 3.7 g/L KCl for biocatalyst stabilization. Most of the feed solutions used for the investigation of the plasmid-based strains contained 10 mg/L tetracycline for plasmid maintenance. In some of the feed solutions the antibiotic was omitted to investigate the stability of the plasmid with time. Tetracycline was not added to the feed solutions used for the chromosomally integrated strains.

3.2 Results and discussion

3.2.1 Plasmid-based strains

Stability of the immobilized biocatalyst was tested first in batch experiments then in the FBR. In the first set of experiments, the use of the immobilized cell beads of strain *Z. mobilis* CP4(pZB5) in serial batch culture was evaluated. The batch fermentation media consisted of 35 g/L glucose and 40 g/L xylose. After 48 hours of fermentation, the beads were washed with 0.05 M KCl and transferred to fresh media. This was done for 4 cycles. The results are tabulated in Table 8.

Table 8. Results of repeated batch experiments performed with immobilized *Z. mobilis* CP4(pZB5) biocatalyst

Cycle #	Glucose(g/l)	Xylose (g/L)	Residual xylose (g/L)	Ethanol(g/L)	Time (hours)	Yield (g/g)
1	33.6	43.9	9.6	31.8	48	0.47
2	29.3	37.9	15	26.0	48	0.46
3	36.8	43.7	15.3	27.1	48	0.42
4	33.6	39.7	25.8	21.3	72	0.45

In all of these experiments, glucose was rapidly and completely consumed. On the other hand, xylose utilization was slower and incomplete. With each batch cycle, there was a slow increase in the residual xylose concentration whereas glucose consumption rates were unchanged. This clearly indicated a gradual loss of xylose metabolism capability in the immobilized cells.

The biocatalyst beads of strain *Z. mobilis* CP4(pZB5) then were tested in the FBR. A solution containing 50 g/L glucose and 13 g/L xylose was fed continuously through the FBR at residence times between 2 to 4 hours. The results are summarized in Table 9. At a dilution rate of 0.24 h^{-1}, an average steady state ethanol concentration of 26.9 g/L was obtained at a yield of 0.44 g ethanol/g sugars (or 86% of theoretical yield). Glucose and xylose conversions were 99.8% and 91.5%, respectively. At a dilution rate of 0.36 h^{-1}, glucose conversion was maintained at 99% while xylose conversion dropped to 79.4%. Ethanol concentration achieved in this case was 26.3 g/L at 88% of theoretical yield. At a higher dilution rate of 0.49 h^{-1}, glucose conversion was essentially complete at 98.4% and xylose conversion was 81%. The ethanol concentration dropped slightly to 25.4 g/L at 86% of theoretical yield. Thus, maximum utilization of xylose occurred at the lowest dilution rate of 0.24 h^{-1}. After 11 days of continuous operation, the dilution rate of 0.24 h^{-1} was repeated. The steady state effluent xylose concentration was 2.72 g/L as compared to 1.1 g/L achieved in the early stages of the experiment. Thus, the xylose conversion dropped from 91.5% to 78.4%. However, the glucose conversion was maintained at 99.8%. This result indicated that there was activity loss toward xylose fermentation after day 11.

Table 9. Steady state results of FBR experiments performed with immobilized *Z. mobilis* CP4(pZB5) biocatalyst

Feed Glucose (g/L)	Feed Xylose (g/L)	Dilution Rate (1/h)	Effluent Glucose (g/L)	Effluent Xylose (g/L)	Effluent Ethanol (g/L)	Glucose Conversion (%)	Xylose Conversion (%)	Ethanol Yield (g/g)
49.9	12.9	0.24	0.11	1.1	26.6	99.8	91.5	0.43
49.1	12.6	0.36	0.59	2.5	25.9	98.8	80.2	0.44
49.1	12.6	0.49	0.8	2.4	25.3	98.4	80.9	0.43

The next set of experiments was performed to test the immobilized cell biocatalyst of strain *Z. mobilis* 31821(pZB5).

The repeated batch experiments were started by placing 25 mL of beads in 60 mL fermentation media. Two sets of sugar concentrations were used: 30 g/L glucose, 30 g/L xylose, and 15 g/L glucose, 15 g/L xylose. Each batch experiment was run for 24 hours, then the beads were recovered, washed with buffer, and transferred to fresh fermentation medium to begin the next batch cycle. This series of experiments was continued over a 30-day period (30 cycles). Samples were taken at the start and end of each cycle. The fermentation results from representative experiments are summarized in Table 10.

Table 10. Results of fermentation of glucose-xylose mixture to ethanol during repeated batch experiments.

Batch #	Time (h)	Sugars	Glucose (g/L)	Xylose (g/L)	Ethanol (g/L)	Yield (g/g)
1	0	High	27.9	34.4	0	
	25.5		0	1.2	29.2	0.48
	0	Low	15.2	17.0	0	
	24.5		0	0.1	14.5	0.46
10	0	High	26.4	28.1	6.8	
	23		0	1.2	32.2	0.48
	0	Low	14.6	14.6	4.3	
	23		0	0.4	17.0	0.44
30	0	High	31.7	33.3	7.7	
	21		0	1.1	37.1	0.46
	0	Low	15.2	16.1	3.5	
	23		0	0.2	18.7	0.49

In both sets of experiments, the xylose fermentation performance was maintained over a 30-day period. This was a significant improvement over the earlier strain. In other words, strain *Z. mobilis* 31821(pZB5) showed a much greater stability toward xylose metabolism and was a strong candidate for long term tests in the FBR.

In order to determine accurately the stability of xylose metabolism, a continuous FBR experiment was performed with a feed solution containing 40 g/L glucose and 20 g/L xylose. A dilution rate of 0.25 h^{-1} was maintained throughout the course of this experiment. The concentration profiles of glucose, xylose and ethanol are shown in Fig. 34. It can be seen that the effluent xylose concentration started to increase sharply after day 19, thereby indicating a decline in the xylose fermentation performance. On the other hand, glucose concentration remained below 1 g/L throughout the experiment. Although the results obtained showed a loss of xylose conversion activity, they actually indicated a significant improvement of this strain over the other strain. The results obtained with the original strain showed that loss of xylose

conversion activity started at about ten days of reactor operation. The loss of xylose conversion capability with time was not likely caused by plasmid instability since the feed solution contained tetracycline, which allowed selection for survival of only plasmid-bearing cells. It could be due to a combination of two events, which were damage of the genes and deactivation of the enzymes of the xylose-converting pathway in non-growing cells.

Figure 34. Determination of stability of strain Z. mobilis 31821 (pZB5) in continuous FBR operation.

Experiments then were conducted to study the performance of strain *Z. mobilis* 31821(pZB5) in the FBR. Two feed solutions were used. The first solution contained 40 g/L glucose and 20 g/L xylose and the second one contained 50 g/L glucose and 10 g/L xylose. Three dilution rates of 0.25, 0.34, and 0.5 h^{-1} were studied. The steady state results are summarized in Table 11. As expected, highest conversion of both sugars was obtained at the lowest dilution rate. At this dilution rate, complete conversion of glucose and greater than 80% conversion of xylose were obtained.

Table 11. Steady state results of FBR experiments with immobilized *Z. mobilis* 31821(pZB5)

Feed Glucose (g/L)	Feed Xylose (g/L)	Dilution Rate (1/h)	Effluent Glucose (g/L)	Effluent Xylose (g/L)	Effluent Ethanol (g/L)	Glucose Conversion (%)	Xylose Conversion (%)	Ethanol Yield (g/g)
42.4	21.9	0.24	0.3	2.3	27.9	99.3	89.5	0.45
37.8	19.6	0.34	0.6	3.6	25.5	98.4	81.6	0.48
37.4	19.5	0.5	3.7	12.7	17.1	90.1	34.9	0.42
50.3	11.3	0.24	0.1	1.8	24.8	99.8	84.1	0.42
50.3	11.3	0.37	1.0	3.6	22.7	98.1	68.1	0.40
50.3	11.3	0.49	2.0	4.6	20.8	96.1	59.3	0.38

Since strain *Z. mobilis* 31821(pZB5) showed high efficiency on conversion of xylose to ethanol, it was decided to test this strain with the actual hydrolysate provided by Arkenol. This feedstock was prepared by the Arkenol's patented concentrated acid hydrolysis process.

Table 12. Steady state results of FBR experiments using immobilized *Z. mobilis* 31821(pZB5) and Arkenol's hydrolysate

Feed Glucose (g/L)	Feed Xylose (g/L)	Dilution Rate (1/h)	Effluent Glucose (g/L)	Effluent Xylose (g/L)	Effluent Ethanol (g/L)	Glucose Conversion (%)	Xylose Conversion (%)	Ethanol Yield (g/g)
48.3	12.6	0.23	0	0.7	29.5	100	94.9	0.49
48.3	12.6	0.32	0.2	0.7	27.9	99.6	94.3	0.47
45.6	13.3	0.56	0.6	1.2	27.4	97.9	91.3	0.48
82.8	27.8	0.21	0.8	2.6	48.3	99	90.6	0.45
82.8	27.8	0.34	1	2.7	50.6	98.8	90.4	0.48
82.8	27.8	0.5	2.4	4.4	48.5	97.1	84.2	0.47
144.4	26.7	0.25	3.4	4.6	69.2	97.6	82.8	0.43
144.4	26.7	0.34	18.3	12.8	58.4	87.3	52.1	0.42
144.4	26.7	0.53	28.3	14.8	47.4	80.4	44.6	0.37
144.4	26.7	1.1	66.8	21.7	32.4	53.7	18.7	0.39

At the start of the experiment, a feed solution containing 48.3 g/L glucose and 12.6 g/L xylose was used. The retention times used were 4.5, 3, and 2 h. After steady state was achieved for the 2-h retention time, the feed solution was replaced with a new feed solution containing 82.8 g/L glucose and 27.8 g/L xylose. Even at high xylose concentration in the second feed, xylose conversion was maintained at high levels. The steady-state results are summarized in Table 12. Complete conversion of glucose was observed at all conditions. At all three retention times used for the first feed solution, xylose conversion at >90% was achieved. When the second feed solution was used, even with a xylose concentration of more than two times that in the first feed solution, xylose conversion was still as high as 84% at the lowest retention time of 2 h. The productivity under these conditions was 25.5 g/L-h, which was more than ten times the typical productivity of ethanol production from a xylose/glucose mixture in a batch reactor. High ethanol yield also was observed. The yield value under all the conditions employed was very close to the theoretical yield of 0.51 g ethanol/g sugar consumed. To test the stability of the biocatalyst, after needed data were collected for all three retention times using the second feed solution, a new feed solution having sugar composition similar to the first feed solution was used. The third feed solution, which contained 52.9 g/L glucose and 11.5 g/L xylose, was used for three days and then was replaced by the fourth feed solution, which contained 58.8 g/L glucose and 11.3 g/L xylose. The retention time was maintained at around 4.5 h for these two feed solutions. The conversion of xylose was maintained at a constant level of near 90% until day 18 when it started to decrease (as indicated by an increase in the effluent xylose concentration.) These results indicated that the xylose metabolism capability of the biocatalyst could be maintained for 18 days. A separate experiment was performed to study ethanol production at very high total sugar concentration. The experiment was started with a synthetic feed containing 41.9 g/L glucose and 18.6 g/L xylose. The retention was kept at between 4.5 and 5 h for four days. Then the Arkenol's hydrolysate feed was used. This feed contained 144.4 g/L glucose and 26.7 g/L xylose, i.e., 175 g/L total sugar. At the highest retention time of 4 h, 70 g/L ethanol was obtained in the effluent, which was equivalent to a productivity of 17.5 g/L-h. The yield was 0.43 g ethanol/g sugars consumed. Almost complete conversion of glucose and 83% conversion of xylose were observed. The conversion of both glucose and xylose decreased when the retention time was lowered. At the lowest retention time of 0.9 h, 32.4 g/L ethanol was obtained in the effluent, equivalent to a productivity of 36 g/L-h. However, only 54% glucose and 19% xylose were consumed. The steady-state results of this experiment are also summarized in Table 12.

To study the requirement for tetracycline, another experiment was performed. The Arkenol's hydrolysate was used to prepare the feed solutions. Tetracycline was omitted from all feed solutions. This experiment was started using a hydrolysate feed solution containing 49 g/L glucose and 12 g/L xylose. A retention time of 4.5 h was used for the first five days before it was changed to 3 and then 2 h after a steady state was reached for each retention time. The first feed solution was completely used after day five just before the retention time was changed to 3 h. The second feed solution contained 52 g/L glucose and 13 g/L xylose. Complete conversion of glucose was achieved throughout the course of the experiment. An average value of 80% conversion of xylose was observed for the first five days. Whereas complete conversion of glucose continued, xylose conversion decreased when the retention time was lowered. At the same time, ethanol concentration also decreased. To test the stability of the biocatalyst, the retention time was brought back to 4.9 h on day nine. Whereas complete glucose conversion still was observed, xylose conversion stayed at 37% instead of increasing to near the level observed

for 4.5 h retention time at the beginning of the experiment (80%). The results clearly indicated that the immobilized cells had lost some of their xylose metabolism capability. When the second feed solution was completely used on day 10, the third feed solution was used. We tried to maintain the same feed composition but due to the non-uniformity of the concentrated Arkenol's hydrolysate, the actual sugar concentrations in the third feed solution were 40 g/L glucose and 13 g/L xylose. Xylose conversion continued to decline although the retention time was kept constant. This confirmed the loss of xylose metabolism capability of the biocatalyst.

The results showed that *Z. mobilis* 31821(pZB5) was a very efficient strain for ethanol production from lignocellulosic hydrolysates using the continuous FBR process. It exhibited very high xylose conversion and also good stability. The only drawback was tetracycline was needed to maintain its xylose metabolism capability over extended use in the FBR. A chromosomally integrated strain with comparable performance would be an ideal candidate for ethanol production from lignocellulosic materials using the FBR technology.

3.2.2 Chromosomally integrated strains

Saccharomyces 424A(LNH-ST)

The stability of xylose metabolism in immobilized *Saccharomyces* 424A (LNH-ST) was evaluated first in the FBR. The feed solution consisted of appropriate concentrations of glucose and xylose, 5 g/L Difco yeast extract, 10 g/L KH_2PO_4, 1 g/L K_2HPO_4 and 3.7 g/L KCl. The experiment was started with a feed solution containing 35 g/L glucose and 22 g/L xylose. The retention time was kept at 4.5 hours. The feed solution ran out on day 8 and was replaced by a new feed solution containing 35 g/L glucose and 20 g/L xylose. The retention time was reduced slightly to 4.0 hours. The concentration profiles of glucose, xylose, and ethanol in the effluent are shown in Fig. 35. The effluent concentrations of glucose, xylose, and ethanol were stable until day 11. On day 12 the conversion of xylose dropped from 55% to 25%. It then dropped further to 19% the next day. The decrease in xylose conversion resulted in a slight decrease in ethanol concentration. Complete glucose conversion was observed throughout the entire period. The average yield is 0.40 g ethanol/g total sugar consumed or 79% of the theoretical yield. The results indicated that under the employed conditions, stable xylose metabolism by immobilized *Saccharomyces* 424A (LNH-ST) could be maintained for 11 days. This was less than the 17-day period observed for *Zymomonas mobilis* 31821 (pZB5). However, it should be recalled that *Z. mobilis* 31821(pZB5) was a plasmid-based strain and it required tetracycline to maintain stable xylose metabolism over that period.

After the stability of xylose metabolism of *Saccharomyces* 424A (LNH-ST) in the FBR was established, experiments were performed to study the effects of feed composition and retention time on ethanol production by this strain. The sugar concentrations were 39 g/L glucose and 20 g/L xylose in the first feed solution, and 49 g/L glucose and 13 g/L xylose in the second one. Three retention times of 4, 3, and 2 hours were studied. The bulk volume of the biocatalyst beads was 550 ml. The steady-state results are summarized in Table 13. Whereas glucose conversion was complete or very near completion under all experimental conditions, xylose conversion was not. Xylose conversion obtained in this case was significantly lower than the conversion obtained with *Z. mobilis* 31821(pZB5) under similar conditions. This indicated that the xylose metabolism pathway in *Z. mobilis* 31821(pZB5) was more efficient than that in the yeast strain.

The general trend for xylose conversion by the immobilized *Saccharomyces* 424A(LNH-ST) in the FBR was it decreased with decreasing retention time. The feed xylose concentration did not have any effect on xylose conversion. This indicated that up to 20 g/L xylose, the concentration of this sugar was not a rate-limiting factor. The yield values of ethanol were similar for both feed solutions and were lower than the yield values obtained for *Z. mobilis* 31821(pZB5) under similar conditions. Whereas *Z. mobilis* 31821(pZB5) produced very little by-products, significant quantities of glycerol were produced by *Saccharomyces* 424A(LNH-ST). In the yeast strain, glycerol concentrations as high as 5 g/L were observed. *Z. mobilis* 31821(pZB5) produced less than 0.5 g/L lactic acid and acetic acid. After the last sample for the 50/10 feed solution was taken on day 12, this feed solution was replaced with a feed solution. Containing 36.3 g/L glucose and 20.6 g/L xylose. The retention time was reset to 4.0 hours. The xylose conversion measured after steady state had been reached was only 27% instead of 47% as expected under the conditions employed. This confirmed the loss of xylose metabolism after 12 days of operation of the FBR.

Figure 35. Determination of stability of strain *Saccharomyces* 424A(LNH-ST) in continuous FBR operation.

Table 13. Steady state results of FBR experiments using immobilized *Saccharomyces* 424A (LNH-ST)

Feed Glucose (g/L)	Feed Xylose (g/L)	Dilution Rate (1/h)	Effluent Glucose (g/L)	Effluent Xylose (g/L)	Effluent Ethanol (g/L)	Glucose Conversion (%)	Xylose Conversion (%)	Ethanol Yield (g/g)
39.3	19.8	0.23	0	10.5	19.2	100	46.8	0.40
39.3	19.8	0.35	0.9	12.9	15.6	97.6	34.5	0.35
39.3	19.8	0.5	2.5	14.6	15.0	93.1	25.4	0.30
48.5	12.8	0.25	0.2	6.4	20.2	99.6	49.6	0.37
48.5	12.8	0.33	2.0	8.5	19.0	95.9	33.6	0.38
48.5	12.8	0.5	2.6	9.0	18.6	94.6	29.8	0.38

Table 14. Steady state results of FBR experiments using a larger quantity of immobilized *Saccharomyces* 424A (LNH-ST) biocatalyst

Feed Glucose (g/L)	Feed Xylose (g/L)	Dilution Rate (1/h)	Effluent Glucose (g/L)	Effluent Xylose (g/L)	Effluent Ethanol (g/L)	Glucose Conversion (%)	Xylose Conversion (%)	Ethanol Yield (g/g)
40.3	18.7	0.24	0	9.2	18.2	100	51.1	0.37
40.3	18.7	0.33	0.3	11.5	17.0	99.3	38.8	0.33
39.6	20.2	0.45	1.6	14.9	18.5	95.9	26.5	0.43
43.2	15.2	0.22	0.11	9.6	19.2	99.8	35.7	0.40
43.2	15.2	0.34	0.5	9.7	20.4	98.9	35.8	0.42
43.2	15.2	0.5	1.7	11.4	18.4	96.1	24.9	0.41

In an attempt to improve the FBR performance, an experiment was performed in which the bulk volume of the biocatalyst was increased from 550 mL to 900 mL. In other words, the entire FBR was filled with these beads and only the expansion section was available for fluidization. The steady-state results are summarized in Table 14. Comparison of the results obtained for this experiment with those obtained for the experiment where 550 mL biocatalyst was used showed that the larger quantity of biocatalyst did not seem to improve the bioreactor performance. This indicated that fluidization was a necessary condition for good performance of this type of reactor configuration.

It was suspected that poor xylose conversion was observed with *Saccharomyces* 424A(LNH-ST) because the experiments were performed under strictly anaerobic conditions whereas the yeast cells might require microaerophilic conditions for optimal performance.

Therefore, we performed an additional experiment in which the feed solution was continuously aerated. This feed solution consequently was air-saturated when it entered the FBR. Since no aeration was provided to the FBR the dissolved oxygen in the feed was quickly consumed by the large number of yeast cells immobilized on the biocatalyst beads. Therefore, the FBR was operated under oxygen-limited conditions instead of strictly anaerobic conditions. This particular experiment used a synthetic feed containing 38 g/L glucose and 21 g/L xylose in the FBR at a retention time of 4.3 h. The experiment was run for nine days, which was well before the biocatalyst was expected to start losing its xylose conversion capability. Almost complete glucose conversion (98%) was observed. However, xylose conversion was only 27%, which was lower than the conversion of 47% obtained under anaerobic conditions using similar feed composition and retention time. The ethanol yield of 0.38 g ethanol/g sugars consumed was comparable with the value obtained under anaerobic conditions. Ethanol concentration in the effluent was 17 g/L, which was slightly lower than the concentration of 20 g/L obtained under anaerobic conditions. The results indicated that oxygen-limited conditions did not improve xylose conversion by immobilized *Saccharomyces* 424A(LNH-ST) in the FBR. Actually better reactor performance was obtained under more anaerobic conditions.

Zymomonas mobilis C25

The chromosomally integrated strain *Zymomonas mobilis* C25 was tested in the FBR using a feed solution containing 40 g/L glucose and 20 g/L xylose at a retention time of 4.2 hours. The experiments were run for one month. In the first experiment, Red Star yeast extract was used as the nutrient source. The results are plotted in Fig. 36a (concentration profiles) and Fig. 36b (sugar conversion). The conversion of xylose in the FBR increased rapidly during the first four days to peak at 69%. The conversion of glucose also increased during this period but at a much lower rate. The increase in conversion rates of both sugars during the first four days was reflected in a decrease in sugar concentrations and an increase in ethanol concentration in the effluent. After day four, xylose conversion suddenly dropped whereas glucose conversion was maintained at the same level. From day 5 to day 9, xylose conversion stabilized at 35%. After day 9, it dropped again but then stabilized for the rest of the experiment. Glucose conversion also dropped slightly after day 9. The average conversion rate of xylose between day 10 and day 31 was 18%. Although it showed some fluctuation, the conversion of glucose over the entire experimental period was significantly more stable than that of xylose. The average glucose conversion for the entire experiment was 88%. The average ethanol yield was 0.33 g ethanol produced per g sugar consumed.

In the second experiment, Difco yeast extract was used as the nutrient source. The results are plotted in Fig. 37a (concentration profiles) and Fig. 37b (sugar conversion). The conversion of xylose followed a pattern similar to the one observed in the first experiment. With the exception of a one-day decrease to a low level after day two, xylose conversion increased to peak at 63% on day six before it started to decrease. After day 11, xylose conversion stabilized. The average conversion of xylose for the rest of the experimental period was 13%. The conversion of glucose was more stable than in the case of Red Star yeast extract. The average conversion of glucose before it started to decrease sharply on day 28 was 97%. The average ethanol yield was 0.31 g ethanol produced per g sugar consumed.

Figure 36. Performance of *Z. mobilis* C25 in FBR using 40/20 glucose/xylose feed at 4.2-h retention time with Red Star yeast extract as nutrient source. (a) effluent concentrations (b) substrate conversion

Figure 37. Performance of *Z. mobilis* C25 in FBR using 40/20 glucose/xylose feed at 4.2-h retention time with Difco yeast extract as nutrient source. (a) effluent concentrations, (b) substrate conversion

The results showed that Difco yeast extract gave higher glucose conversion but lower xylose conversion compared to Red Star yeast extract. The production of by-products, mainly xylitol and lactic acid, was observed in both experiments. By-product formation could be the cause for the low ethanol yield obtained.

To compare the performance of the chromosomally integrated *Z. mobilis* strain with the chromosomally integrated yeast strain, the experiment was repeated with *Saccharomyces* 424A(LNH-ST) using Difco yeast extract as the nutrient source. Many FBR experiments were performed with this yeast strain in the past, but we decided to perform one more experiment using the same batch of Difco yeast extract as the one used for the experiment with the chromosomally integrated *Z. mobilis* strain. The results are plotted in Fig. 38a (concentration profiles) and Fig. 38b (sugar conversion). Complete conversion of glucose and 40% conversion of xylose were observed during the first 13 days. After that the conversion of both sugars started to decrease because the beads started to clump together and caused severe restriction of substrate transfer to the immobilized cells. This was also observed a number of times in the past. The problem of biocatalyst aggregation in the case of *Saccharomyces* 424A(LNH-ST) can be partially alleviated by increasing the feed flow rates. Increasing feed flow rates will decrease retention time, which in turn will cause higher productivity but lower substrate conversion. The average ethanol yield before bead aggregation occurred was 0.36 g ethanol produced per g sugars consumed and for the entire experimental period was 0.32 g ethanol produced per g sugars consumed.

In summary, under the conditions tested in the FBR, *Saccharomyces* 424A(LNH-ST) showed lower initial conversion of xylose than *Z. mobilis* C25. However, xylose conversion by the yeast strain seemed to be more stable than by the microbial strain. Glucose conversion by both strains in the FBR was equivalent.

Escherichia coli KO11

Only one experiment on ethanol production by immobilized *E. coli* KO11 was studied in the FBR. The medium was the same as the one used for previous FBR studies using immobilized *Saccharomyces* and *Z. mobilis* strains. The pH of the medium was adjusted to 6.5 before sterilization. The pH in the FBR was maintained at 6.5 and the retention time was set at 4 hours. The effluent concentration profiles of glucose, xylose, and ethanol are shown in Fig. 39. Compared to the recombinant xylose-fermenting *Saccharomyces* and *Z. mobilis* strains studied under similar conditions, *E. coli* KO11 did not perform as well. Highest glucose conversion was at 60% whereas xylose conversion at the start of the experiment was at 30% but then steadily decreased and ethanol concentration never exceeded 10 g/L. Average ethanol yield during the first nine days was 0.39 g ethanol produced per g sugars consumed. The yield dropped to 0.26 g ethanol produced per g sugars consumed on day ten when more than 3 g/L lactic acid was observed in the effluent. Since contamination was suspected the experiment was terminated on day 11.

Figure 38. Performance of *Saccharomyces* 424A(LNH-ST) in FBR using 40/20 glucose/xylose feed at 4.6-h retention time with Difco yeast extract as nutrient source. (a) effluent concentrations, (b) substrate conversion

Figure 39. Continuous ethanol fermentation in the FBR by *E. coli* K011.

3.3 Economic analysis

A study of the effects of FBR technology on ethanol production cost was performed by Mark Ruth at NREL. Since sugar streams with insoluble solids will plug the FBR, the analysis was based on a process with a clear fermentation broth. For this reason, the concentrated acid process was chosen for the base process. The modeled process consists of the following areas: biomass handling, two stages of concentrated acid hydrolysis of the biomass, acid recovery and recycle, fermentation, ethanol recovery, waste-water treatment, lignin combustion to produce steam and electricity, and utilities. The ancillary areas (biomass handling, ethanol recovery, waste-water treatment, lignin combustion, and utilities) were unchanged from the enzymatic base case studied at NREL.

The concentrated acid hydrolysis process design and many of the process parameters were developed from U.S. Patent 5,782,982 held by Arkenol, Inc. The sugar solution recovered from the chromatography column is neutralized and overlimed with the gypsum removed before fermentation. After overliming, the solution contains approximately 11% glucose and 6% xylose. That sugar solution is fermented by recombinant *Z. mobilis* in a submerged culture to produce ethanol. The fermentation takes place in a cascading train of continuous stirredt tank

bioreactors with a design residence time of 2.5 days. The glucose-to-ethanol and xylose-to-ethanol yields are 92% and 85%, respectively. A seed train is required to produce 10% inoculum for the train. The only nutrient provided to the train is corn steep liquor at 0.25% (w/w) of the solution within the first fermenter. The fermentation train is kept at 30°C by cooling water supplemented with chilled water during 20% of the operation time annually. Seven percent of the sugars entering the train are lost to contamination. The beer produced in fermentation is held in a surge tank and then pumped to ethanol recovery. The remaining areas of the ethanol production area are the same in the NREL's enzyme-based process.

The FBR technology is different from submerged culture technology in the area between overliming and the beer well. The four 1,000,000 gallon submerged fermenters are replaced by four taller, skinnier 38,000 gallon FBR reactors that have 60% of their working volume filled with the immobilized-cell biocatalyst. The biocatalyst beads have a void fraction of 30%, so the actual volume of the beads taken up only 42% of the total working volume of the reactor. The working volume in the reactors is assumed to be 90% of the total volume. The cells stay at a much higher concentration in the FBR's than in the submerged culture reactors because they do not wash out with the beer. Because the cells are at a much higher concentration, they consume sugars much more rapidly and require a one-hour retention time in fermentation instead of 60 hours as is required with the submerged culture reactors. The increased cell concentrations also result in less cell mass production and higher ethanol yields so the glucose to ethanol yield was increased from 92% to 95% and the xylose to ethanol yield was increased from 85% to 90%. Because less cell mass is produced, the corn steep liquor requirement was reduced from 0.25% to 0.1%. The seed train was eliminated because the FBR's do not require inoculum. However, the beads within each reactor need to be replaced once very three months, so four reactors were chosen to allow a spare to be out of service at all times and a catalyst loading system capital cost was added.

The capital cost of the FBR is $590,000 per reactor and was scaled from the cost reported by Fluor Daniel (Fluor Daniel, 1994). A bead cost of $20 per cubic foot was also taken from the Fluor Daniel report and results in an annual bead cost of $460,000. The capital and operating costs of the pumps were scaled from the pump costs for the submerged culture reactors.

The overall ethanol production cost was reduced by $0.035/gal with the FBR technology. The reasons for the reduction are increased ethanol yields and reduced nutrient cost. The capital costs for each system are almost identical (the FBR capital cost is about 0.7% higher than the capital cost for the submerged culture system due to increased complexity in the fermentation area). The nutrient cost in the FBR system is $1,000,000 less annually in the FBR system than in the submerged culture system. That reduction is approximately equivalent to $0.02/gal ethanol and more than compensates for the annual bead cost of $460,000.

4. Scale-up of the FBR technology

The FBR technology has been tested at demonstration scale (Webb et al., 1995). The reactor used in this study was 2.5 m tall with a 10.2 cm ID. The substrate was glucose. The feed concentrations ranged from 90 to 170 g/L and the dilution rate from 0.7 to 1.4 h^{-1}. Three feed solutions, which included a 30-40% glucose solution, a 1.5% yeast extract solution, and process water, were kept in separate containers. The final glucose concentration was adjusted by changing the ratios of the glucose and process water feed streams. Minimal procedures were

used for mitigation of contaminant growth. These conditions, which were even less stringent than those employed in bench-scale experiments, included:

1. Rinsing of feed lines twice daily with 60°C water. Normal operation resumed within ten minutes.
2. Refrigeration of the yeast extract solution.
3. Replacement of feed containers with each charge of fresh feed.

The reactor was not sterilized, nor were the feed streams.

In this demonstration-scale study, glucose conversion ranged from 80 to 99.7%. The productivity ranged from 59 to 170 g/L-h, which was equal to or greater than observed in bench-scale experiments (40-110 g/L-h). Ethanol yields (80 to 95% of theoretical yield) were lower than observed in bench-scale experiments (97% of theoretical yield). The lower yields might be the results of free-cell contaminant growth in the fluid phase. The results demonstrated thescalability of the FBR technology.

Despite many demonstrated advantages the FBR has not been used for ethanol production at the commercial scale. However, this type of reactor has been used successfully for full-scale production of methane by anaerobic digestion of organic wastes. From a process engineering point of view the two systems, i.e., ethanol fermentation and methane production, have many similarities. In both systems the process development engineer will have to be concerned with biocatalyst stability, entrainment of biocatalyst in the effluent, control of pH and temperature, mixing, and gas disengagement. Therefore, the experience learned in methane generation can also be applied to ethanol production.

One of the main concerns in the scale-up of the FBR for ethanol production is biocatalyst stability. Structural integrity of the biocatalyst beads has been verified in the laboratory-scale FBR. In most of the experiments, the reactor was operated for at least one month and structural failure of the biocatalyst was completely absent even with heavy cell growth on the surface and within the beads. In the full-scale FBR, the possibility of the biocatalyst beads at the bottom of the reactor being crushed by those above is minimal. First of all, instead of using one single tall reactor, many units of equal size can be used. This will reduce the height of the reactors and subsequently reduce the weight exerting on the biocatalyst at the bottom. This type of arrangement was used in an economic analysis performed by Fluor Daniel. Secondly, because of the constant fluidization of the biocatalyst these beads always are in motion and hence will never have to bear the weight of those above as in the case of a packed-bed reactor. Biocatalyst entrainment in the effluent also should not be a problem. Although the biocatalyst will rise with the gas bubbles they will sink when the gas escape near the top of the reactor. A small number of beads may still be floating but they can be easily kept inside the reactor with a screen.

Temperature and pH control is not difficult to maintain. Again due to the constant fluidization of the biocatalyst beads high degree of mixing can be realized in the fermentation broth. This fluid motion will aid in distribution of heat and the base solution used for pH control. The methane-producing organisms require much more stringent control of pH and temperature than the ethanol-producing organisms. Since failure of FBR used for anaerobic digestion due to pH or temperature has not been reported there should not be any concern for such failure in the case the ethanol FBR.

Carbon dioxide is produced in the FBR in the form of very small gas bubbles. These bubbles carry the biocatalyst beads with them when they rise. When the bubbles detach from the beads to continue their journey these beads will fall downward only to be carried upward again later. These effects provide good mixing for the reactor contents. After leaving the biocatalyst beads behind to continue to rise further, the gas bubbles still maintain their small size. Because of their size these small bubbles will not coalesce to form larger bubbles. Therefore, surface boiling due to bursting of large gas pockets will not occur. Not only that loss of biocatalyst beads in the effluent is avoided but highly efficient gas disengagement also can be realized.

In summary, scale-up of the FBR technology for commercial production of ethanol production can be carried out with proper process design.

5. Conclusions

The following conclusions can be made from the results discussed in the previous sections:

1. The FBR was a highly effective system for ethanol production from corn-derived and lignocellulosic sugars. Both feed stocks could be used to produce ethanol at yields very close to the theoretical values and at volumetric productivities at least one order of magnitude higher than those typically obtained in batch process using conventional stirred tank fermenters. The reactor could be operated continuously for over a month with very good stability. There was no loss of the biocatalyst beads from the reactor over the entire normal course of the operation and minimal deactivation. The κ-carrageenan-based immobilized biocatalyst was stable. There were no obvious signs of structural failure of these beads. Minimal sterility requirement were needed and the system was resistant to contamination due to the low liquid residence time.

2. Co-immobilized enzyme-microbe systems allow the potential to perform simultaneous saccharification and fermentation (SSF). Both co-immobilized biocatalyst systems, namely the glucoamylase-*S. cereviasiae* and glucoamylase-*Z. mobilis,* are suitable for production of ethanol from soluble starch. The average ethanol yield of the glucoamylase-*S. cereviasiae* system was 0.45 g ethanol/g starch consumed or 80% of the theoretical yield. In the case of the glucoamylase-*Z. mobilis* system the average ethanol yield was 0.49 g ethanol/g starch consumed or 89% of the theoretical yield.

3. When dry-milled corn starch was used for ethanol production, the solids in the feed streams had to be removed first because the FBR was unable to handle feed streams with high solid contents.

4. An SHF (separate hydrolysis and fermentation) system was much more effective for ethanol production from dry-milled corn starch than an SSF system because in the SHF it was possible to carry out the two consecutive steps, namely the hydrolysis of soluble starch by immobilized glucoamylase and the fermentation of the sugars to ethanol by immobilized *Z. mobilis*, at their different optimum conditions, rather than at a compromise non-optimal condition. In the SSF system to ensure viability of the organism the FBR had to be operated at temperatures below 35^{o}C, at which the hydrolysis rate of glucoamylase was only about 15

to 20% of its optimum rate at 55°C. The results clearly indicated the need for a highly effective thermophilic ethanol-producing organism, which will allow hydrolysis and fermentation to be carried out simultaneously in one single reactor at the temperature optimum for both the enzyme and the organism.

5. An SHF process using the FBR technology was developed for production of ethanol from dry-milled corn starch using immobilized glucoamylase and immobilized *Z. mobilis* in two consecutive reactors. An economic analysis was performed for this process with USDA. The results showed savings of one to three cents per gallon of ethanol produced compared to a traditional batch process using conventional stirred tank fermenters in a state-of-the-art dry-mill ethanol plant.

6. A mathematical model was developed for ethanol production from glucose or from soluble starch in the FBR. The model can be used to predict concentration profiles of starch and glucose within a biocatalyst beads as well as the concentration profiles of starch, glucose, and ethanol along the length of the FBR under a set of process conditions such as feed concentration and feed flow rate. The predicted results allow determination of optimum bead size and optimum operating conditions of the FBR.

7. Five recombinant organisms were tested in the FBR for ethanol production from lignocellulosic sugars. These included two plasmid-based strains, *Z. mobilis* CP4(pZB5) and *Z. mobilis* 31821(pZB5), and three chromosomally integrated strains, *Z. mobilis* C25, *Saccharomyces* 424(LNH-ST), and *E. coli* KO11.

8. Strain *Z. mobilis* CP4(pZB5) was not suitable for continuous operation in the FBR. Even with tetracycline in the feed solutions the strain lost its xylose metabolism capability in about ten days. *Z. mobilis* 31821(pZB5) was a much more stable strain and was suitable for continuous use in the FBR. With tetracycline in the feed solutions it maintained its xylose metabolism capability for a period of 17 days. However, without tetracycline it lost this capability after five days of continuous operation.

9. *Z. mobilis* 31821(pZB5) had very high xylose conversion efficiency. With feed solutions containing 40 g/L glucose and 20 g/L xylose, and 50 g/L glucose and 10 g/L xylose, greater than 84% conversion of xylose was observed at a dilution rate of 0.24 h^{-1}. In both cases complete conversion of glucose was achieved. The xylose conversion rate was well above the goal of 75% xylose conversion set for a process using lignocellulosic sugars to produce ethanol.

10. *Z. mobilis* 31821(pZB5) was also tested with Arkenol's rice straw hydrolysate, which was obtained by the concentrated hydrolysis process. The hydrolysate displayed no toxicity toward the organism. It also was proven to be a good feed stock for ethanol production. At the highest sugar concentrations tested, which were 144 g/L glucose and 27 g/L xylose, and a dilution rate of 0.25 h^{-1}, the conversion rates of glucose and xylose were 98% and 83%, respectively. The ethanol concentration was 70 g/L, which gave a productivity of 17 g/L-h. This was almost ten times the typical productivity of 2 to 3 g/L-h obtained in batch fermentations using lignocellulosic sugars.

11. An economic model was developed for a process using the FBR technology with immobilized *Z. mobilis* biocatalyst for ethanol production from lignocellulosic sugars obtained by concentrated acid hydrolysis. The results indicated savings of about three cents per gallon of ethanol produced compared to a typical batch process using stirred tank fermenters.

12. Both *Saccharomyces* 424A(LNH-ST) and *Z. mobilis* C25 displayed loss of xylose metabolism capability with time. The yeast strain was able to maintain xylose metabolism at the level equal to the initial level for 13 days whereas the bacterial strain seemed to lose that capability sooner. Both of these strains showed an ethanol yield lower than the yield obtained with the plasmid-baased strain *Z. mobilis* 31821(pZB5) due to formation of by-products.

13. *E. coli* KO11 did not perform as well as the other two chromosomally integrated strains tested. Maximum glucose conversion of only 60% was achieved. This strain also displayed instability of xylose metabolism with time.

References

AIba, S., Humphrey, A. E., and Millis, N. F. (1973), *Biochemical Engineering,* Academic Press, New York, 2nd Edition, 115-116.

Bajpai, P. K., and Margaritis, A. (1985), *Enzyme Microbiol. Technol.* 7, 462-464.

Begovich, J. M. and Watson, J. S. (1978), *Fluidization*, J. F. Davison and D. L. Kearns (Editors) Cambridge University Press, Cambridge, 190.

Burchardt, G., and Ingram, L. O., (1992), *Appl. Environ. Microbiol.*, 58, 1128-1133.

Crueger, W., and Crueger, A. (1982), *Biotechnology: A Textbook of Industrial Microbiology,* Science Tech, Madison, WI.

Davison, B. H., and Scott, C. D. (1988), *Appl. Biochem. Biotechnol.* 18, 19-34.

Doelle, H. W., Kirk, L., Crittenden, R., and Toh, H. (1993), *Crit. Rev. Biotechnol.* 13, 57-98.

Godia, F., Casas, C., and Sola, C. (1987), *Process Biochem.* 22(2), 43-48.

Hamdane, A. M., Wilhelm, M., and Riba, J. P. (1988), *The Chemical Engineering J.*, 39, B25-B30.

Harshbarger, D., Bautz, M., Davison, B. H., Scott, T. C., and Scott, C. D. (1995), *Appl. Biochem. Biotechnol.* 51/52, 593-604.

Ho, N. W. Y., Chen, Z. D., and Brainard, A. (1998), *Appl. Environ. Microbiol.*, 64, 1852-1859.

Inloes, D. S., Michaels, A. S., Robertson, C. R., and Martin, A. (1985), *Appl. Microbiol. Biotechnol.* 23, 85-91.

Kim, C. H., Lee, G. M., Abidin, Z., Han, M. H., and Rhee, S. K. (1988), *Enzyme Microbiol. Technol.* 10, 426-430.

Kim, C. H., Abidin, Z., Ngee, C., and Rhee, S. (1992), *Biores. Technol.* 40, 1-6.

Ladish, M. R., Lin, K. W., Voloch, M., and Tsao, G. T. (1983), *Enzyme Microbiol. Technol.* 5, 82-102.

Lantero, O. J., Brewer, J. W., and Sarber, S. M. (1995), U.S. Patent 5,472,861.

Lee, J. H., Pagan, R. J., and Rogers, P. L. (1983), *Biotechnol. Bioeng*. 25, 659-669.

Lee, K. J. and Rogers, P. L. (1983), *Chem. Eng. Sci.*, 47, 3419-3429.

Madson, P. W. and Locco, D. B. (1999), Paper 6-03 presented at the 21st Symposium on Biotechnology for Fuels and Chemicals, Fort Collins, CO.

Miranda, M. and Murado, M. A. (1991), *Enzyme Microbiol. Technol.* 13, 142-150.

Petersen, J. N., and Davison, B. H. (1995), *Biotechnol. Bioeng.* 46, 139-145.

Rogers, P.L., Bramall, L., and McDonald, I. J. (1978), *Can. J. Microbiol.* 24, 372-380.

Silman, R. W. (1984), *Biotechnol. Bioeng.* 26, 247-251.

Sun, M. Y., Ph.D. Thesis, University of Tennessee – Knoxville (1998).

Webb, O. F., Scott, T. C., Davison, B. H., and Scott, C. D. (1995), *Appl. Biochem. Biotechnol.* 51/52, 559-568.

Webb, O. F., Davison, B. H., and Scott, T. C. (1996), *Appl. Biochem. Biotechnol.* 57/58, 639-647.

Zhang, M., Eddy, C., Deanda, K., Finkelstein, M., and Picataggio, S. (1995), *Science* 267, 240-243.

Table 7. Summary of operating costs for base case process and FBR process cases.

	Residence Time (min)	Yield (fraction of theoretical)	Ethanol conc. (g/L)	Total oper. cost ($1000/yr)	DDGS credit ($1000/yr)	Net oper. cost ($1000/yr)	Ethanol production (gal/yr)	Net oper. cost (cents/gal)	Savings (cents/gal)
Base case		0.954	94	7,408	6,480	16,715	15,035	111.17	—
FBR Case 1	60	0.98	72.2	7,333	6,187	16,933	15,378	110.11	1.06
FBR Case 2	60	0.954	70.3	7,343	6,516	16,614	14,970	110.98	0.19
FBR Case 3	120	0.98	72.2	7,686	6,187	17,286	15,378	112.41	–1.23
FBR Case 4	120	0.954	70.3	7,696	6,516	16,967	14,970	113.34	–2.17
FBR Case 5	20	0.98	72.2	7,017	6,187	16,617	15,378	108.06	3.12
FBR Case 6	20	0.954	70.3	7,036	6,516	16,307	14,970	108.93	2.24

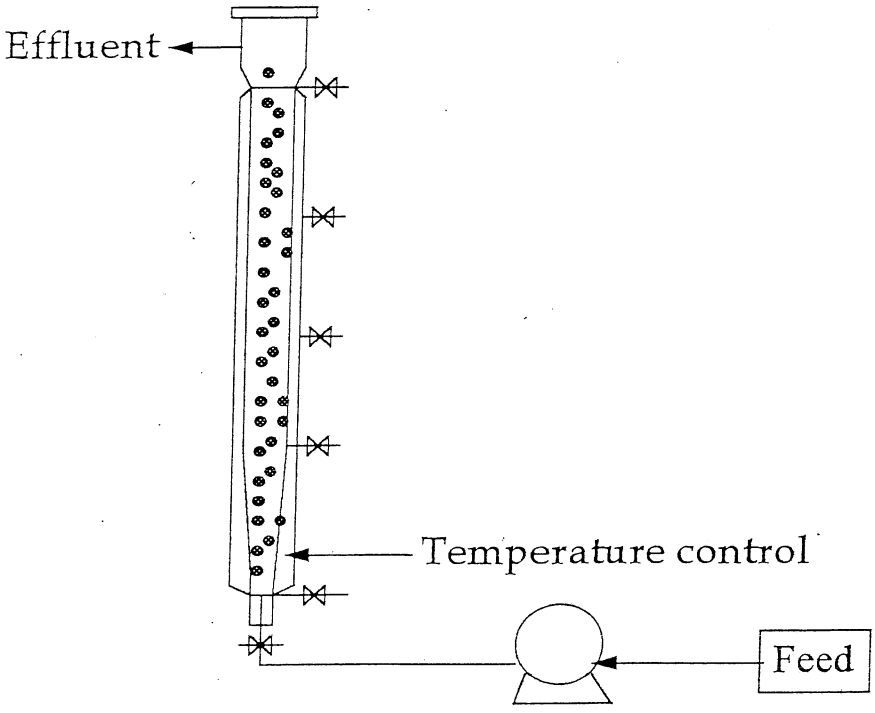

Figure 1. Schematic diagram of the fluidized-bed reactor (FBR) used for study of ethanol production from soluble starch solutions.

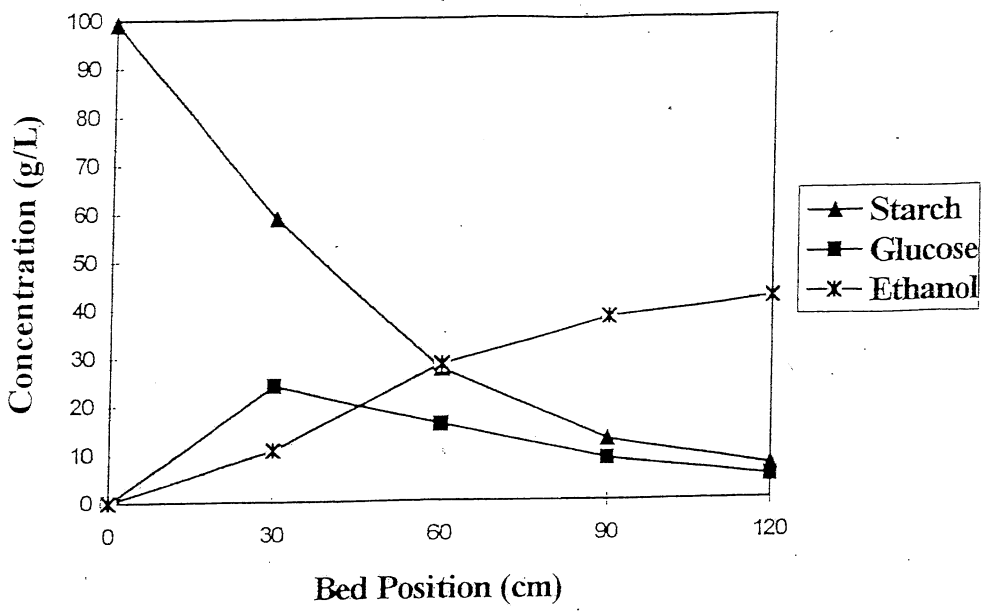

Figure 2. Example of concentration profiles along the length of the FBR using the glucose amylase-*S. cerevisiae* biocatalyst.

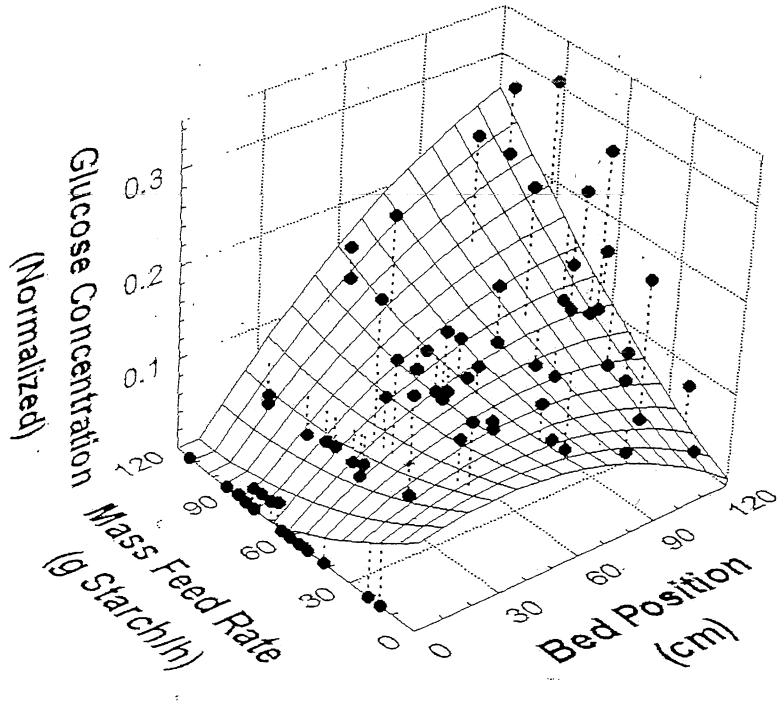

Figure 3. The effect of starch mass loading on FBR performance with the glucose amylase-*S. cerevisiae* biocatalyst.

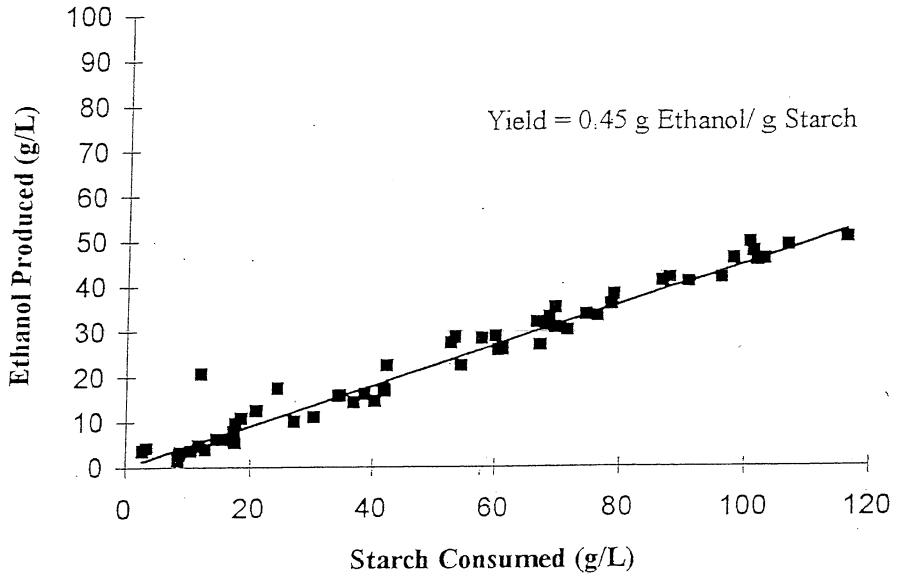

Figure 4. Determination of average ethanol yield by the glucose amylase-*S. cerevisiae* biocatalyst in the FBR.

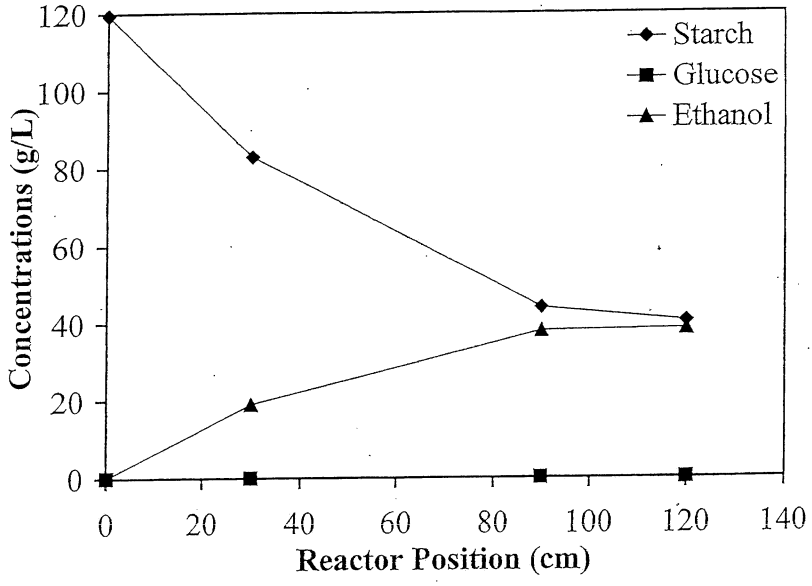

Figure 5. Example of concentration profiles along the length of the FBR using the glucose amylase-*Z. mobilis* biocatalyst.

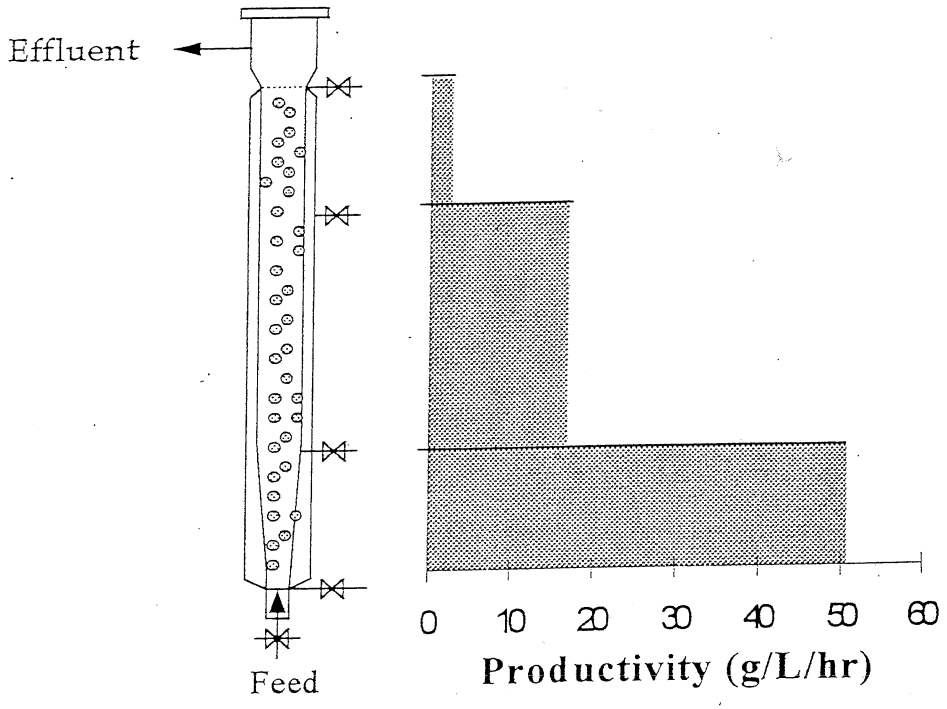

Figure 6. Ethanol volumetric productivity at different sections of the FBR using the glucose amylase-*Z. mobilis* biocatalyst.

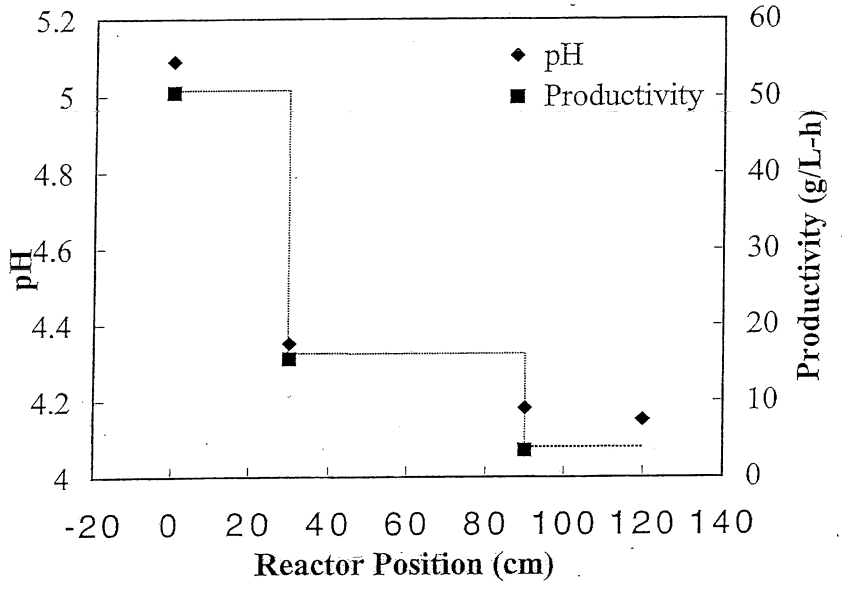

Figure 7. pH profiles along the length of the FBR using the glucose amylase-*Z. mobilis* biocatalyst.

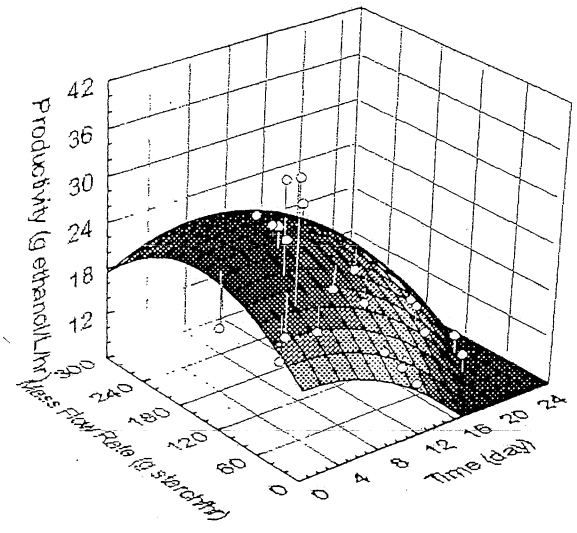

Figure 8. The effect of starch mass feed rate and time of operation on ethanol productivity in the FBR using the glucose amylase-*Z. mobilis* biocatalyst.

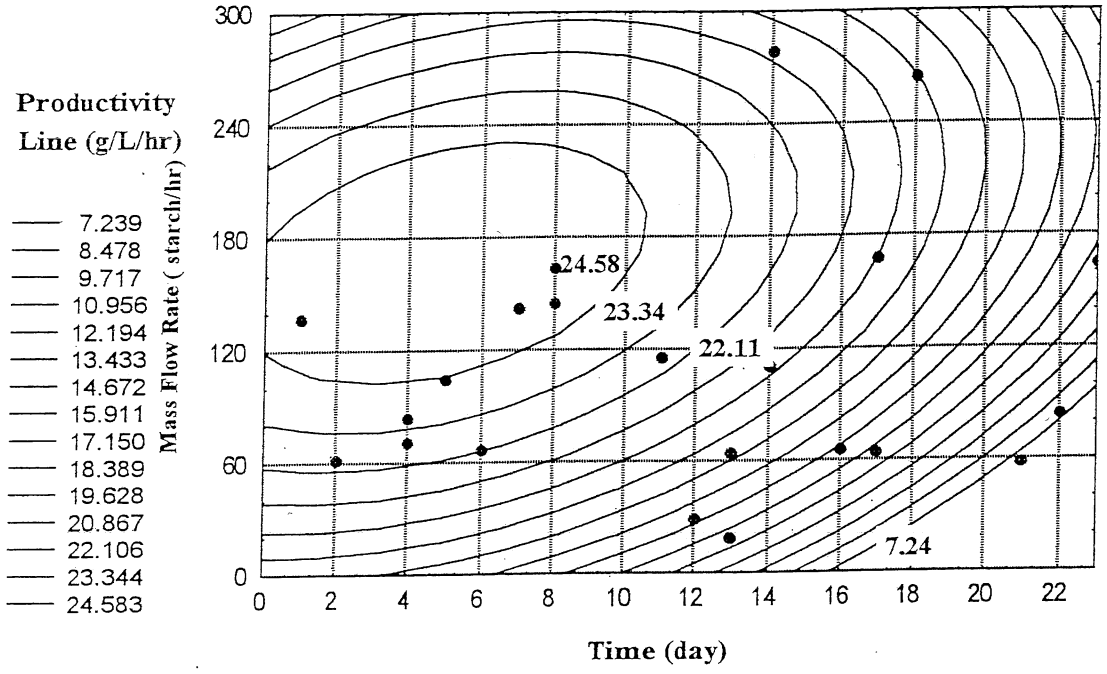

Figure 9. The contour plot of productivity versus starch mass feed rate and time to determine the optimum mass feed rate the FBR using the glucose amylase-*Z. mobilis* biocatalyst.

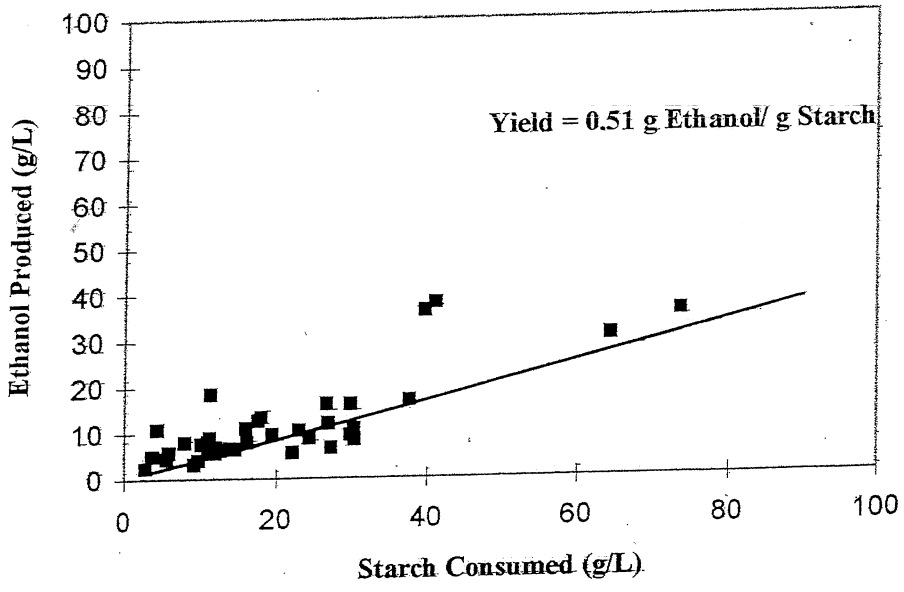

Figure 10. Determination of average ethanol yield by the glucose amylase-*Zymomonas mobilis* biocatalyst in the FBR.

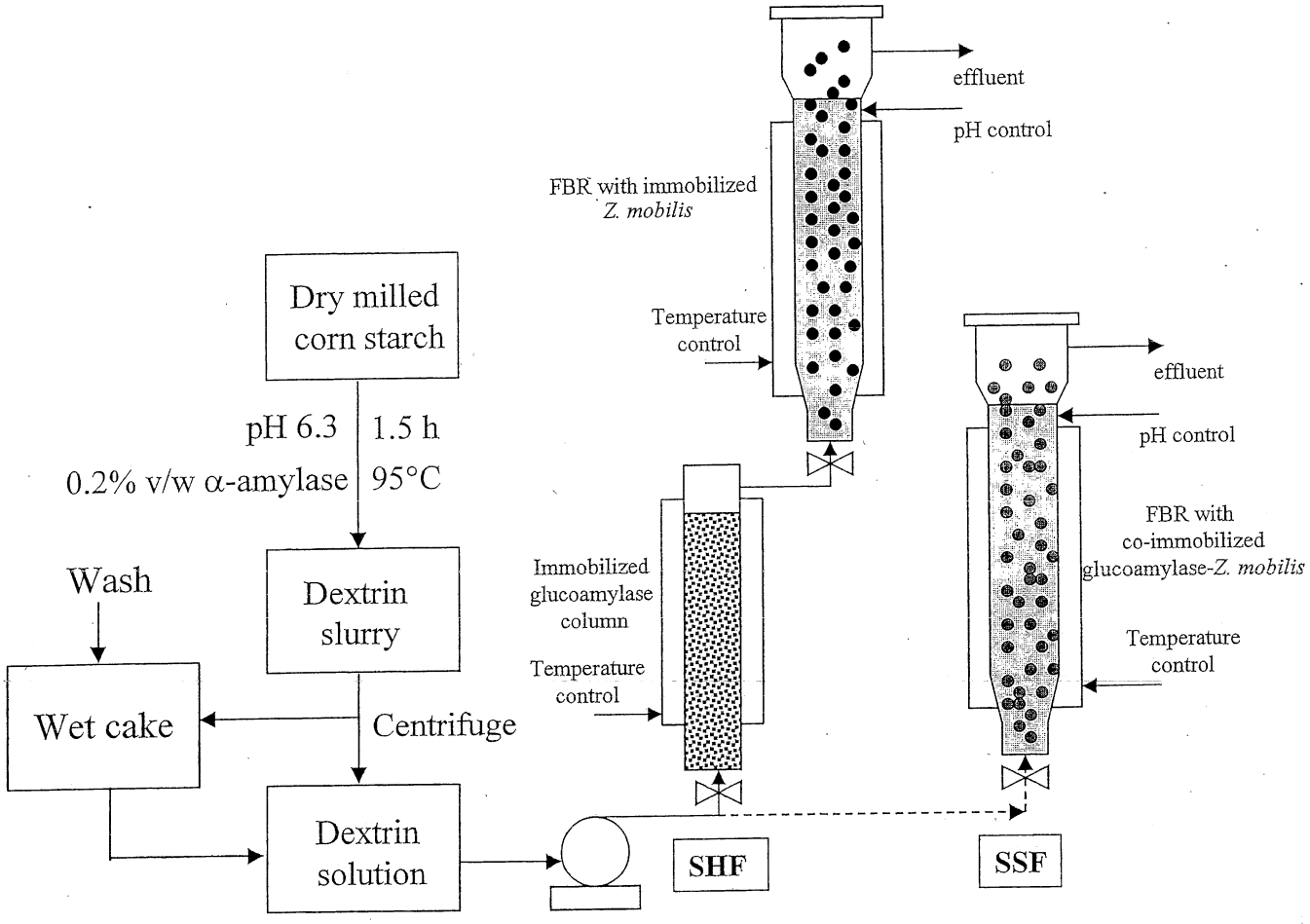

Figure 11. Schematic diagrams of the simultaneous saccharification and fermentation (SSF) and separate hydrolysis and fermentation (SHF) processes.

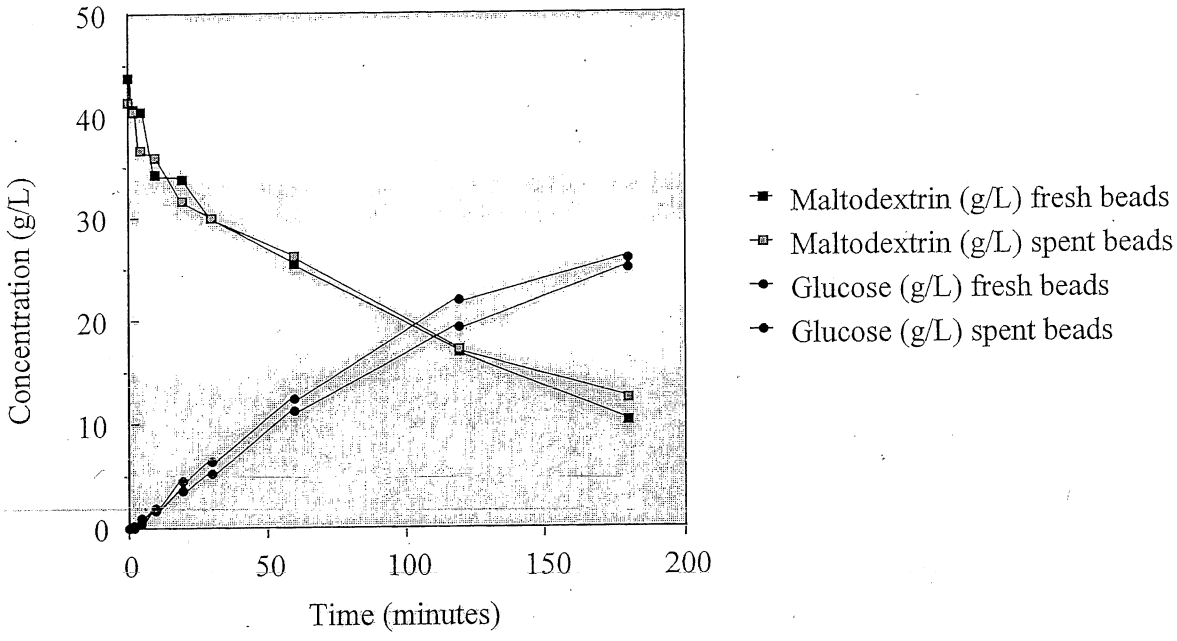

Figure 12. Comparison of soluble starch hydrolysis by fresh glucoamylase-*Z. mobilis* beads and spent (22 batch cycles) beads.

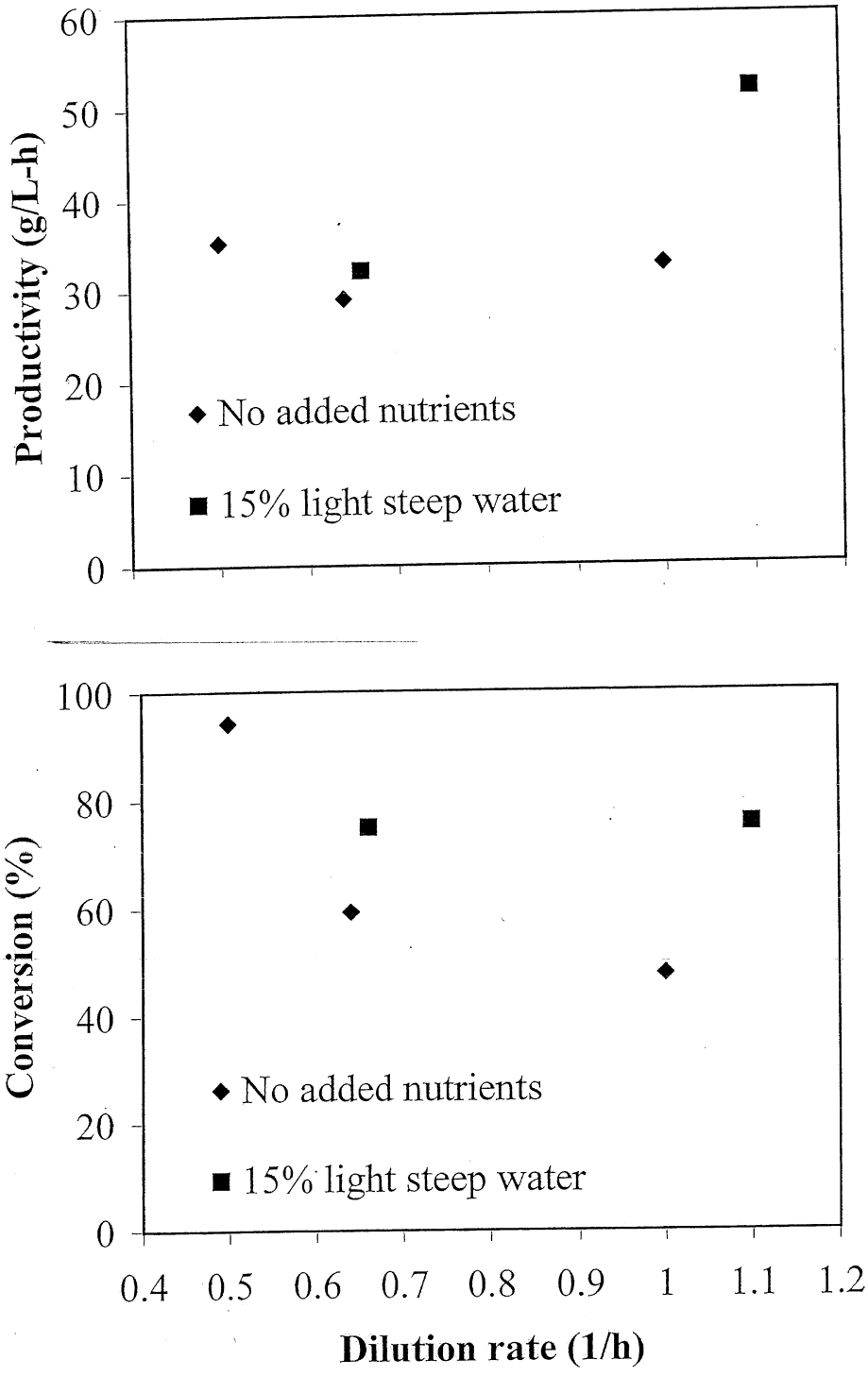

Figure 13. Volumetric ethanol productivity and dry-milled cornstarch-derived glucose feed conversion as a function of dilution rate for the SHF process.

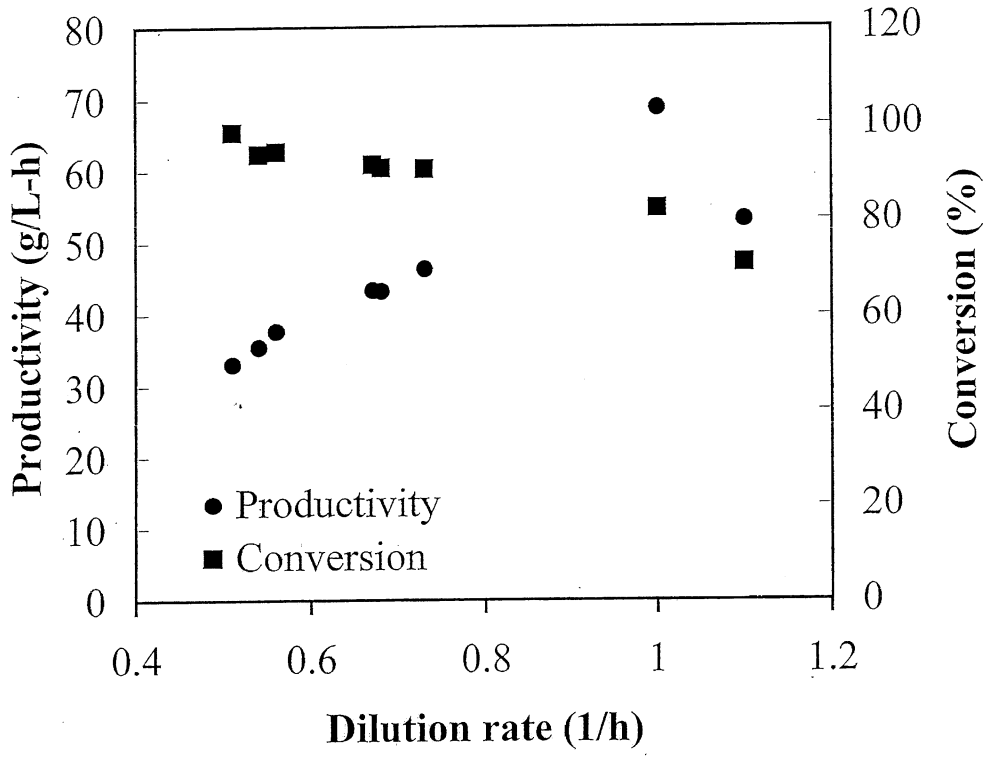

Figure 14. Volumetric ethanol productivity and synthetic glucose feed conversion as a function of dilution rate for the SHF process.

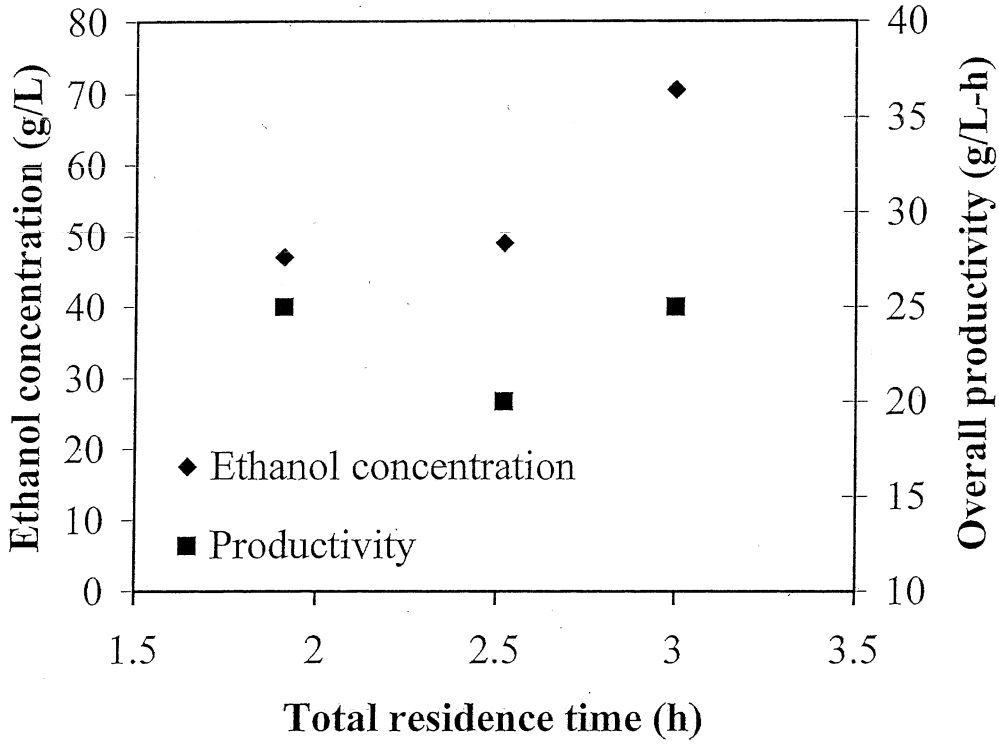

Figure 15. Overall volumetric ethanol productivity and ethanol concentrations obtained from hydrolyzed cornstarch feed by the SHF process using immobilized glucose amylase and *Z. mobilis*. The results are plotted as a function of the total residence time.

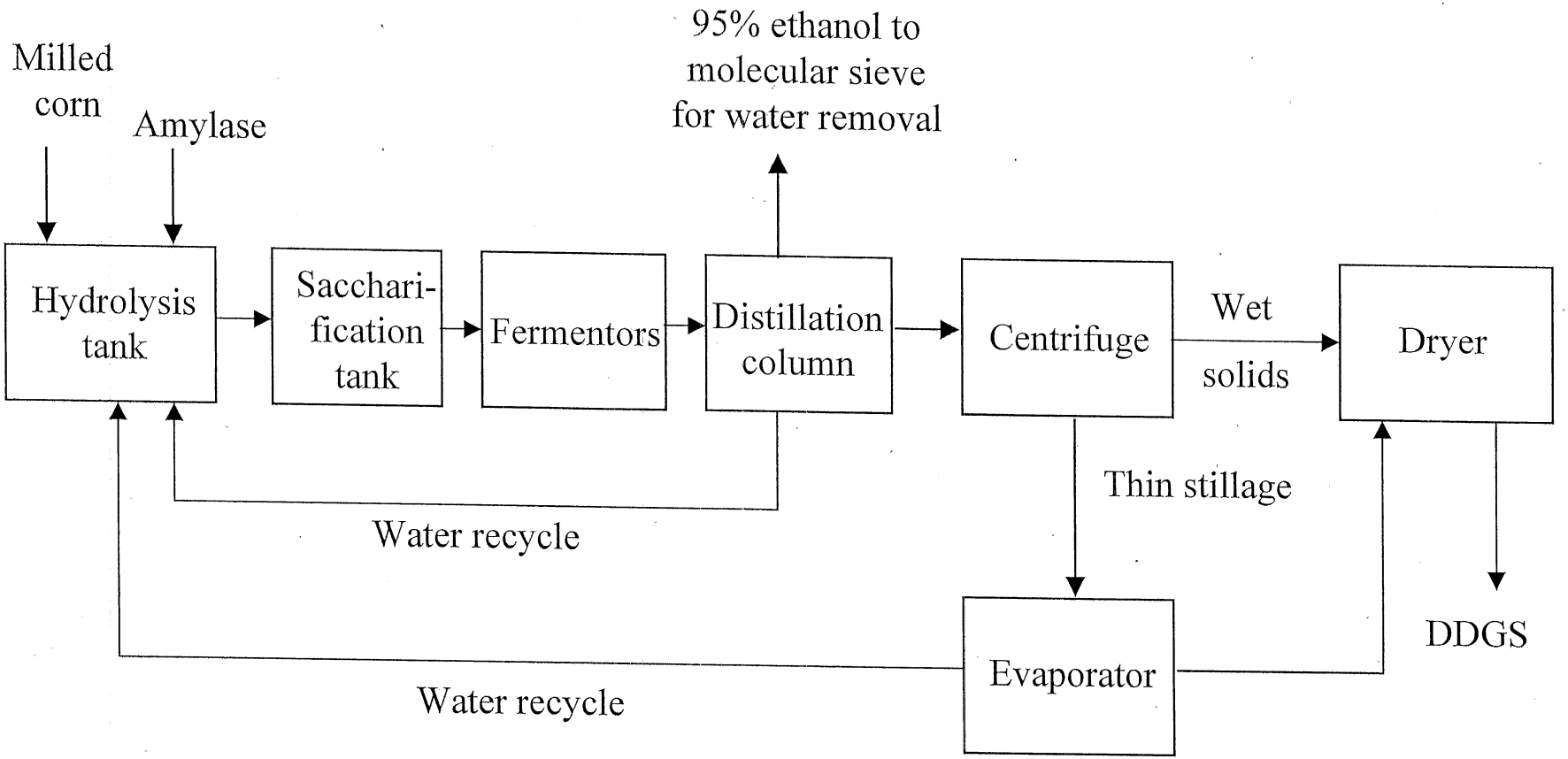

Fig. 16. Base case dry-mill corn starch to ethanol process.

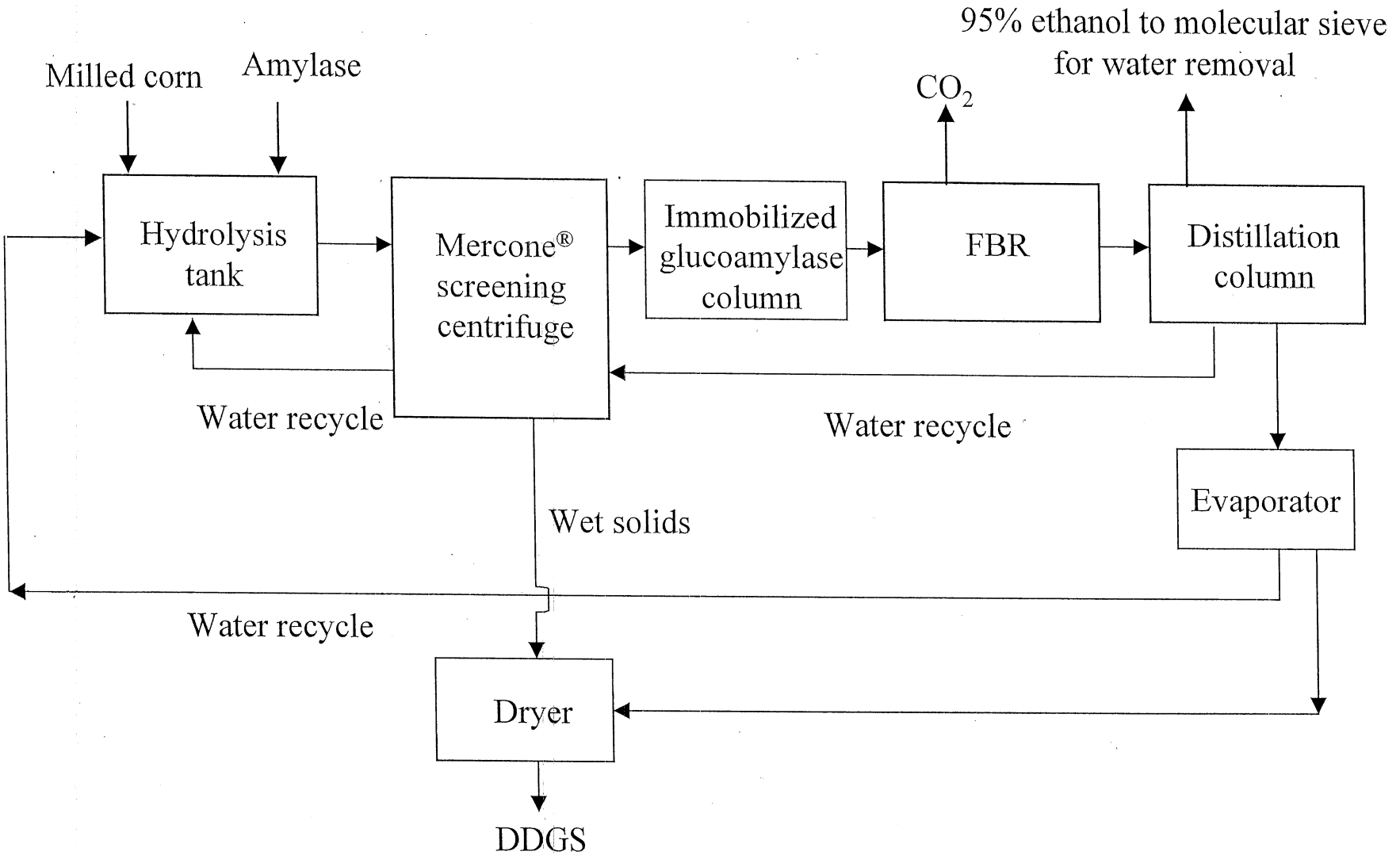

Fig. 17. FBR ethanol process.

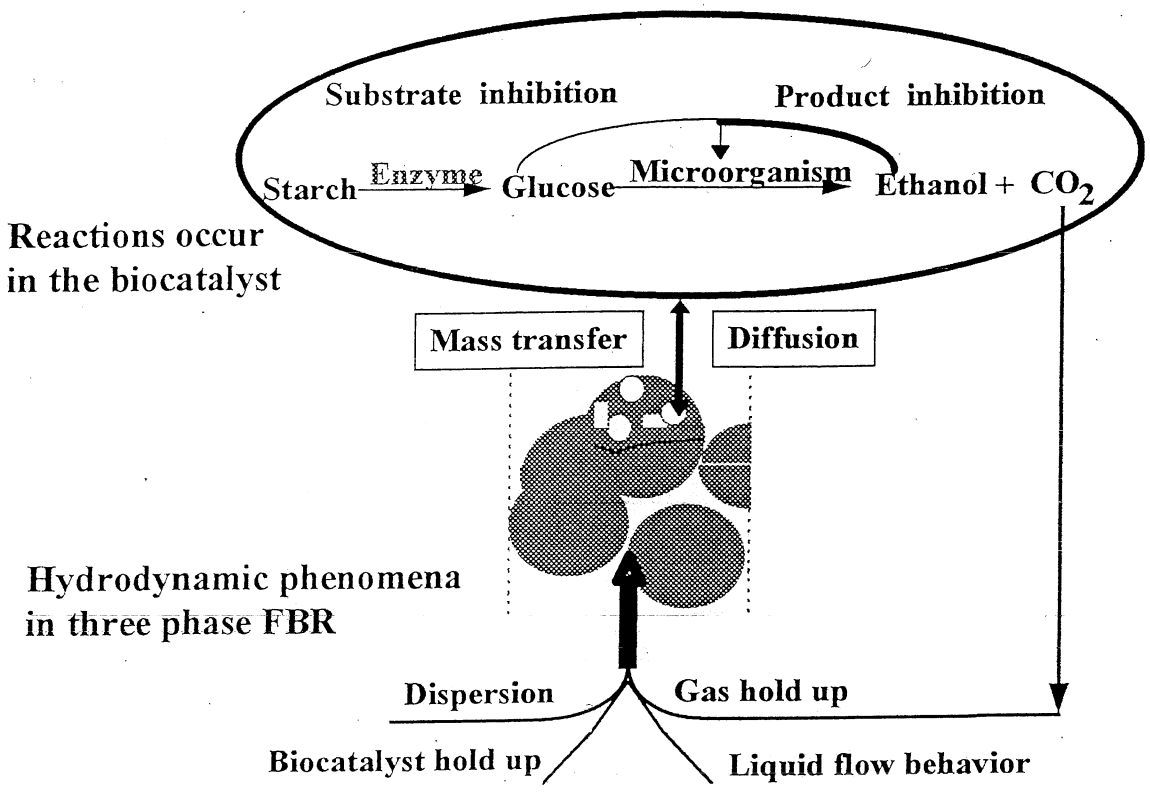

Figure 18. The mechanisms inside the reactor

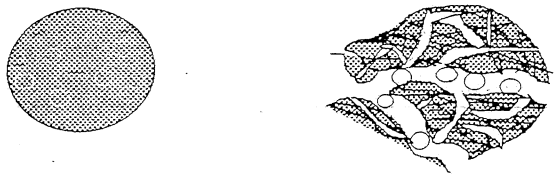

The schematic of the co-immobilized microorganism - GA biocatalyst

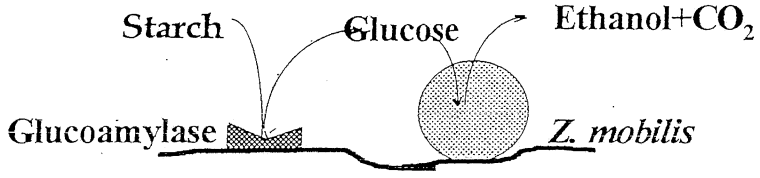

$$(C_6H_{10}O_5)_n + (n-1)H_2O \xrightarrow{\gamma_S} nC_6H_{12}O_6 \xrightarrow{\gamma_g} 2nCH_3CH_2OH + 2nCO_2$$

Figure 19. The reactions and mechanism inside the co-immobilized GA-*Z. mobilis* biocatalyst

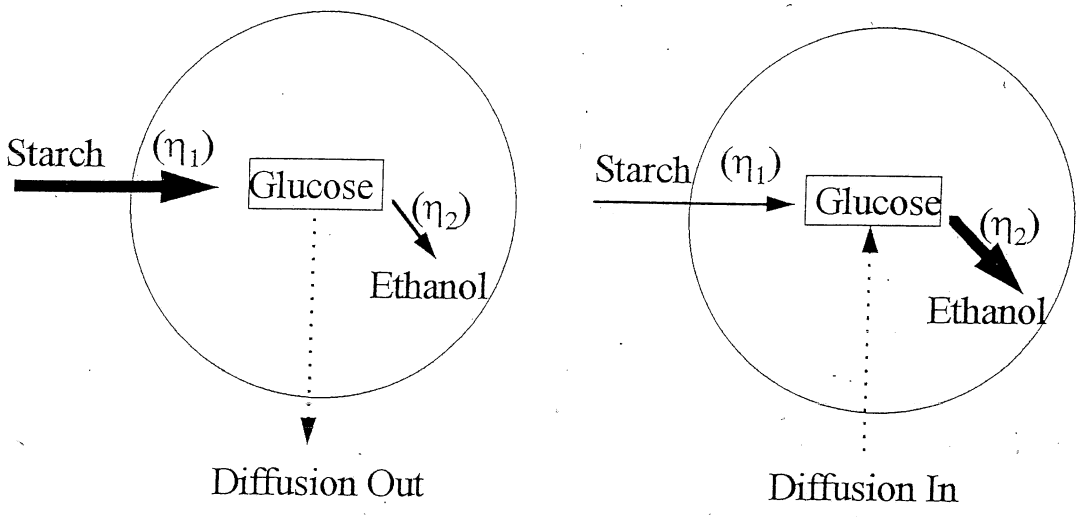

Figure 20. Mass flow and two effectiveness factors of the co-immobilized biocatalyst bead.

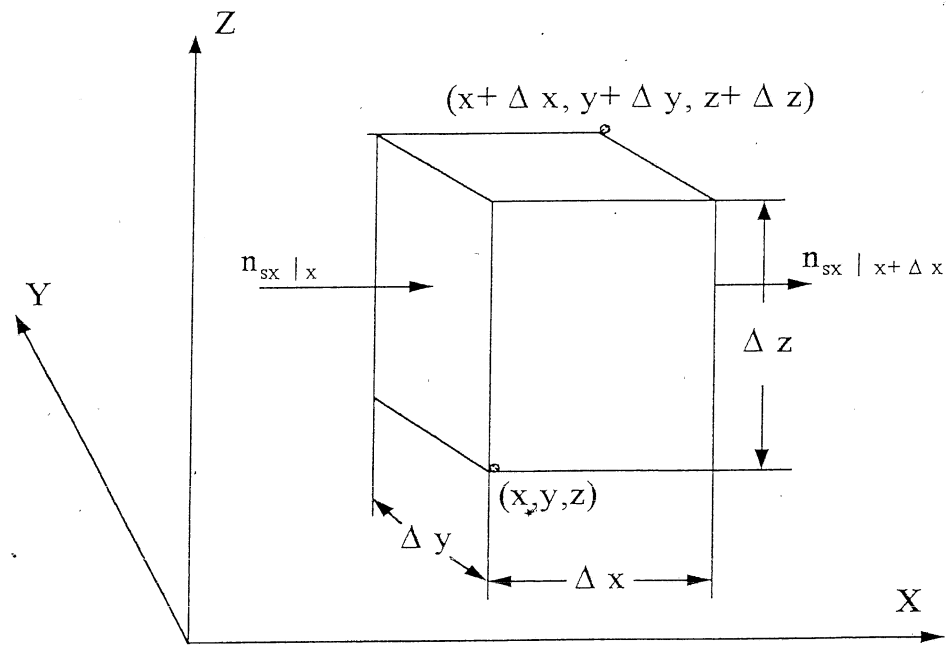

Figure 21. Stationary volume element $\Delta x \Delta y \Delta z$ through which the fluid is moving.

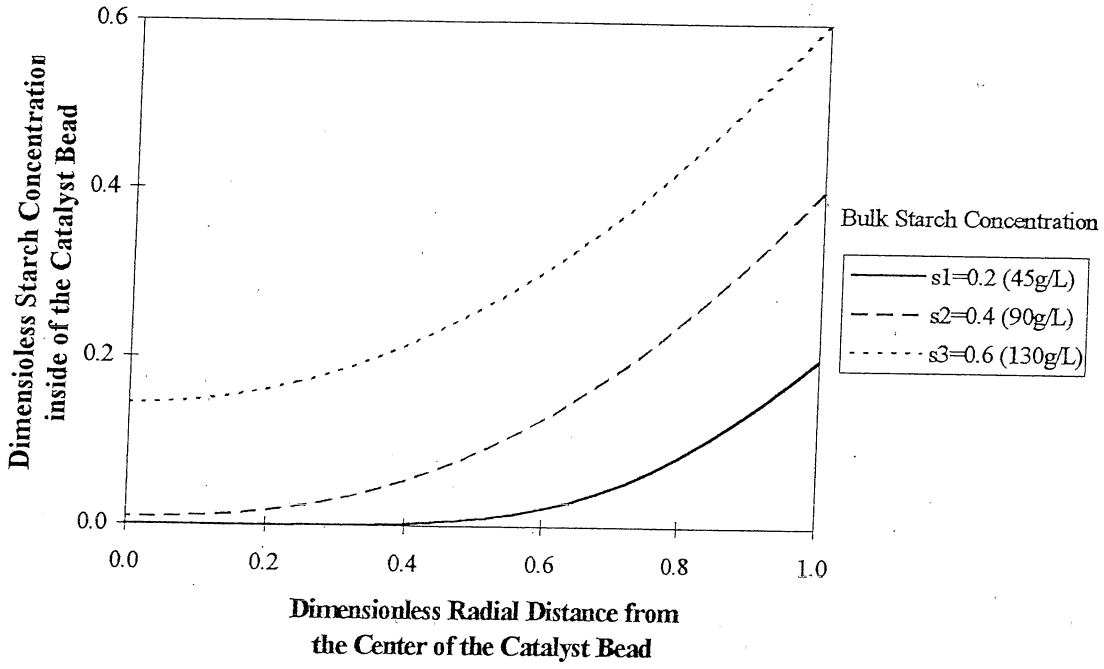

Figure 22. Starch concentration profile inside the bead along the radial distance from the center of the bead at the different bulk starch concentrations.

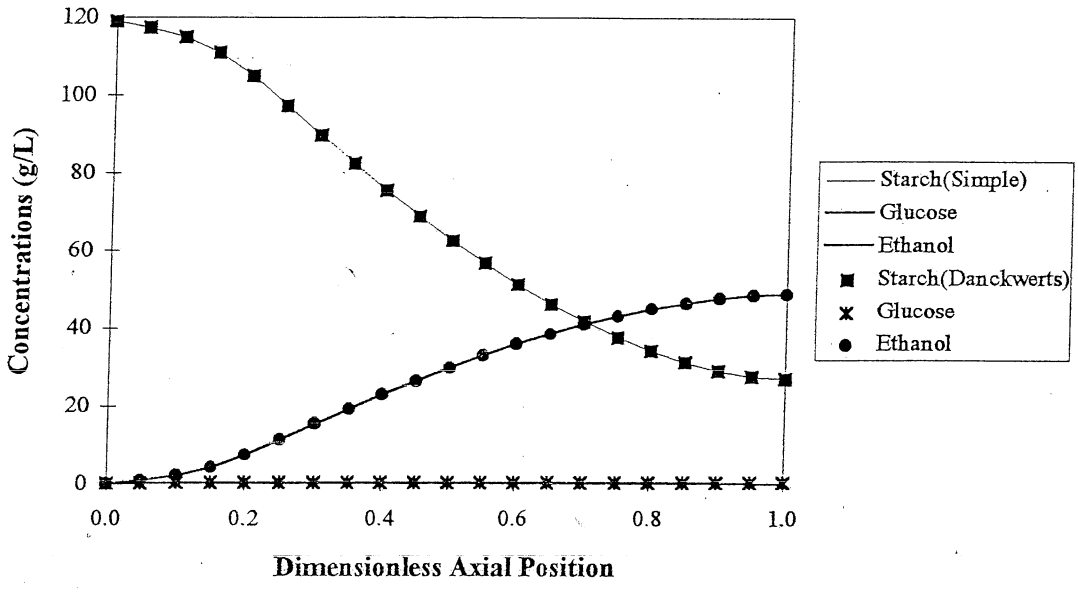

Figure 23. The comparison of the mathematical model results solved using the plug flow boundary condition (simple) and the Danckwerts boundary condition. (flow rate 0.6 L/hr, enzyme loading = 150 ml, and catalyst bead diameter = 0.2 mm)

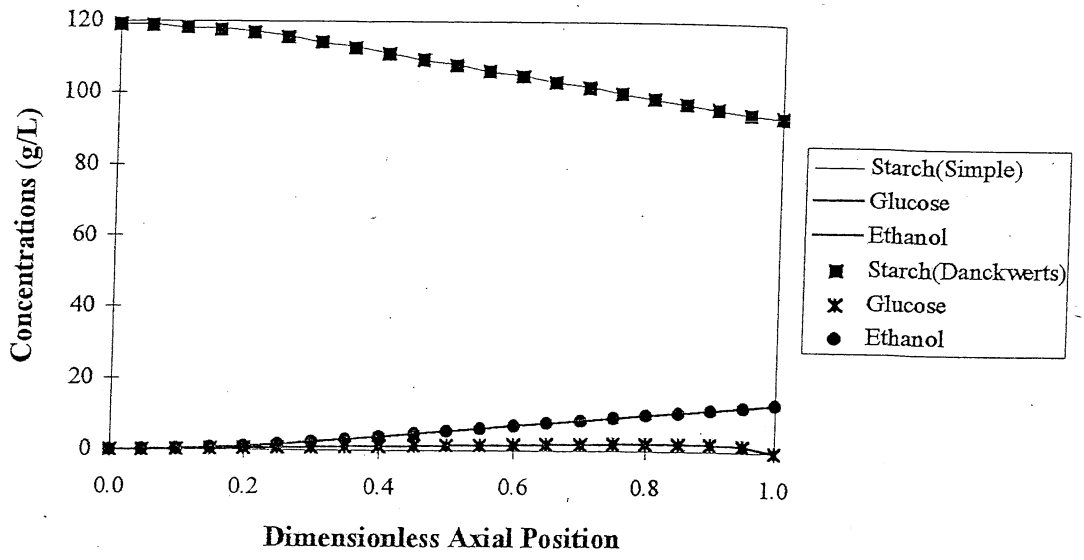

Figure 24. The comparison of the mathematical model results solved using the plug flow boundary condition (simple) and the Danckwerts boundary condition. (flow rate is 2 L/hr, enzyme loading = 375 ml, and catalyst bead diameter = 0.4 mm)

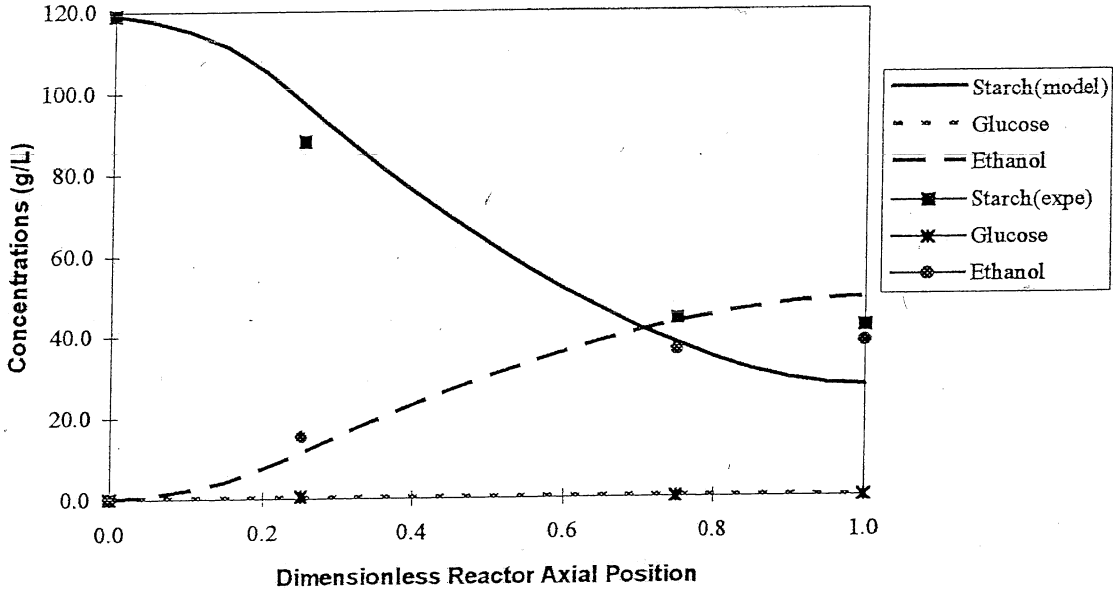

Figure 25. The starch concentration profile comparison between the model results and the experimental data. (experimental condition: flow rate = 0.6 L/hr, feed concentration = 119 g/L)

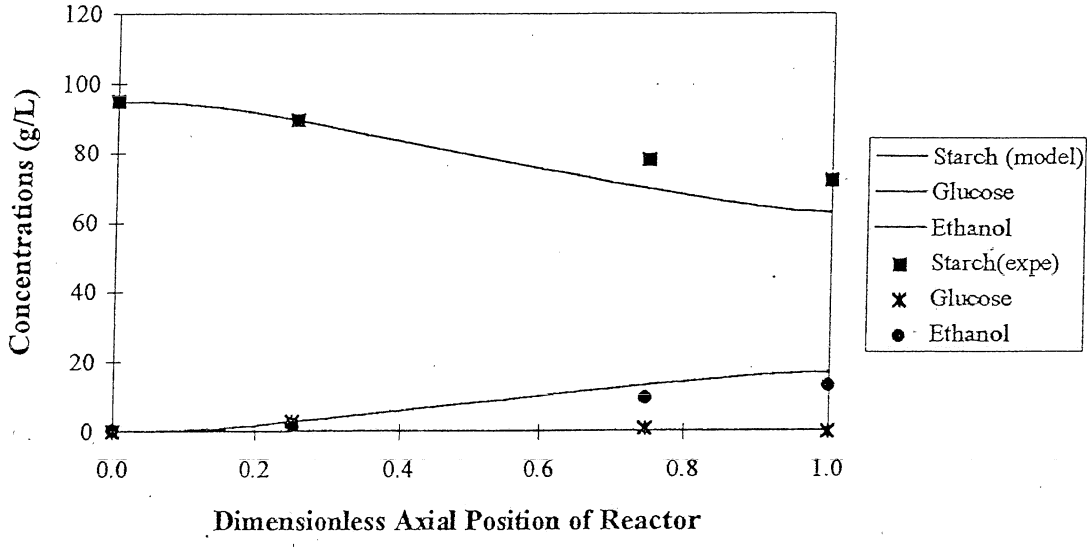

Figure 26. The starch concentration profile comparison between the model results and the experimental data. (Experiment condition: Flow rate = 2 L/hr, Feed concentration = 95 g/L)

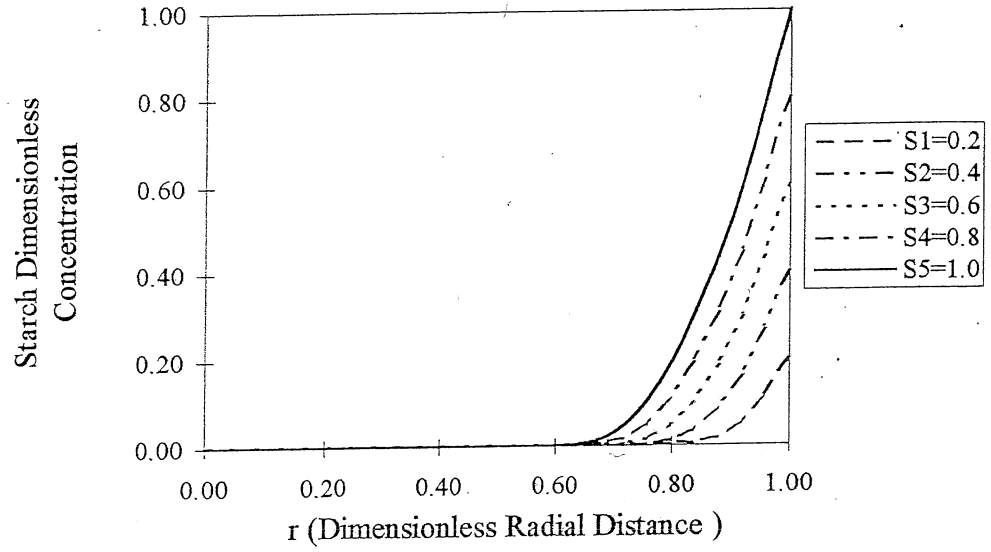

Figure 27. The starch concentration profile in the catalyst bead at different bulk starch concentrations.

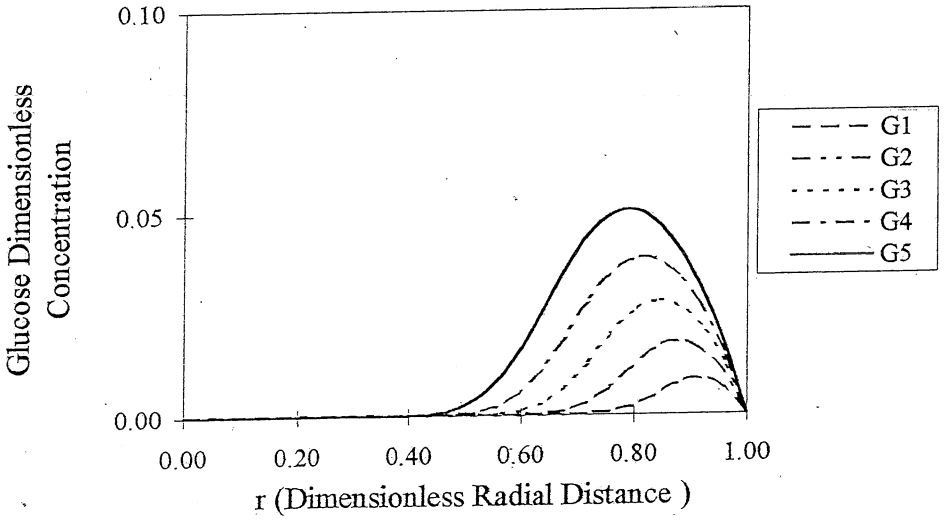

Figure 28. Glucose concentration profiles corresponding to the different starch bulk concentrations. Glucose concentration G1 corresponds to bulk starch.

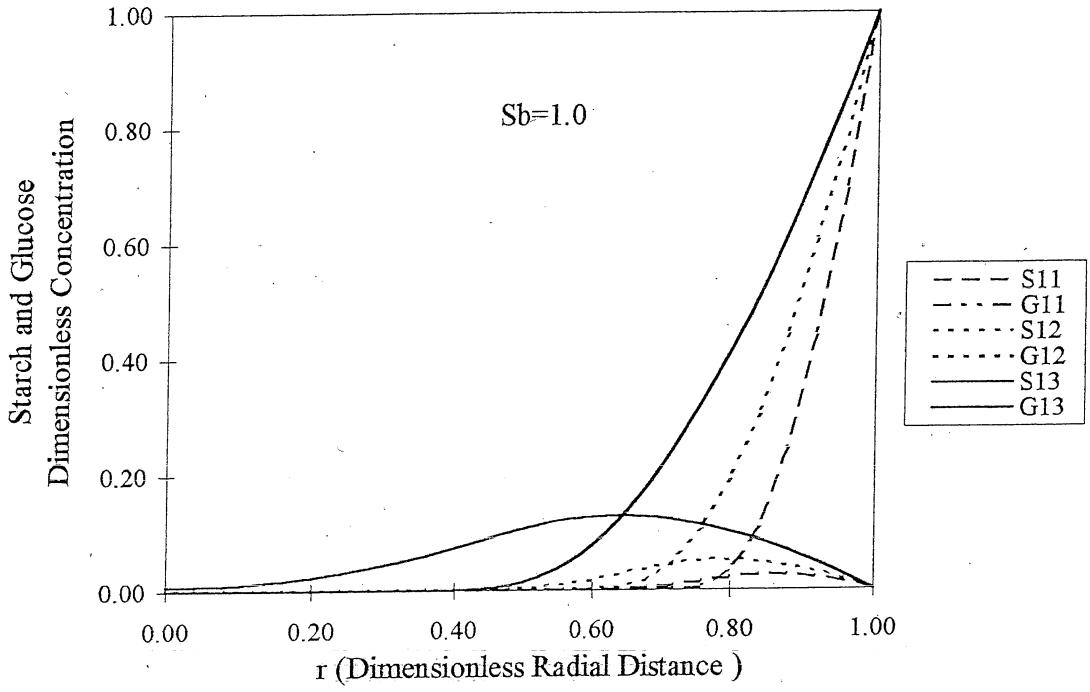

Figure 29. Starch and glucose concentration profiles at the different starch diffusivities. Bead Radius = 2mm, Starch bulk concentration Sb = 1.0, glucose bulk concentration = 0.0, starch S11, glucose G11 (Ds =0.002 cm^2/hr); S12, G12 (Ds = 0.004 cm^2/hr); S13, G13 (Ds = 0.008 cm^2/hr)

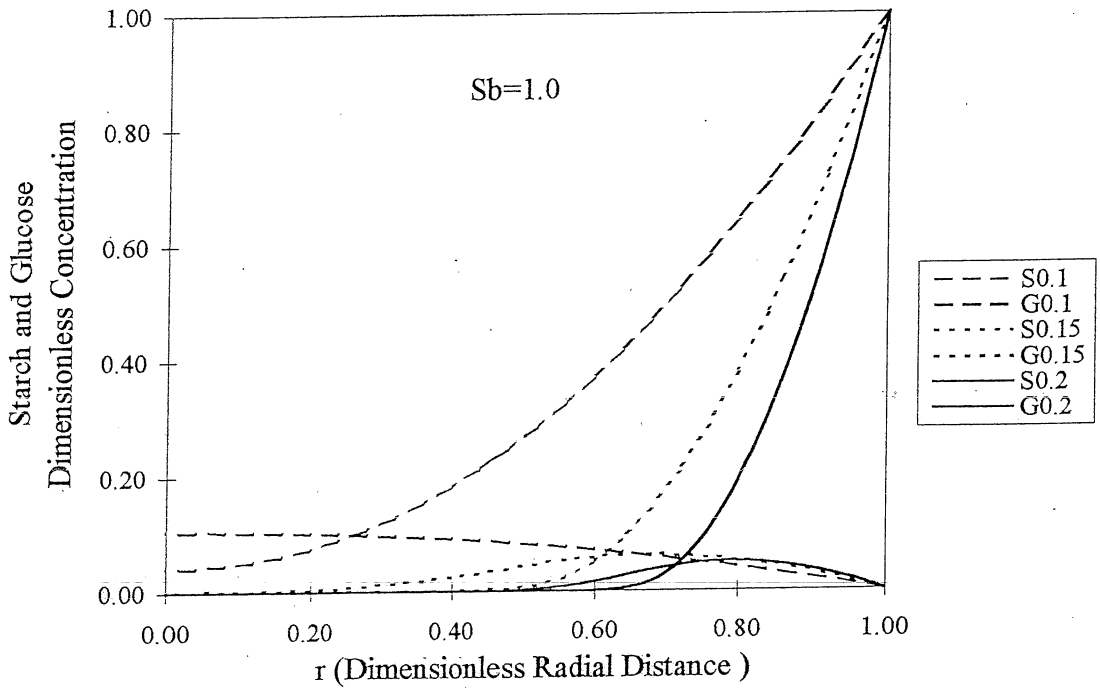

Figure 30. Starch and glucose concentration profiles for different sizes of catalyst bead. S0. 1 is starch concentration, G0. 1 is glucose concentration at r = 0.1 cm; S0. 15; G0. 15 (r = 0.15 cm); S0.2, G0.2 (r = 0.2 cm).

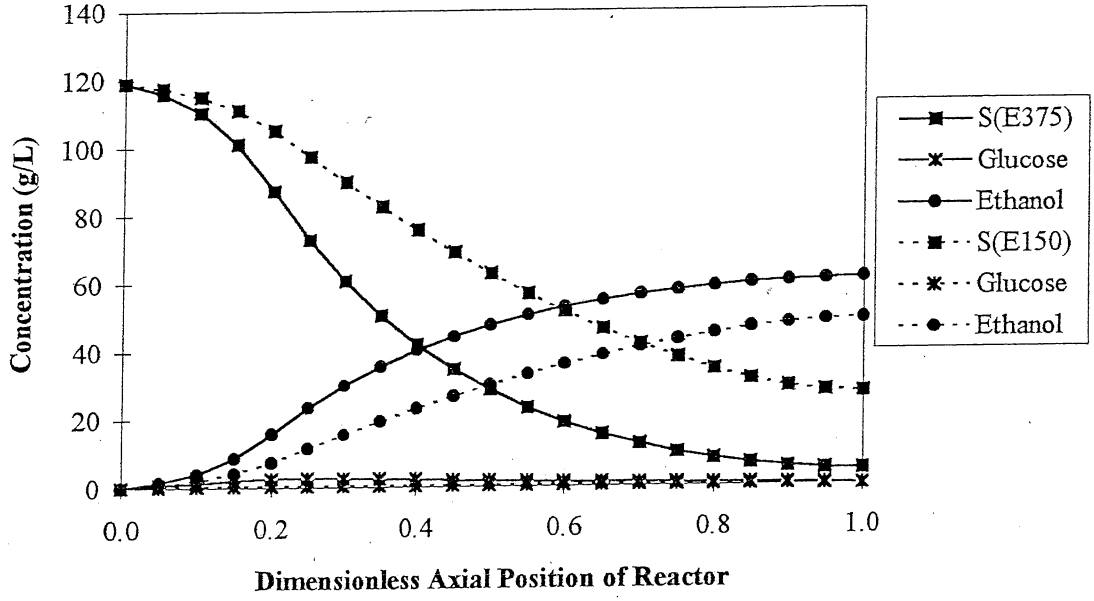

Figure 31. The comparison of concentration profiles in the reactor with different catalyst enzyme loading.

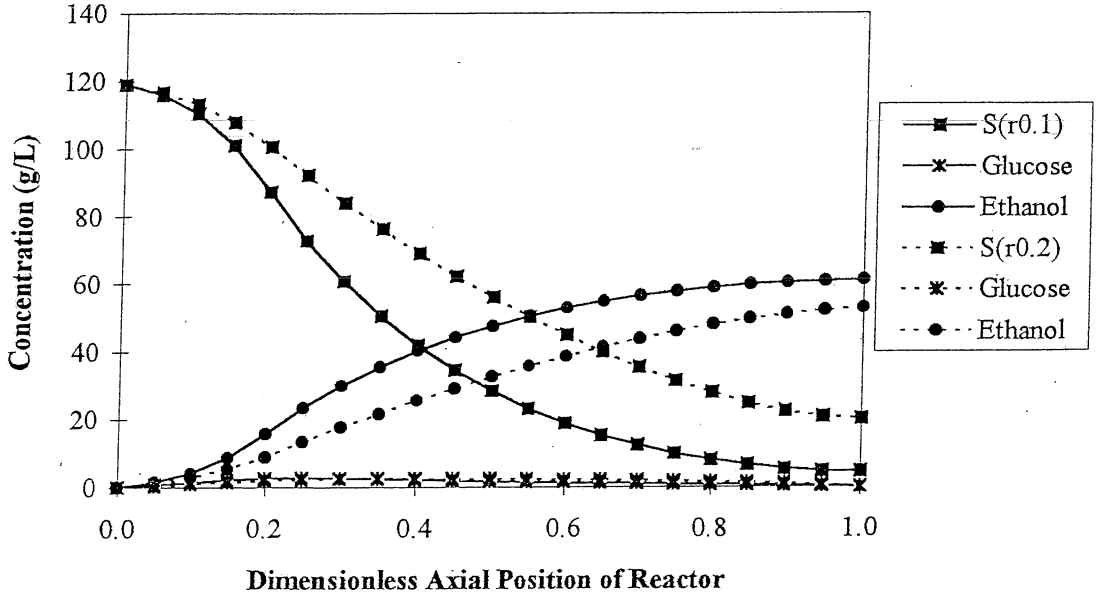

Figure 32. The comparison of concentration profiles in the reactor with different catalyst enzyme loading.

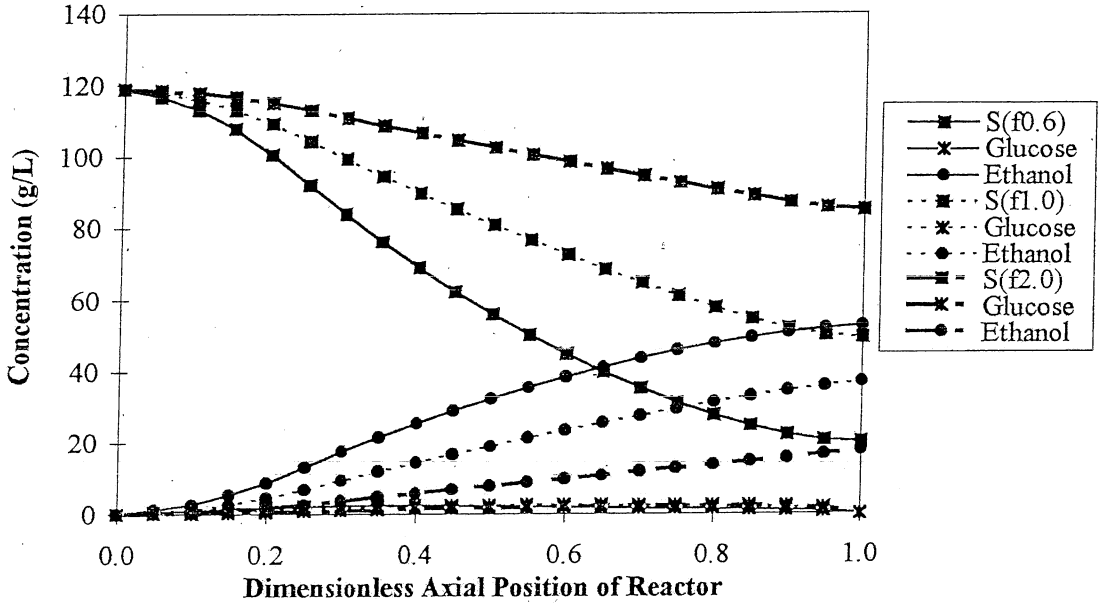

Figure 33. The influence of the feed flow rate on the concentration profiles in the reactor.

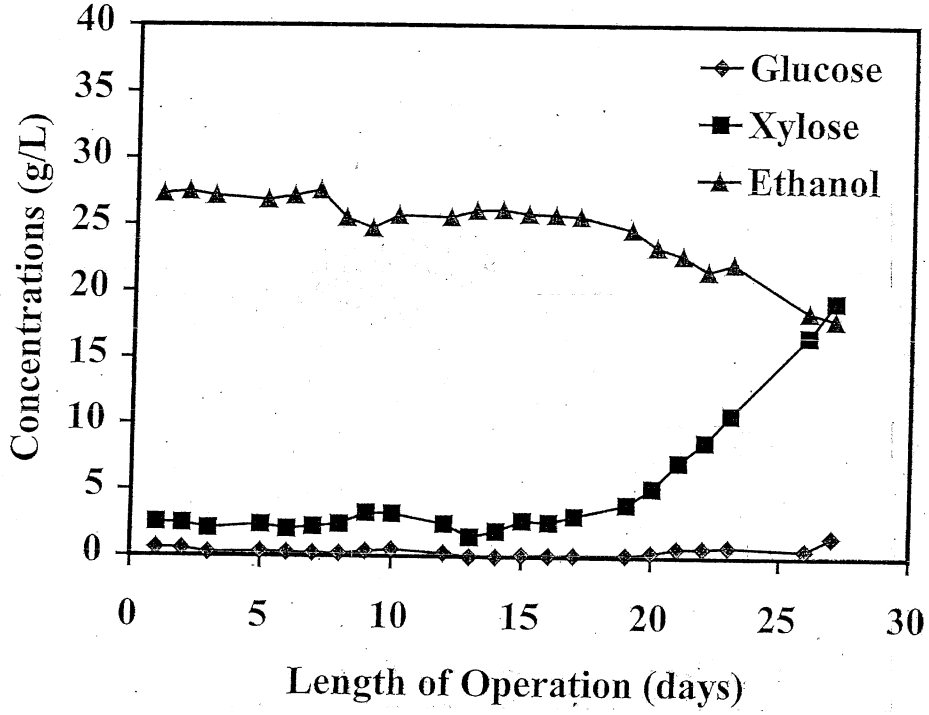

Figure 34. Determination of stability of strain *Z. mobilis* 31821 (pZB5) in continuous FBR operation.

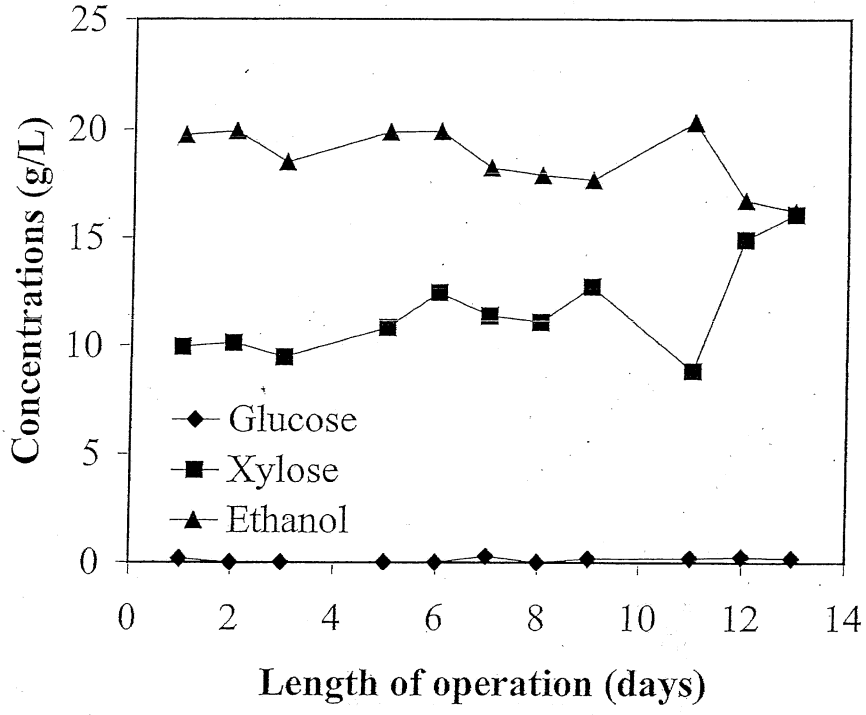

Figure 35. Determination of stability of strain *Saccharomyces* 424A (LNH-ST) in continuous FBR operation.

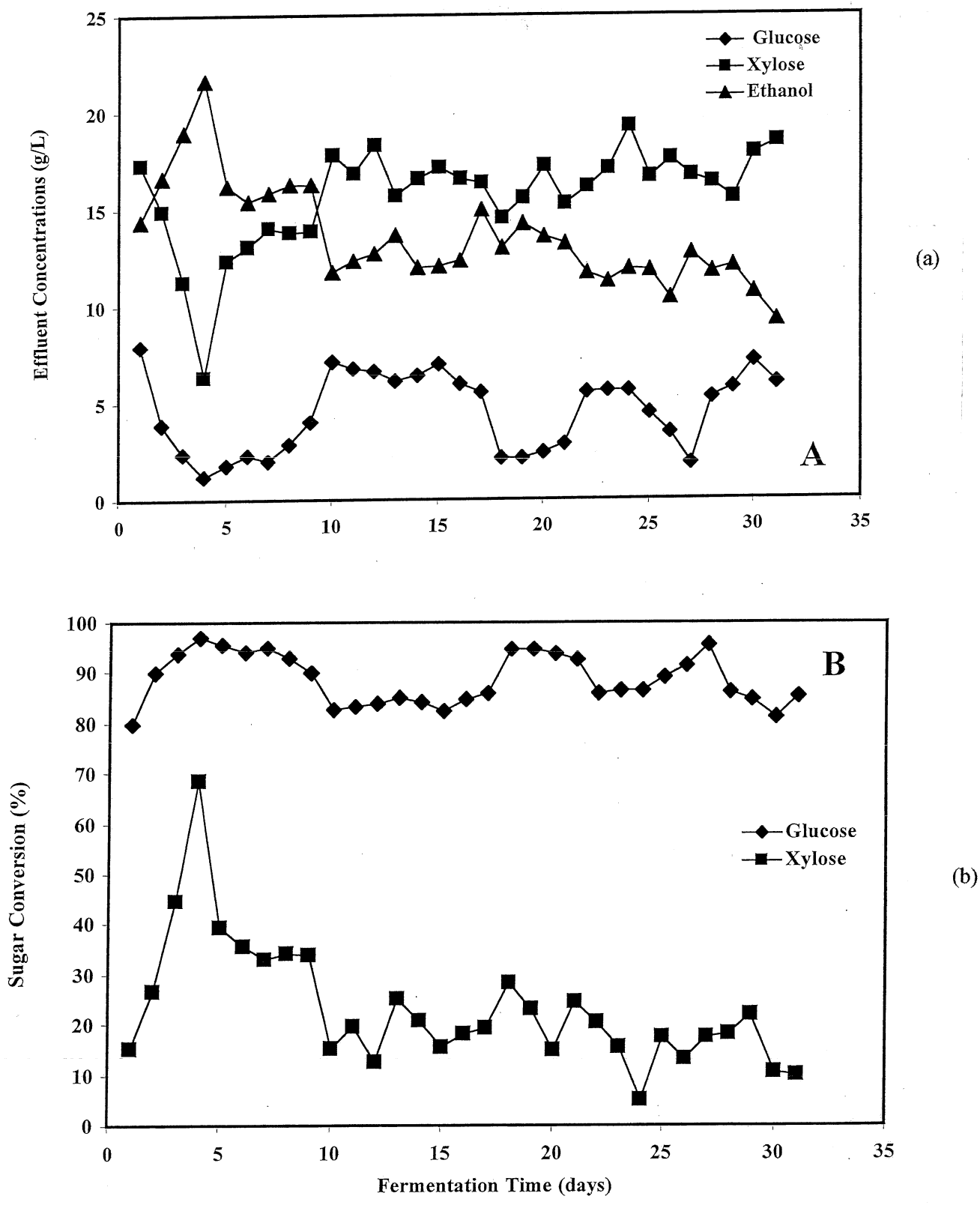

Figure 36. Performance of *Z. mobilis* C25 in FBR using 40/20 glucose/xylose feed at 4.2- h retention time with Red Star yeast extract as nutrient source.

(a) Effluent concentrations

(b) Substrate conversion

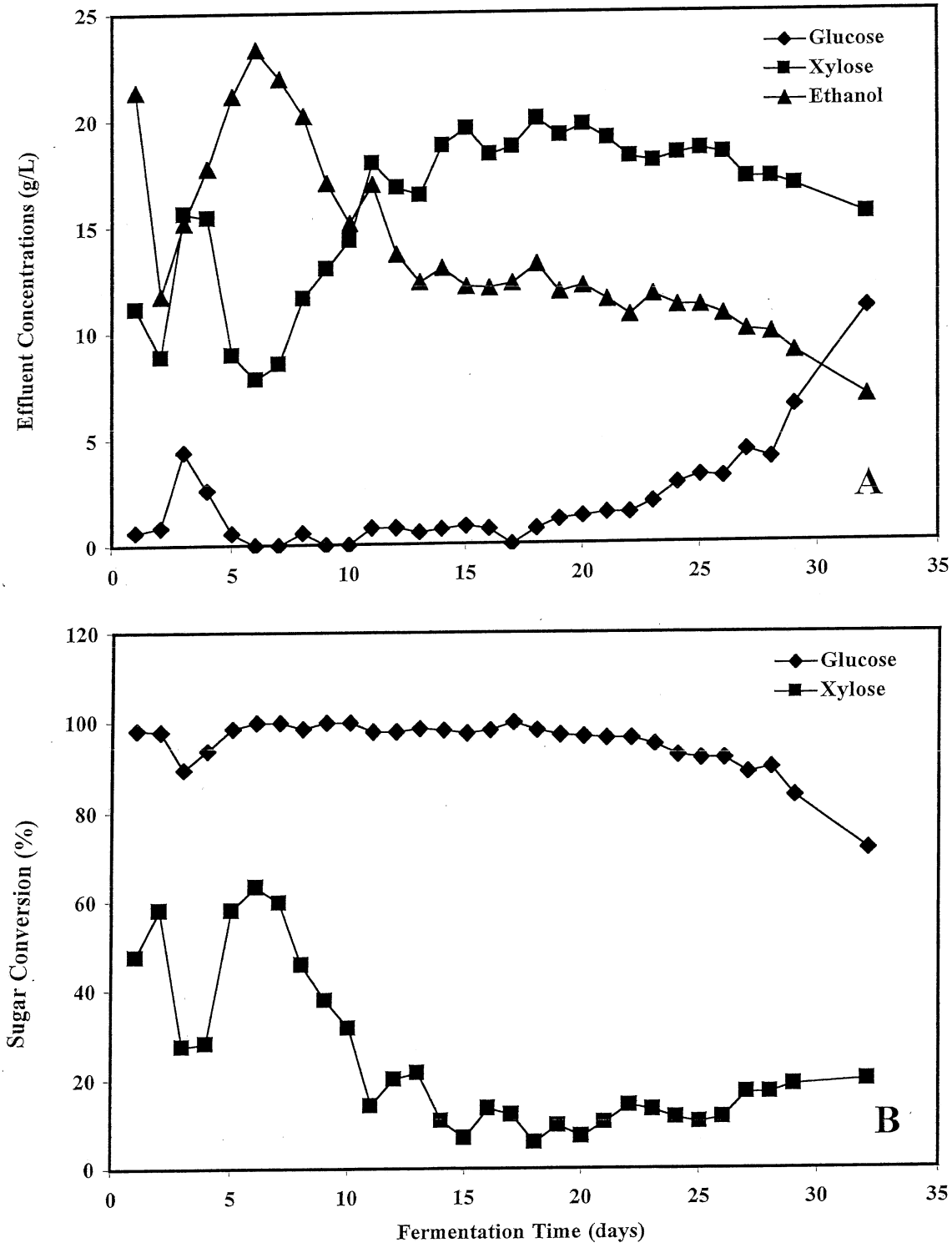

Figure 37. Performance of *Z. mobilis* C25 in FBR using 40/20 glucose/xylose feed at 4.2- h retention time with Difco yeast extract as nutrient source.

(a) Effluent concentrations

(b) Substrate conversion

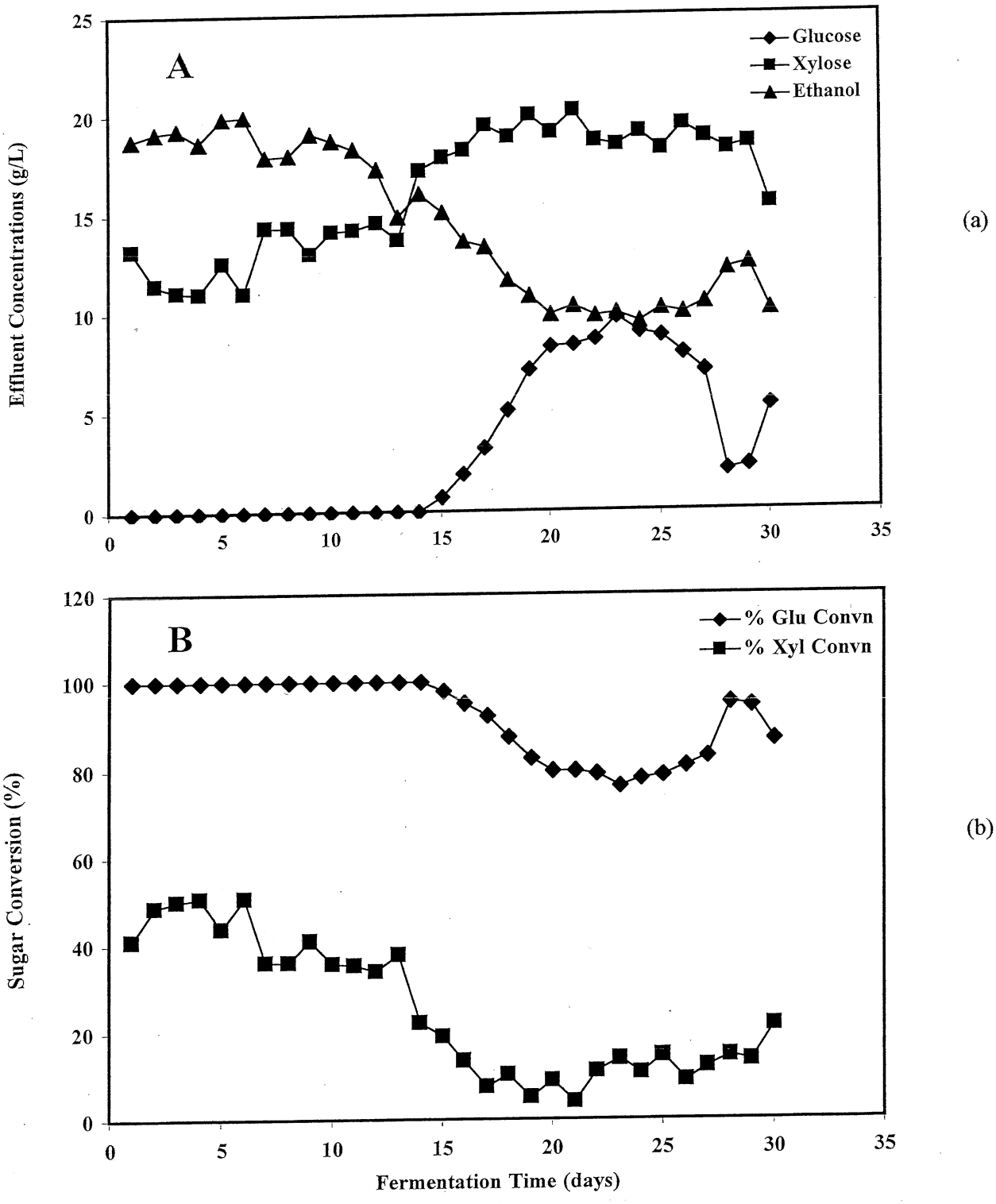

Figure 38. Performance of *Saccharomyces* 424A (LNH-ST) in FBR using 40/20 glucose/xylose feed at 4.2- h retention time with Difco yeast extract as nutrient source.

(c) Effluent concentrations

(d) Substrate conversion

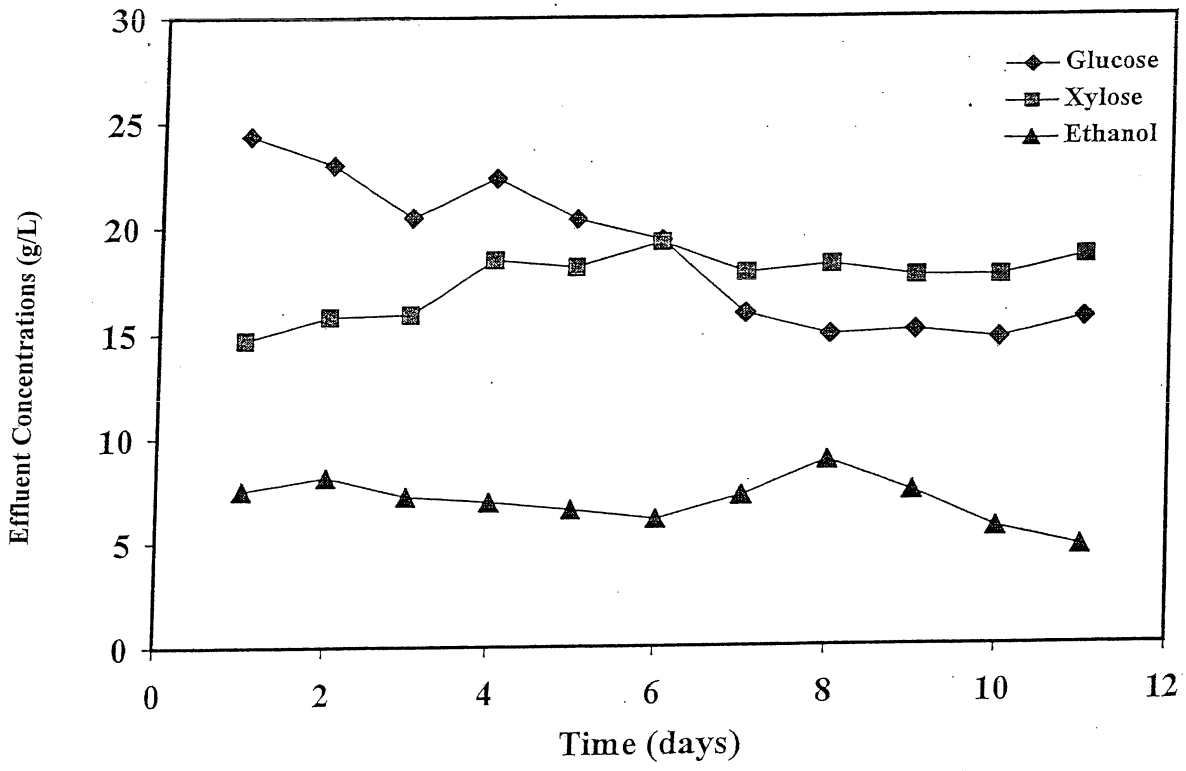

Figure 39. Continuous ethanol fermentation in the FBR by *E. coli* K011.